THE
PHYSICAL REVIEW
A Journal of Experimental and Theoretical Physics Established by E. L. Nichols in 1893
VOL. 53, NO. 6 MARCH 15, 1938 SECOND SERIES

Radioactivity Induced in the Rare Earth Elements by Fast Neutrons

M. L. POOL AND L. L. QUILL
Departments of Physics and Chemistry, Ohio State University, Columbus, Ohio
(Received January 15, 1938)

With the exception of illinium, thulium and lutecium all the rare earth elements have been bombarded with slow and fast neutrons. The fast neutrons were obtained from the Li+D reaction. Deuterons of 6.3 Mev were produced by the cyclotron at the University of Michigan. The following periods for electron emission have been observed: La^{140} (31 hr.), Pr^{142} (19 hr.), Nd^{147} (84 hr.), Nd'^{149} (2.0 hr.), Nd^{151} (21 min.), Il^{144} (12.5 hr.), Sm^{151} (21 min.), Sm^{153} (46 hr.), Eu^{152} (9.2 hr.), Tb^{160} (3.3 hr.), Dy^{165} (2.5 hr.), Ho^{164} (47 min.), Ho^{166} (30 hr.), Er^{169} (12 hr.) and Er^{171} (5.1 hr.) The following periods for positron emission have been observed: Ce^{139} (2.1 min.), Pr^{140} (3.5 min.), Eu^{150} (27 hr.), Tb^{158} (3.6 min.), Dy^{159} (2.2 min.) and Er^{165}(1.1 min.). There seems to be at least two isotopes which are isomeric: one is Gd^{159} (3.5 min., 17 hr.) and the other is Yb^{175} (2.1 hr., 14 hr.). From radioactivity data it is necessary to postulate the existence of four new stable isotopes: Gd^{152}, Dy^{160}, Er^{164} and Yb^{170}. With the fast neutron bombardment seventeen n-$2n$ type of reactions have been found.*

INTRODUCTION

THE initial work of Fermi[1] and of Amaldi *et al.*[2] in 1934 showed that certain of the rare earth elements could be made weakly radioactive by neutrons from a radon-beryllium source. These workers and others extended the study and in 1936 Hevesy and Levi summarized all such findings.[3] Since 1936 very few new data have been added.

This lack of additional work is probably due to the unusual number of difficulties encountered with this group of elements. Many of the elements can be had only in small quantities. The task of chemically separating one of the rare earth elements from others of the same group is in general long and tedious since their chemical reactions are so nearly identical that fractional separation is usually necessary. Inability to separate rapidly one rare earth from its neighbors obviously inhibits the analysis of the radioactive products formed in samples bombarded with neutrons or deuterons.

The influences of the above-named difficulties are seen in the existing induced radioactivity data as compiled by Hevesy and Levi. For many of the elements the data show contradicting periods, an extremely weak intensity of the radioactivity and meager evidence for associating a period with a definite nucleus.

Clearly much exacting work with pure and strongly radioactive samples is needed before the induced radioactive properties of the rare earths can be ascertained. The cyclotron, conceded to

* *Note added in proof:* Samples of gadolinium, erbium and ytterbium used in these experiments were sent to Professor A. J. Dempster of the University of Chicago who has kindly analyzed them in his mass spectrograph. He replies that the predicted stable isotopes Gd^{152}, Er^{164}, and Yb^{170} have been found as well as three other new isotopes. With his own dysprosium the existence of stable Dy^{160} is confirmed and in addition another dysprosium isotope is found. The high purity of gadolinium, erbium and ytterbium is also verified. Details will be published in a paper by Professor Dempster in the near future.

[1] Fermi, Ricerca Scient. **1**, 330 (1934).

[2] Amaldi, Fermi, Rasetti and Segrè, Nuovo Cimento **11**, 442 (1934).

[3] Hevesy and Levi, K. Dansk-Acad. **14**, No. 5 (1936).

produce slow neutrons in much greater abundance than the strongest radon-beryllium source, answers the need of strongly radioactive samples. A number of the rare earths of unusual purity had been prepared by one of us (L.L.Q.). Furthermore, it has recently been pointed out that fast neutrons, ranging in energies up to 20 Mev, induce strong radioactivity in a large number of elements and are of great aid (because of the *n*-2*n* process) in assigning radioactive periods to nuclei.[4]

It is the primary purpose of this paper to report the action of fast neutrons on the rare earth group of elements. However, most of the rare earth elements were also irradiated with slow neutrons. In a few cases deuteron bombardment was employed.

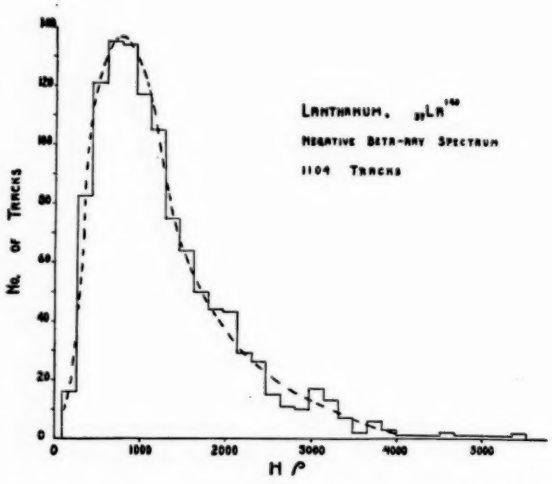

FIG. 1. Beta-ray spectrum of La^{140}. By inspection the upper limit is 4080*H* (0.8 Mev).

EXPERIMENTAL

The fast neutrons were obtained by bombarding a block of metallic lithium with 6.3 Mev deuterons. The lithium was securely fastened to a water cooled copper plate. The material to be irradiated with fast neutrons was placed in an aluminum, copper or glass container and attached to the copper plate. The container, copper plate, and lithium target were in a chamber that could be evacuated.

The slow neutrons were obtained by bombarding metallic beryllium with deuterons. The material to be irradiated with slow neutrons was surrounded by 15 cm or more of paraffin and placed about two feet from the beryllium target.

The deuterons of 6.3 Mev were furnished by the cyclotron at the University of Michigan.

The intensity of the induced radioactivity was measured by a Wulf string electrometer. A six-inch Wilson cloud chamber filled with hydrogen and placed in a magnetic field was used to examine the beta-rays.

RESULTS

Lanthanum

Amaldi *et al.* found lanthanum inactive after strong irradiation under water.[5] However, Marsh and Sugden, using 400 millicuries of radon, found a rather weak activity with a half-life of 46 hours.[6] In the following research lanthanum oxide, La_2O_3, was used. Arc spectrum analysis showed the absence of other rare earths. A bombardment of five to ten microampere-hours with deuterons gave an activity that could easily be followed five half-lives.

This activity, which had a half-life of 31 hours, was found to be associated with the lanthanum fraction in the following series of chemical separations: The bombarded lanthanum was dissolved in dilute hydrochloric acid. To this solution was then added a small amount of barium chloride and cerium chloride solutions. The lanthanum and cerium were precipitated with oxalic acid from the resulting solution as the oxalates. The barium was precipitated from the filtrate as barium sulfate, which was found to be inactive. The lanthanum and cerium oxalates were dissolved in concentrated nitric acid, the resulting solution then being almost neutralized with ammonium hydroxide (just acid to litmus). A small amount of calcium oxide and some potassium bromate were added and the mixture evaporated almost to dryness. The residue was boiled with water, filtered and washed. The cerium remained in the precipitate and the lanthanum was precipitated from the filtrate by oxalic acid. The cerium precipitate was virtually inactive, whereas the lanthanum oxalate precipitate showed the 31-hr. activity.

[4] Pool, Cork and Thornton, Phys. Rev. **51**, 890 (1937); **52**, 239 (1937).

[5] Amaldi, D'Agostino, Fermi, Pontecorvo, Rasetti and Segrè, Proc. Roy. Soc. **149**, 522 (1935).

[6] Marsh and Sugden, Nature **136**, 102 (1935).

The reactions for this activity are,

$$_{57}La^{139}+{}_1d^2\rightarrow{}_{57}La^{140}+{}_1p^1$$
$$_{57}La^{140}\rightarrow{}_{58}Ce^{140}+{}_{-1}e^0 \text{ (31 hr.)}.$$

A histogram based upon the measurement of 1104 negative beta-ray tracks is shown in Fig. 1. By inspection the upper limit is placed at 0.8 Mev. This value of the energy together with the period gives on the Sargent plot a point which falls on the first Sargent curve. The interpretation is that the beta-ray transition is a permitted one.

Fast neutron bombardment of lanthanum also gave the 31-hr. period and in addition a period of 85.6 min. This latter period is undoubtedly due to $_{56}Ba^{139}$ since an 85.6-min. period was obtained by bombarding barium with deuterons and observing the activity in the barium sulphate precipitate.[7] This interpretation is substantiated by Amaldi *et al.*[5] who obtained with slow neutron bombardment of barium a period of 80 min. in the barium chemical separation. The fast neutron reaction equations are,

$$_{57}La^{139}+{}_0n^1\rightarrow{}_{56}Ba^{139}+{}_1p^1$$
$$_{56}Ba^{139}\rightarrow{}_{57}La^{139}+{}_{-1}e^0 \text{ (85.6 min.)}.$$

Cerium

Amaldi *et al.*[5] and Marsh and Sugden[6] found cerium inactive. The question of neutron excited alpha-ray activity in cerium has been discussed by Döpel and by Fünfer.[8]

In the following study the cerium used was the dioxide, CeO_2. Although it was found to be free of other rare earths, the purest available sample had a natural beta- and gamma-activity which was probably due to thorium contamination. The intensity of the activity in a ten gram sample of CeO_2 was about equal to the background of the ionization chamber. Since thorium is strongly activated by fast neutrons, this impurity becomes a serious problem.

In order to compensate as much as possible for this contamination a sample of NH_4OH+Th was made which had the same natural activity as the cerium sample. Both samples were then irradiated with fast neutrons at the same time. The NH_4OH+Th decay curve was subtracted from the cerium decay curve and the resultant decay attributed to the cerium. This procedure gave a 2.1-min. positron period which was about ten times as intense as the induced thorium radioactive background. Since fast neutron bombardment of thorium alone resulted in an induced thorium activity which was totally electron emitting, the carrier of the 2.1-min. positron activity is very probably Ce^{139}. The reaction equations are

$$_{58}Ce^{140}+{}_0n^1\rightarrow{}_{58}Ce^{139}+2{}_0n^1$$
$$_{58}Ce^{139}\rightarrow{}_{57}La^{139}+{}_1e^0 \text{ (2.1 min.)}.$$

Deuteron bombardment of cerium gave longer periods in the cerium chemical separation, but since thorium is also strongly activated by deuterons the results are too confusing for analysis at present.

Praseodymium

Amaldi *et al.*[5] found a 5-min. and a 19-hr. period, the latter being water sensitive. Marsh and Sugden[6] verified the 19-hr. period and attributed the activity to Pr^{142}. However, they were unable to detect the 5-min. period.

In the following study praseodymium oxide, Pr_2O_3, containing about 99 percent praseodymium and 1 percent lanthanum, was used. The presence of lanthanum did not interfere since it is not easily activated.

With fast neutrons a very strong 3.5-min. period was observed which is by far the strongest positron period in the rare earth group of elements. The 19-hr. period was also observed and measured as 18.7 hr. Since praseodymium has only one stable isotope, the reaction equations for the short period may be written:

$$_{59}Pr^{141}+{}_0n^1\rightarrow{}_{59}Pr^{140}+2{}_0n^1$$
$$_{59}Pr^{140}\rightarrow{}_{58}Ce^{140}+{}_1e^0 \text{ (3.5 min.)}.$$

With slow neutron bombardment only the 19-hr. period was observed and the assignment made by Marsh and Sugden is confirmed.

Neodymium

Amaldi *et al.*[5] found a very weak 1-hr. period. Marsh and Sugden[6] were unable to find any induced radioactivity with neutrons from a 400-millicurie radon-beryllium source. With a 500-millicurie source McLennan and Rann[9] observed

[7] Pool and Cork, Phys. Rev. **51**, 1010 (1937).
[8] Döpel, Zeits. f. Physik **99**, 161 (1936); Fünfer, Physik. Zeits. **37**, 693 (1936).
[9] McLennan and Rann, Nature **136**, 831 (1935).

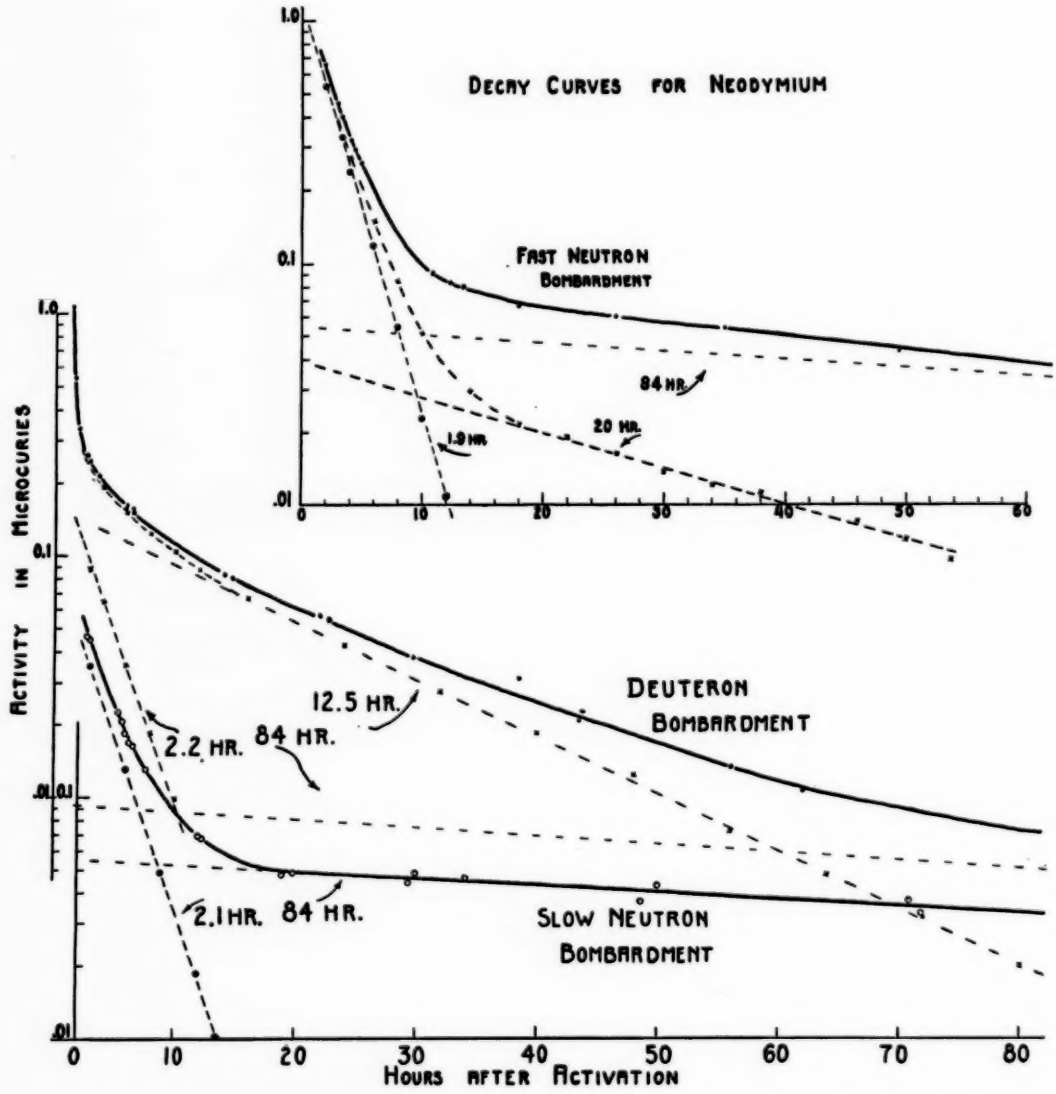

FIG. 2. Decay curves for neodymium. The periods shown are 84 hr. (Sm^{147}), 2 hr. (Sm^{149}), 20 hr. (Pr^{142}) and 12.5 hr. (Il^{144}). The curves extending beyond 80 hr. after activation are not shown. The 21-min. (Sm^{151}) slow neutron period is also not shown.

a 35-min. period which gave an initial intensity of eight impulses per minute in a Geiger counter.

In the following experiments the neodymium oxide, Nd_2O_3, used showed, by arc spectrum analysis, the absence of other rare earths.

The very much greater neutron equivalent of the cyclotron is easily evident from the fact that in four hours of slow neutron bombardment three periods were easily evident, 21 min., 2.0 hr. and 84 hr. They all emitted electrons. The relative rates of formation of the nuclei responsible for these radioactive periods are, respectively, 0.8 : 1 : 1.7. With fast neutron bombardment the observed periods were 2.0 hr., 20 hr. and 84 hr.; the relative rates of formation are 1 : 0.22 : 1.2. The decay curves are shown in Fig. 2.

Since the 21-min. period is produced by slow but not by fast neutron bombardment and since Nd^{150} is the heaviest neodymium isotope,[10] it is reasonable to assign this activity to Nd^{151}.

In order to assign the 2.0-hr. and 84-hr. periods the relative abundance of the stable

[10] Dempster, Phys. Rev. **51**, 289 (1937).

nuclei and the rate of formation of the radioactive nuclei (branching ratio) must be compared. The ratio of the abundance of Nd^{146}/Nd^{148} is 2.4.[11] For slow neutron bombardment the ratio of the rate of formation of the 84-hr. period to the 2-hr. period is 1.7. This ratio for fast neutron bombardment is 1.2 and the ratio of abundance of Nd^{148}/Nd^{150} is 1.15. Consequently, these data suggest, in view of no other guiding information, that the 84-hr. period should be attributed to Nd^{147} and the 2-hr. period to Nd^{149}. The reaction equations would then be

for slow n $\quad {}_{60}Nd^{146}+{}_0n^1\rightarrow{}_{60}Nd^{147}+{}_0\gamma^0$

for fast n $\quad {}_{60}Nd^{148}+{}_0n^1\rightarrow{}_{60}Nd^{147}+2{}_0n^1$

$\qquad {}_{60}Nd^{147}\rightarrow{}_{61}Il^{147}+{}_{-1}e^0$ (84 hr.)

for slow n $\quad {}_{60}Nd^{148}+{}_0n^1\rightarrow{}_{60}Nd^{149}+{}_0\gamma^0$

for fast n $\quad {}_{60}Nd^{150}+{}_0n^1\rightarrow{}_{60}Nd^{149}+2{}_0n^1$

$\qquad {}_{60}Nd^{149}\rightarrow{}_{61}Il^{149}+{}_{-1}e^0$ (2.0 hr.).

The weak 20-hr. period obtained with fast neutron bombardment is best assigned to Pr^{142}

$${}_{60}Nd^{142}+{}_0n^1\rightarrow{}_{59}Pr^{142}+{}_1p^1$$
$${}_{59}Pr^{142}\rightarrow{}_{60}Nd^{142}+{}_{-1}e^0 \text{ (19 hr.)}.$$

With deuteron bombardment the 2-hr. and 84-hr. periods were observed as well as a new period of 12.5 hours. The relative rate of formation of the nuclei responsible for these periods are, respectively, 1 : 1.5 : 3.7.

In order to eliminate the effects of sodium, potassium and other contaminations easily activated by deuterons, chemical separation of neodymium oxide was made as follows. The irradiated neodymium oxide was dissolved in warm hydrochloric acid to which was added a small amount of salt. The neodymium was precipitated with oxalic acid. The mixture was cooled to room temperature and filtered. The activity of the precipitated neodymium oxalate was then measured.

Because of the time required for the chemical separation, periods appreciably shorter than the 2-hr. period could not be observed. The 12.5-hr. period was quite strong and has been followed for six half-lives. However, it is uncertain to which nucleus this period should be assigned. The best assignment seems to be Il^{144} according to the equations

$${}_{60}Nd^{143}+{}_1d^2\rightarrow{}_{61}Il^{144}+{}_0n^1$$
$${}_{61}Il^{144}\rightarrow{}_{62}Sm^{144}+{}_{-1}e^0 \text{ (12.5 hr.)}.$$

If a stable samarium isotope should be found at mass number 145 or 146, the assignment of the 12.5-hr. period to Il^{145} or Il^{146} would be equally plausible.

[11] Mattauch and Hauk, Naturwiss. **48**, 780 (1937).

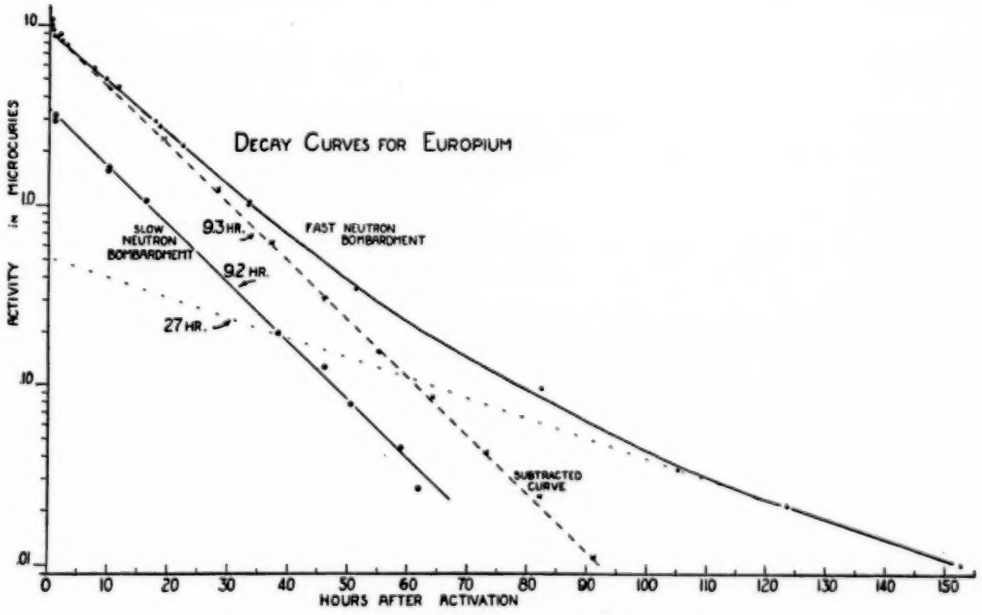

FIG. 3. Decay curves for europium.

Samarium

A 40-min.[5, 6] period and a "longer period" [6] have been reported.

By arc spectrum analysis the samarium oxide, Sm_2O_3, used in the following study showed no other rare earths present.

Fast and slow neutrom bombardment gave the same periods, 21-min. and 46-hr. For slow neutron bombardment the branching ratio of the 46-hr. period to the 21 min. period is 7.7. For fast neutron bombardment this ratio is 1.4. The ratio of the abundance of the stable isotopes Sm^{152}/Sm^{150} is 5.2 and that for Sm^{154}/Sm^{152} is 0.8. These data strongly suggest that the 21-min. period should be assigned to Sm^{151} and the 46-hr. period to Sm^{153}. The reaction equations are

for slow n $\quad {}_{62}Sm^{150}+{}_0n^1\rightarrow{}_{62}Sm^{151}+{}_0\gamma^0$

for fast n $\quad {}_{62}Sm^{152}+{}_0n^1\rightarrow{}_{62}Sm^{151}+2{}_0n^1$

$\qquad {}_{62}Sm^{151}\rightarrow{}_{63}Eu^{151}+{}_{-1}e^0$ (21 min.)

for slow n $\quad {}_{62}Sm^{152}+{}_0n^1\rightarrow{}_{62}Sm^{153}+{}_0\gamma^0$

for fast n $\quad {}_{62}Sm^{154}+{}_0n^1\rightarrow{}_{62}Sm^{153}+2{}_0n^1$

$\qquad {}_{62}Sm^{153}\rightarrow{}_{63}Eu^{153}+{}_{-1}e^0$ (46 hr.).

Europium

Marsh and Sugden[6] found a strong 9.2-hr. slow neutron period.

Arc spectrum and magnetic susceptibility measurements of the europium oxide, Eu_2O_3, used in the present research showed the europium to be of exceptional purity.

The decay curves for slow and fast neutron bombardment of europium are shown in Fig. 3. The 9.2-hr. period is confirmed. For fast neutron bombardment a weak 27-hr. positron period in addition to the 9.2-hr. period is also present. The 27-hr. period is attributed to Eu^{150} instead of to I^{148} or I^{150} primarily because positron activity is not found on the heavy isotope side of an element.

The 9.2-hr. period is assigned to Eu^{152} instead of to Eu^{154} since this period is strongly produced by fast neutron bombardment. The equations are

for slow n $\quad {}_{63}Eu^{151}+{}_0n^1\rightarrow{}_{63}Eu^{152}+{}_0\gamma^0$

for fast n $\quad {}_{63}Eu^{153}+{}_0n^1\rightarrow{}_{63}Eu^{152}+2{}_0n^1$

$\qquad {}_{63}Eu^{152}\rightarrow{}_{64}Gd^{152}+{}_{-1}e^0$ (9.2 hr.)

for fast n $\quad {}_{63}Eu^{151}+{}_0n^1\rightarrow{}_{63}Eu^{150}+2{}_0n^1$

$\qquad {}_{63}Eu^{150}\rightarrow{}_{62}Sm^{150}+{}_1e^0$ (27 hr.).

Since gadolinium is not known to have a stable isotope with mass number 152 and since the 9.2-hr. period emits electrons and is assigned to Eu^{152}, it is necessary to postulate the existence of a stable Gd^{152}. Radioeuropium decays into this new stable isotope as shown in the third equation above.

Gadolinium

Amaldi *et al.*[5] observed an 8-hr. period which was water-sensitive. Marsh and Sugden[6] found gadolinium inactive. With fourteen grams of material McLennan and Rann[9] observed a 6.4-hr. period which gave an initial intensity of sixteen impulses per minute in a Geiger counter.

In this present study gadolinium oxide, Gd_2O_3, was used. High purity was indicated by the absence, in arc spectrum analysis, of any other rare earth elements.

Periods of 3.5-min. and 17-hr. were obtained with both slow and fast neutron bombardment. The branching ratio of these periods for both methods of production is also nearly the same. It is therefore likely that both the 3.5-min. and 17-hr. activity should be assigned to Gd^{159}. This assignment is substantiated by fast neutron bombardment of terbium as indicated below.

Terbium

Marsh and Sugden obtained a weak 3.9-hr. period [6]

The terbium used in the following experiments was prepared by G. Urbain. Slow neutron bombardment gave a 3.3-hr. period which emitted electrons. With fast neutron bombardment a 3.6-min. and 17-hr. period were obtained and the 3.3-hr. period was not evident. About half of the 3.6-min. activity was due to positrons.

Since the 3.6-min. and 17-hr. periods appeared only with fast neutron bombardment of terbium, and with both slow and fast neutron bombardment of gadolinium, support is thereby added to the previous contention that Gd^{159} is isomeric.

The reaction equations for fast neutron bombardment of terbium may be written as follows:

${}_{65}Tb^{159}+{}_0n^1\rightarrow{}_{65}Tb^{158}+2{}_0n^1$

$\qquad {}_{65}Tb^{158}\rightarrow{}_{64}Gd^{158}+{}_1e^0$ (3.6 min.)

${}_{65}Tb^{159}+{}_0n^1\rightarrow{}_{64}Gd^{159}+{}_1p^1$

$\qquad {}_{64}Gd^{159}\rightarrow{}_{65}Tb^{159}+{}_{-1}e^0$ (3.5 min. 17 hr.).

Since the 3.3-hr. period emits electrons and is assigned to Tb^{160} and since there is no known stable isotope in dysprosium at mass number

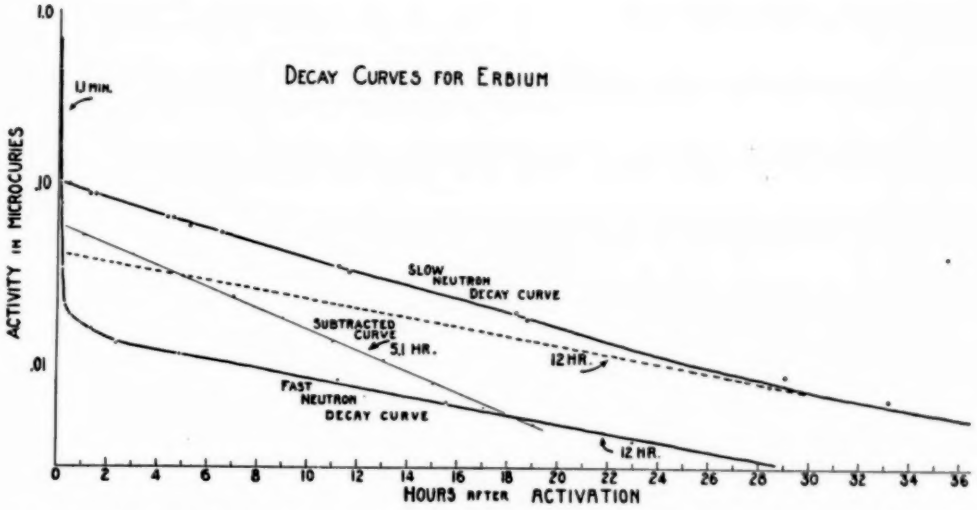

FIG. 4. Decay curves for erbium. The periods shown are 12 hr. (Er^{169}), 5.1 hr. (Er^{171}) and 1.1 min. (Er^{165}). The latter is a very strong positron period.

160, it is necessary to postulate the existence of stable Dy^{160}. Radioterbium then decays into this stable nucleus as follows:

$$_{65}Tb^{159}+{}_0n^1\rightarrow{}_{65}Tb^{160}+{}_0\gamma^0$$
$$_{65}Tb^{160}\rightarrow{}_{66}Dy^{160}+{}_{-1}e^0 \text{ (3.3 hr.)}.$$

Dysprosium

A 2.5-hr. period, the strongest slow neutron period yet known, has been previously found.[6, 12]

For the following experiments Professor Hopkins loaned the authors very pure material that had been used for atomic weight determinations.

With slow neutron bombardment the 2.5-hr. period was verified. With fast neutron bombardment a weak 2.2-min. positron period was found as well as the 2.5-hr. period. This 2.5-hr. period was unusually strong which suggests a stable Dy^{166} isotope. However, the intensity of the radioactivity was not sufficiently strong to force the postulation of the existence of such a stable dysprosium isotope.

The 2.2-min. period is best assigned to Dy^{159} since stable Dy^{160} has been postulated. The reaction equations are as follows:

$$_{66}Dy^{160}+{}_0n^1\rightarrow{}_{66}Dy^{159}+2{}_0n^1$$
$$_{66}Dy^{159}\rightarrow{}_{65}Tb^{159}+{}_1e^0 \text{ (2.2 min.)}.$$

Holmium

Periods of 2.6 hr.,[6, 9] 33 hr.,[3] and 35 hr.[12] have been reported.

[12] Hevesy and Levi, Nature **136**, 103 (1935).

For the following experiments Dr. Kremers loaned the authors a holmium-rich yttrium mixture.

Because the holmium contained yttrium the holmium sample and a pure yttrium sample were bombarded at the same time with fast neutrons. The holmium activity was so much stronger than the yttrium activity that no appreciable difficulties were encountered. A 30-hr. and a 47-min. period were observed. The 47-min. period emits electrons and is assigned to Ho^{164}. This assignment necessitates postulating a stable isotope of erbium at mass number 164. The reaction equations for the 47-min. period may be written

$$_{67}Ho^{165}+{}_0n^1\rightarrow{}_{67}Ho^{164}+2{}_0n^1$$
$$_{67}Ho^{164}\rightarrow{}_{68}Er^{164}+{}_{-1}e^0 \text{ (47 min.)}.$$

Erbium

The previous work on this element has resulted in the observation of a variety of radioactive periods, 4.5 min.,[9] 7 min.,[6] 2.9 hr.,[13] 12 hr.,[12] 13 hr.,[3] and 38 hr.[6]

For the following experiments erbium oxide, Er_2O_3, was used. The purity was about 99 percent or better; traces of holmium and yttrium were present.

Slow neutron bombardment gave two weak periods, 5.1 hr. and 12 hr., both electron active. Fast neutron bombardment gave a strong 1.1 min. positron period and a weak 12-hr. period

[13] Sugden, Nature **135**, 469 (1935).

and a very weak 51-min. period. The 51-min. period is probably due to a slight holmium impurity. The decay curves are shown in Fig. 4. Since the 5.1-hr. period is not present with fast neutron bombardment, it is assigned to Er^{171}. The 12-hr. period, obtained with both fast and slow neutron bombardment, is assigned to Er^{169}. Since the 1.1-min. period is positron active, it is assigned to Er^{165}. The reactions with fast neutrons are as follows:

$$_{68}Er^{170}+{}_0n^1\rightarrow{}_{68}Er^{169}+2{}_0n^1$$
$$_{68}Er^{169}\rightarrow{}_{69}Tu^{169}+{}_{-1}e^0 \text{ (12 hr.)}$$
$$_{68}Er^{166}+{}_0n^1\rightarrow{}_{68}Er^{165}+2{}_0n^1$$
$$_{68}Er^{165}\rightarrow{}_{67}Ho^{165}+{}_1e^0 \text{ (1.1 min.)}.$$

This strong 1.1-min. positron period distinguishes Er^{165} as being the heaviest element in the periodic system yet known to emit positrons. This observation is significant because the probability of K electron capture increases, supposedly, very rapidly with atomic number and as a competitive process in all positron radioactive decay may become even much greater than the probability of positron emission itself.

Thulium

With slow neutron bombardment half-life periods of 3.5 mo.,[12] 4 mo.[14] and 8 mo.[15] have been reported.

Since thulium was not available no additional information can be given in this paper.

Ytterbium

A period of 3.5-hr. has been reported.[6, 12]

In the following experiments ytterbium oxide, Yb_2O_3, was used. It was prepared by the method of Yntema,[16] being precipitated electrolytically as $YbSO_4$. No exact analysis was made but it was probably about 98–99 percent Yb_2O_3 with thulium and lutecium as probable impurities.

Both fast and slow neutron bombardment gave periods of 2.1 hr. and 41 hr. The branching ratio for these two periods was the same by both methods of activation, even though Yb^{174} is three times as abundant as Yb^{176}. Therefore, both periods are assigned to Yb^{175}. The fast neutron reaction equations are

$$_{70}Yb^{176}+{}_0n^1\rightarrow{}_{70}Yb^{175}+2{}_0n^1$$
$$_{70}Yb^{175}\rightarrow{}_{71}Lu^{175}+{}_{-1}e^0 \text{ (2.1 hr., 41 hr.)}.$$

[14] Neuninger and Rona, Wiener Akad. Anzeiger. **73**, 159 (1936).
[15] Curie and Preiswerk, Comptes rendus **203**, 787 (1936).
[16] Yntema, J. Am. Chem. Soc. **52**, 2782 (1930).

TABLE I. *Induced radioactivities in the rare earth elements. Arrangement and notation similar to that used by Livingston and Bethe.*[17]

Raa Element					
Z	A	Class	Raa Particle	Half-life T	Produced by
56	Ba^{139}	A	e^-	85.6 min.	Ba-n-γ, Ba-d-p, La-n-p
57	La^{140}	A	e^-	31 hr.	La-n-γ, La-d-p
58	Ce^{139}	B	e^+	2.1 min.	Ce-n-2n
59	Pr^{140}	A	e^+	3.5 min.	Pr-n-2n
60	Nd^{147}	A	e^-	84 hr.	Nd-n-γ, Nd-n-2n
	Nd^{149}	A	e^-	2.0 hr.	Nd-n-γ, Nd-n-2n
	Nd^{151}	A	e^-	21 min.	Nd-n-γ
61	Il^{144}	C	e^-	12.5 hr.	Nd-d-n
62	Sm^{151}	A	e^-	21 min.	Sm-n-γ, Sm-n-2n
	Sm^{153}	A	e^-	46 hr.	Sm-n-γ, Sm-n-2n
63	Eu^{150}	B	e^+	27 hr.	Eu-n-2n
	Eu^{152}	A	e^-	9.2 hr.	Eu-n-γ, Eu-n-2n
64	Gd^{159}	B	e^-	3.5 min., 17 hr.	Gd-n-γ, Gd-n-2n, Tb-n-p
65	Tb^{158}	B	e^+	3.6 min.	Tb-n-2n
	Tb^{160}	A	e^-	3.3 hr.	Tb-n-γ
66	Dy^{159}	B	e^+	2.2 min.	Dy-n-2n
	Dy^{165}	A	e^-	2.5 hr.	Dy-n-γ, Dy-d-p
67	Ho^{164}	B	e^-	47 min.	Ho-n-2n
	Ho^{166}	A	e^-	30 hr.	Ho-n-γ
68	Er^{165}	A	e^+	1.1 min.	Er-n-2n
	Er^{169}	A	e^-	12 hr.	Er-n-γ, Er-n-2n
	Er^{171}	A	e^-	5.1 hr.	Er-n-γ
69	Tu^{170}	A	e^-	8 mo.	Tu-n-γ
70	Yb^{175}	A	e^-	2.1 hr., 41 hr.	Yb-n-γ, Yb-n-2n
71	Lu^{176}	E	e^-	3.6 hr., 6 da.	Lu-n-γ

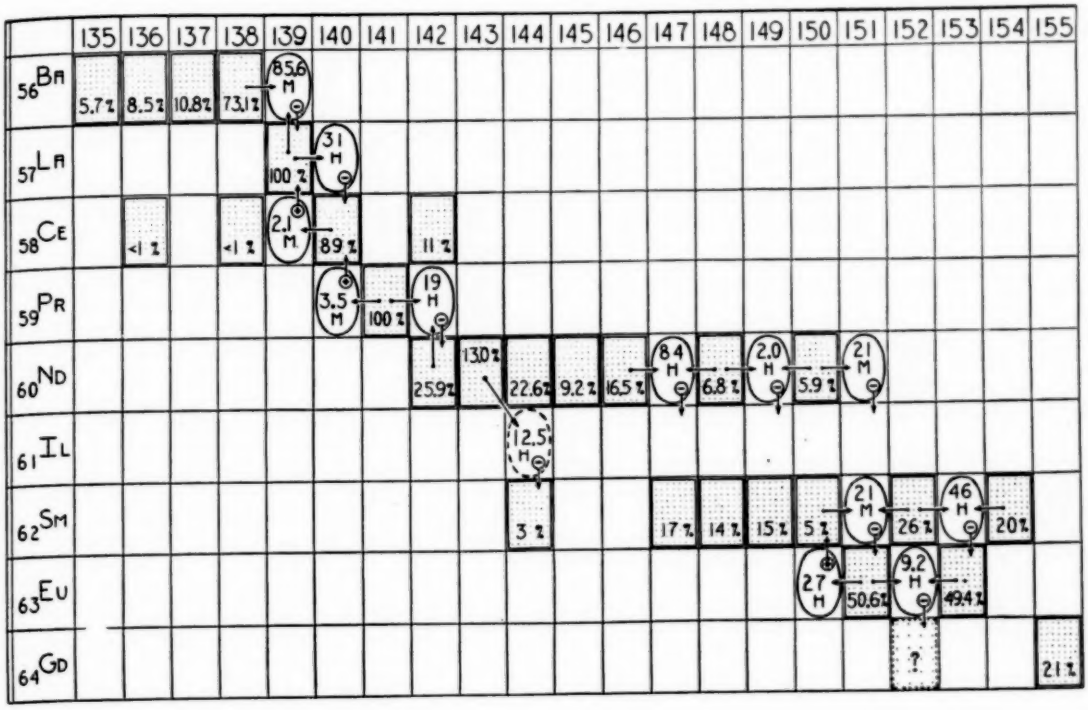

(a)

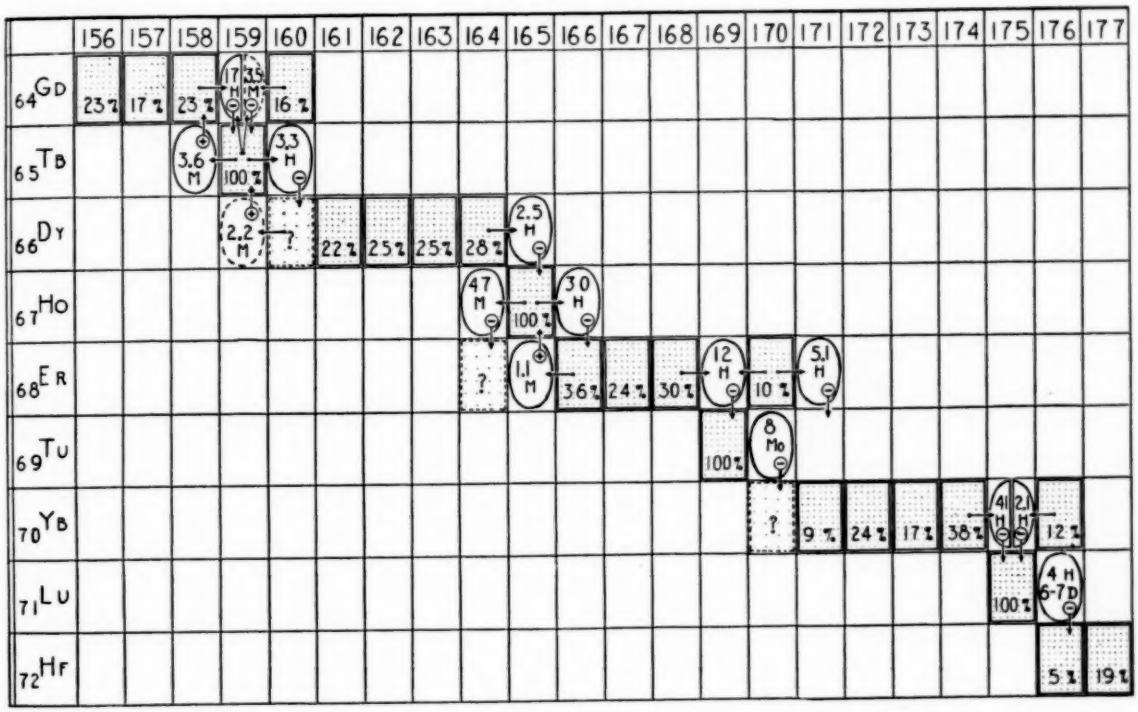

(b)

FIG. 5. Rare earth chart. Stable isotopes are shown by rectangles. Predicted stable isotopes are shown by question mark. Radioactive isotopes are shown by ellipses. Arrows indicate method of production or disintegration. Isomeric nuclei are represented by half-ellipses.

TABLE II. *Rate of formation of radioactive nuclei.*

SUBSTANCE BOMBARDED	TYPE OF BOMBARDMENT	PERIOD T	ASSIGNMENT	TYPE OF REACTION	RELATIVE RATE OF FORMATION
La	fast n	85.6 min. 31 hr.	Ba^{139} La^{140}	n-p n-$2n$	1.0 4.7
Pr	fast n	3.5 min. 19 hr.	Pr^{140} Pr^{142}	n-$2n$ n-γ	3.5 1.0
Nd	slow n	21 min. 2 hr. 84 hr.	Nd^{151} Nd^{149} Nd^{147}	n-γ n-γ n-γ	0.8 1.0 1.7
	fast n	2 hr. 19 hr. 84 hr.	Nd^{149} Pr^{142} Nd^{147}	n-$2n$ n-p n-$2n$	1.0 0.22 1.2
	deuteron	2 hr. 12.5 hr. 84 hr.	Nd^{149} Il^{144} Nd^{147}	d-p d-n d-p	1.0 3.7 1.5
Sm	slow n	21 min. 46 hr.	Sm^{151} Sm^{153}	n-γ n-γ	1.0 7.7
	fast n	21 min. 46 hr.	Sm^{151} Sm^{153}	n-$2n$ n-$2n$	1.0 1.4
Eu	fast n	9.3 hr. 27 hr.	Eu^{154} Eu^{152}	n-$2n$ n-$2n$	6.5 1.0
Gd	slow n	3.5 min. 17 hr.	Gd^{159} Gd^{159}	n-γ n-γ	1.0 3.6
	fast n	3.5 min. 17 hr.	Gd^{159} Gd^{159}	n-$2n$ n-$2n$	1.0 5.7
Tb	fast n	3.6 min. 17 hr.	Tb^{158}, Gd^{159} Gd^{159}	n-p n-p	1.0 2.6
Dy	fast n	2.2 min. 2.5 hr.	Dy^{159} Dy^{165}	n-$2n$ n-γ	1.0 24.0
Ho	fast n	47 min. 30 hr.	Ho^{164} Ho^{166}	n-$2n$ n-γ	1.0 3.0
Er	slow n	5.1 hr. 12 hr.	Er^{171} Er^{169}	n-γ n-γ	0.7 1.0
(Ho)	fast n	1.1 min. 51 min. 12 hr.	Er^{165} Ho^{164} Er^{169}	n-$2n$ n-$2n$ n-$2n$	8.0 .043 1.0
Yb	slow n	2.1 hr. 41 hr.	Yb^{175} Yb^{175}	n-γ n-γ	1.0 1.24
	fast n	2.1 hr. 41 hr.	Yb^{175} Yb^{175}	n-$2n$ n-$2n$	1.0 1.27

Lutecium

Radioactive periods of 3.6 hr.,[9] 4 hr.,[6, 3] and 6 to 7 days[3] have been reported.

No observations on lutecium were made in this study.

SUMMARY AND DISCUSSION

Livingston and Bethe[17] have summarized in Table LXIX of their article the available data on induced radioactivities as of July 1, 1937. Following the same plan of presentation and using the same symbols, we have in Table I summarized the data collected in this research on the rare earth group of elements.

Since the relative rate of formation of radioactive nuclei for a given type of bombardment was useful in assigning some of the radioactive periods, Table II shows the relative rates for all the induced radioactive reactions involving two or more periods.

In the rare group of elements the n-$2n$ type of reaction is very prominent in the production of new radioactive periods. Seventeen such reactions were observed. Fig. 5 shows the rare earth region of the periodic table with the stable isotopes represented by rectangular blocks. The radioactive isotopes are represented by ellipses. A dotted ellipse signifies that the assignment is questionable. The isomeric nuclei are represented by half-ellipses.

That Nd^{151} and Sm^{151} both have a 21-min. period is worthy of note. Provided Il^{151} is unstable, which seems quite likely, it is possible that Nd^{151} has a very short life compared to 21 min. It would thus change to Il^{151} which also, in a very short time, would change to Sm^{151}. This samarium isotope which has the real 21 min. period would change to stable Eu^{151}. This proposed series of transformations from Nd^{151} to Eu^{151} involves a triple beta-ray process.

If a stable illinium isotope exists it will have to be isobaric with either neodymium or samarium. However, no examples of stable neighboring isobars in the rare earths are known; the nearest example is Sb and Te. Should no stable illinium isotopes exist at mass numbers 147 and 149, then Nd^{147} (84 hr.) and Nd^{149} (2.0 hr.) would decay by a double beta-ray process into samarium.

ACKNOWLEDGMENTS

The authors are very grateful to Professor J. M. Cork and Dr. R. L. Thornton for the opportunity of one of us (M.L.P.) to work in their laboratory with the cyclotron at the University of Michigan. To Professor B. S. Hopkins of the University of Illinois we give thanks for the loan of a large quantity of very pure dysprosium. Likewise we thank Dr. H. C. Kremers of Cleveland for the loan of the holmium-rich material. Mr. E. Rosenbaum made some of the chemical separations. Mr. B. R. Curtis kindly helped with some of the cloud chamber pictures. One of us (M.L.P.) is very grateful to have been the recipient of the Elizabeth Clay Howald Scholarship for 1936–37.

[17] Livingston and Bethe, Rev. Mod. Phys. 9, 245 (1937).

Proton Induced Radioactivities

L. A. DuBridge, S. W. Barnes, J. H. Buck and C. V. Strain
University of Rochester, Rochester, New York

(Received January 27, 1938)

Results are tabulated of the radioactivities produced by 4 Mev protons in targets of $_{7}$N, $_{8}$O, $_{20}$Ca, $_{24}$Cr, $_{27}$Co, $_{30}$Zn, $_{34}$Se, $_{42}$Mo, $_{46}$Pd, $_{48}$Cd, $_{49}$In. In most cases the reactions are of the p-n type, and lead to isotopes which emit either + or − electrons. A detailed study was made of O, Zn and Se. The reaction $O^{18}(p,n)F^{18}$ (107 min.) shows a threshold at 2.56 Mev and a positron energy of 0.74 Mev in good agreement with the energy relations. The cross section for the reaction at 4 Mev is about 2×10^{-25} cm² and there is a resonance maximum at 3.55 Mev. The cross section for the reaction $O^{16}(p,\gamma)F^{17}$ is 4000 times smaller. The isomeric Br^{80} periods (17.4 min. and 4.45 hr.) are observed in the reaction $Se^{80}(p,n)Br^{80}$. At 4 Mev the ratio of the short to long period activities for infinite bombardment is about 15 but the thresholds are at about 3.0 and 3.2 Mev, respectively. The cross section for the reaction is about 0.6×10^{-26} cm² at 4 Mev.

I. Introduction

THE present report is an extension and summary of work briefly described in earlier communications[1] on nuclear reactions produced by protons of energies up to 4 Mev. Since previous observations with protons had been confined to energies below about 1 Mev our first experiments were exploratory in nature. These preliminary experiments are summarized herein together with more complete data on certain of the more interesting reactions.

The cyclotron used for this work follows closely, except for size, the design developed at Berkeley.[2] The magnet, of Armco iron, has a pole diameter of 26 inches tapered at 45 degrees to a 20-inch tip, accommodating a 20-inch accelerating chamber. A 26-inch chamber which uses the full pole diameter is now being installed. The diameter of the last ion path in the smaller chamber is 17 inches. The beam emerges through a Pt foil window (0.1 mil) into a target chamber at atmospheric pressure. With an oscillator frequency of 21 megacycles and a resonant magnetic field of about 14,000 gauss the calculated beam energy is 4.2 Mev. After emerging through the Pt window the range of the beam was about 4.8 mils of Al, corresponding to an energy of 3.9 Mev. After allowance is made for the stopping power of the Pt window the beam energy in the chamber is close to the computed value of 4.2 Mev. In some of the later experiments the beam energy was raised, by increasing the frequency, to 4.2 Mev after emergence. The proton currents were usually between 1 and 3 μa. Since the resonance conditions were chosen to accelerate protons (not molecular ions) there is no danger of deuteron or other ion contamination in the beam.

The homogeneity of a cyclotron beam is of some interest. This certainly will depend very greatly on the design of chamber, arrangement of shims and other factors. We have attempted an evaluation for our particular case by measuring the current to a collector (in the target chamber) in front of which Al foils could be inserted. The collector current is plotted against foil thickness (in mils of Al) in Fig. 1. The upper curve is for the magnetic field set at the value to give maximum total beam. For the lower curve the magnetic field was increased a few tenths of a percent above this value. The beam homogeneity is thereby greatly improved and there is an increase in intensity of the long range portion. The dashed curve (S) indicates the theoretical straggling to be expected for an initially homogeneous beam. The observed straggling is about three times greater, which could be accounted for by a 4 percent energy spread (half-width) in the beam. Since, however, observed straggling even for a homogeneous beam usually exceeds the theoretical by a factor of 1.5 to 2 we may conclude that the actual energy spread of the primary proton beam is not more than ±2 percent from the mean, that is, ±80 kv at a mean value of 4 Mev.[2a] Further

[1] S. W. Barnes, L. A. DuBridge, *et al.*, Phys. Rev. **51**, 775 (1937); Phys. Rev. **51**, 995 (1937); Phys. Rev. **51**, 1012 (1937).

[2] E. O. Lawrence and M. S. Livingston, Phys. Rev. **45**, 608 (1934); E. O. Lawrence and D. Cooksey, Phys. Rev. **50**, 1131 (1936).

[2a] Cf. M. C. Henderson and M. G. White, Rev. Sci. Inst. **9**, 19 (1938).

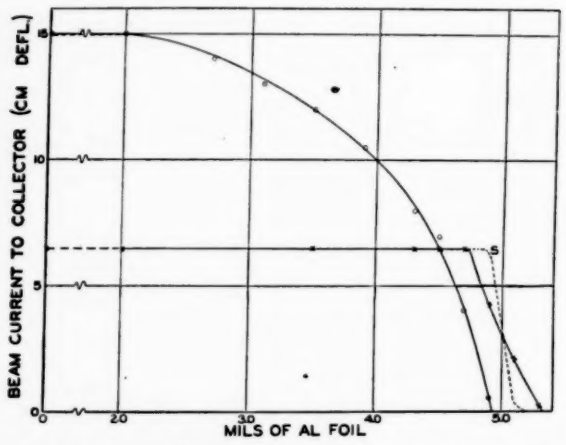

FIG. 1. Curves showing degree of homogeneity of proton beam from cyclotron. Open circle, resonance field; cross, field above resonance; S, theoretical straggling.

evidence for homogeneity will be found in the excitation curve for the O^{18} p-n reaction to be described below which shows a resonance peak whose half-width is about 100 kv.

Most of the activities herein reported were measured with an ionization chamber and amplifier unit of the type described by Hafstad.[3] The chamber was filled with nitrogen at 1 atmosphere. Its sensitivity as compared with a Geiger-Müller counter is such that 100 counts/min. on the counter corresponds to a 1 cm deflection of the amplifier-galvanometer. The sensitivity to β-rays, periodically checked against a constant natural source, is such that a 1 cm steady deflection is produced by the passage through the chamber of about 12 β-rays per sec. The solid angle subtended is such as to collect 1/10 of the β-rays from a given source. For strong samples the sensitivity is quickly changed by the galvanometer shunt. The initial activities of the proton-bombarded samples varied widely from a fraction of a microcurie to about 0.1 millicurie but were generally of the order of 10 microcuries.

II. General Discussion of Proton Reactions

In the energy region below 1 Mev two types of proton reactions are known,[4] namely, p-γ and p-α. (A p-d reaction is observed in the single case Be^9 (p-d) Be^8.) In our earliest work[1] radioactivities were observed in a number of cases where p-γ and p-α reactions would lead only to stable isotopes. These could be explained by assuming a p-n type reaction. This was confirmed by chemical tests, by the identification of certain known periods, and by observation of neutrons produced by the proton beam. A more detailed study of this new type of reaction was then made.

The type reaction is

$$Z^A+H^1\rightarrow(Z+1)^A+n^1.$$

Since neighboring isobaric isotopes are almost unknown in the periodic table the product nucleus $(Z+1)^A$ will almost always be unstable and will either emit positrons or electrons.

Case A. Positron emission

$$(Z+1)^A\rightarrow Z^A+e^+. \quad (1)$$

The mass-energy relation becomes

$$Z^A+H^1+E_p=(Z+1)^A+n^1+E_n$$
$$=Z^A+e^++(e^-)+n^1+E_n+E_+,$$

where E_p = proton energy, E_n = neutron energy, E_+ = maximum positron energy.

The minimum value of E_p will be that for which $E_n=0$. Hence

$$E_{p0}=n^1-H^1+2e+E_+=1.80+E_+ \text{ Mev}. \quad (2)$$

Also

$$E_{p0}=(n^1-H^1)+[(Z+1)^A-Z^A]$$
$$=0.78+\Delta_1 \text{ Mev}, \quad (3)$$

where we have taken $(n^1-H^1)=0.00084$ mu[5] $=0.78\pm0.07$ Mev and Δ_1 stands for the mass difference of the two adjacent isobars (expressed in Mev). If E_+ is known the threshold for the reaction, E_{p0}, is determined and the measurement of either E_+ or E_{p0} determines Δ_1. Since positron energies usually lie between 0.2 and 5 Mev the threshold for this reaction will never be less than about 2 Mev and in most cases not greater than about 7 Mev.

Case B. Electron emission

$$(Z+1)^A\rightarrow(Z+2)^A+e^-. \quad (4)$$

[3] L. R. Hafstad, Phys. Rev. **44**, 201 (1933).
[4] M. S. Livingston and H. A. Bethe, Rev. Mod. Phys. **9**, 245 (1937). Hereafter referred to as LB.
[5] See LB. p. 373.

In this case the mass relations are

$$E_{p0}=(n^1-H^1)+[(Z+1)^A-Z^A] \\ =0.78+\Delta_1 \text{ Mev} \quad (5)$$

and

$$E_{p0}=(n^1-H^1)+E_-+[(Z+2)^A-Z^A] \\ =0.78+E_-+\Delta_2 \text{ Mev}, \quad (6)$$

where Δ_2 is the mass difference between the isobars differing by 2 in atomic number. Evidently $\Delta_1-\Delta_2=E_-$. In this case measurements of E_{p0} and E_- will determine the mass differences of three isobaric isotopes. Since stable isobars differing by 2 in atomic number are commonly both stable the mass difference Δ_2 may be expected to be small. Hence the threshold for the reaction will be of the order of $(0.78+E_-)$ Mev, e.g., from 1 to 4 Mev. For the same β-ray energy the threshold may then be 1 Mev lower than for the positron emitting case.[6] Examples of these relations will be considered below.

Results

Of the large number of activities found in the first exploratory work with high energy protons three elements, O, Se, and Zn, showed such strong activity that they were selected for more detailed study. These will be discussed first, followed by a tabular summary of other reactions.

A. Oxygen

Targets containing oxygen in any form when exposed to the proton beam show two strong activities of 1.23 ± 0.1 min. and 107 ± 4 min. The first checks with the known[7] period of F^{17} which is probably formed by the reaction $O^{16}(p,\gamma)F^{17}$. The second is in agreement with the period for F^{18} formed by Snell[8] in the reaction Ne-*d*-α and by Pool, Cork and Thornton[9] in the reaction F-*n*-2*n*. This period appears only in the fluorine precipitate (CaF_2 from bombarded NaOH). The active F^{18} isotope may be produced by proton bombardment of oxygen by either of two reactions: $O^{17}(p,\gamma)F^{18}$ or $O^{18}(p,n)F^{18}$. The former can hardly contribute more than a small fraction of the total F^{18} activity, as will be shown below. As a further test we have bombarded samples of water, kindly supplied to us by Professor H. C. Urey, in which the O^{18} concentration was about 4.5 times the normal. The 107-min. activity produced in this water was between 3 and 4 times as great as in ordinary water, in rough agreement with the concentration ratio. The difficulty of handling liquid targets and of avoiding activity due to contamination of the cell by air and water vapor have precluded more precise comparisons. Since Dr. Urey states that the O^{17} concentration is only about twice normal in this water the results give strong evidence for attributing the 107-min. activity to the reaction involving O^{18}.

Excitation functions.—The thick target (quartz) excitation functions for the F^{17} and F^{18} periods are shown in Fig. 2, each corrected for the finite bombardment time. It is seen that the F^{17} period (1.23 min.) can be detected at energies as low as 1.6 Mev while the F^{18} activity sets in sharply at about 2.6 Mev and then rises so rapidly that at 4 Mev it is four times stronger than the F^{17}. This indicates that two different types of process must be in operation. The $O^{17}(p,\gamma)F^{18}$ process would be expected to behave in the same way as the $O^{16}(p,\gamma)F^{17}$, the latter being stronger by a factor of 2500, the ratio of abundance. We attribute the main part of the F^{18} activity therefore to the O^{18}-*p*-*n* reaction, and the energy relations to be given presently confirm this hypothesis.

By the method of stacked Al foils, bombarded in O_2, the thin-film excitation curve for the F^{18} activity was obtained as shown in Fig. 3. The lower curve (triangles) was obtained with a homogeneous initial beam of 3.8 Mev and shows a pronounced peak at 3.55 Mev. This curve was repeated many times with different foils and foil arrangements. Later when the initial energy was raised to 4.1 Mev the upper curve (circles) was repeatedly observed. Since the high energy beam was less homogeneous and since the straggling was also greater in the thicker absorbing layers the peak is flattened out as would be expected. This peak is reflected in the thick target curves where it is found also for the O^{16}-*p*-γ reaction. Its

[6] Cf. LB. p. 315.

[7] The data are tabulated by L. N. Ridenour and W. J. Henderson, Phys. Rev. **52**, 889 (1937). We have not yet accounted for our failure to obtain a closer check on the value 1.07 ± 0.1 min. for this period obtained in the careful experiments of these authors. The limits of error however just overlap.

[8] A. H. Snell, Phys. Rev. **51**, 142 (1937).

[9] M. L. Pool, J. M. Cork and R. L. Thornton, Phys. Rev. **52**, 239 (1937).

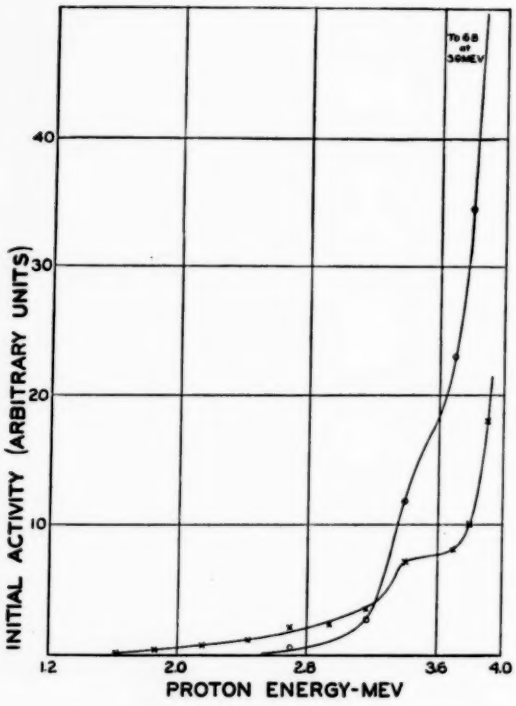

FIG. 2. Thick target excitation curves for the F^{17} and F^{18} periods each corrected for the finite bombardment time. O=F^{18}, ×=F^{17}.

position is considerably above the top of the potential barrier (2.4 Mev according to Bethe's formula[10]). It may simply represent a flattening of the rise in penetration probability or may indicate a resonance level. The rapid rise of the yield above 3.7 Mev suggests further levels above the barrier.

When corrected for bombardment time the activity at the peak of the curve (3.55 Mev) corresponds to the production of about one F^{18} atom per 10^9 protons. The effective range of the F^{18} recoil atoms is calculated (following Newson[11]) to be about 0.075 cm. The cross section for the reaction at 3.55 Mev (taking into account the abundance of O^{18}) is thus roughly 0.75×10^{-25} cm². At 4 Mev it is about three times larger. The average cross section calculated from the solid target data is about 0.6×10^{-25} cm². The latter value is about 4000 times greater than for the $O^{16}(p\text{-}\gamma)F^{17}$ reaction, the cross section for which is 0.15×10^{-28} cm². The F^{17} activity is four times weaker than the F^{18} though the abundance ratio favors the former by a factor of 500 and the effective beam range is twice as great.[12]

Energy relations.—The extrapolated threshold for the production of F^{18} is found to be close to 2.56 ± 0.04 Mev. From Eq. (4) we have then

$$E_+ = 2.56 - 1.80 = 0.76 \pm 0.07 \text{ Mev.}$$

The positron absorption curve in Al is shown in Fig. 4. The end point corresponds to a maximum energy of 0.74 Mev in excellent agreement with the prediction. This agreement incidentally furnishes good evidence for the accuracy of the accepted mass difference $(n^1 - H^1) = 0.78$ Mev.

Applying Eq. (3) we obtain the mass of F^{18}

$$F^{18} = O^{18} + 1.76 \text{ Mev}$$
$$= 18.00557 \pm 0.00025 \text{ mass units,}$$

if the accepted value[5] of 18.00369 for O^{18} is used. The uncertainty in the mass of F^{18} is due mainly to the uncertainty in this value.

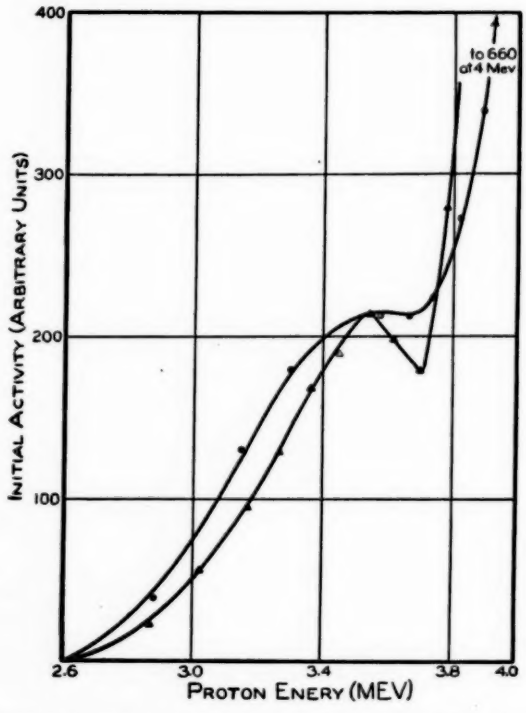

FIG. 3. Curve for thin-film excitation for the F^{18} activity. Lower curve (triangles) for 3.8 Mev protons; upper curve (circles) 4.1 Mev protons.

[10] H. A. Bethe, Rev. Mod. Phys. **9**, 172 (1937).
[11] H. W. Newson, Phys. Rev. **51**, 620 (1937).

[12] In view of this large ratio one might assume the F^{17} to be produced by the reaction $O^{17}(p-n)F^{17}$. But since the positron energy for F^{17} is 2.1 Mev this reaction is energetically excluded for protons below 3.9 Mev, though it actually occurs down to 1.6 Mev.

B. Zinc

Proton bombardment of Zn results in a strong radioactivity which is resolved into three periods: 18.2 min. (electron), 68 min. (positron) and 82 hour (electron). The two short periods appear in the Ga precipitate and are at once identified with the known periods of Ga^{70} and Ga^{68}, respectively. The reactions are then $Zn^{70}(p\text{-}n)Ga^{70}$ (18.2 min.) and $Zn^{68}(p\text{-}n)Ga^{68}$ (68 min.). Ga^{68} might also be formed by the reaction $Zn^{67}(p\text{-}\gamma)Ga^{68}$ but this would appear to be less probable.

The thick target excitation function for the electron-emitting Ga^{70} (18.2 min.) activity shows a threshold at about 1.6 Mev. In contrast, the positron emitting isotope Ga^{68} is not produced at proton energies under about 3.6 Mev. The positron energy as recently measured by Ridenour and Henderson[7] is 1.85 Mev leading to an expected threshold of 3.63 Mev.

The 82-hour period which is always present in activated Zn does not come down with Cu, Zn, Ga or Ge precipitates. It is probably due to an impurity though we find this period in none of the most probable impurity elements so far investigated.

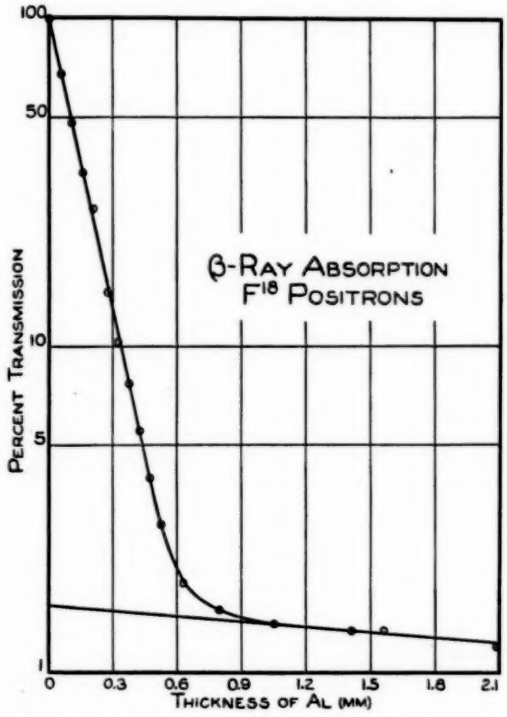

FIG. 4. Positron absorption curve in aluminum.

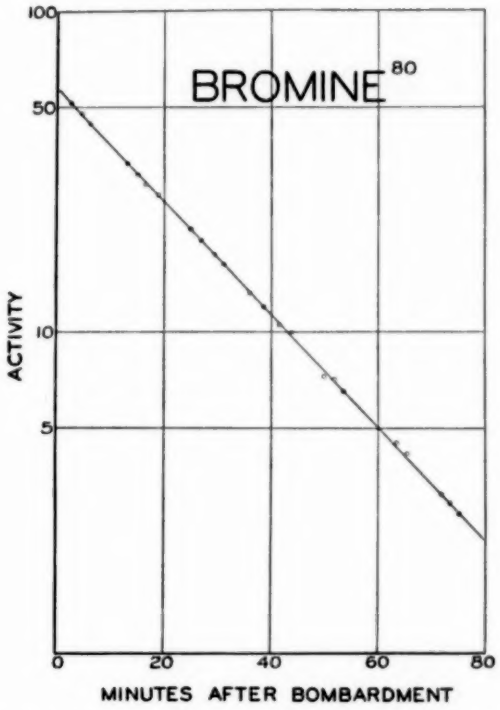

FIG. 5. Decay curve for the activity of Br^{80}. (17.4 min.)

C. Selenium

The strongest radioactivity so far found in proton bombardment appears in Se. A ten-minute bombardment with 2 μa of 4 Mev protons gives an initial activity of the order of 0.1 millicurie. The decay curves show three periods, all electron-emitting: 17.4 ± 0.25 min., 4.45 ± 0.10 hr. and 33.0 ± 1.0 hr. The two short periods are at once identified with the isomeric Br^{80} and the long period with Br^{82}. The values are in good agreement with Snell's[13] except for the 17.4-min. period which he reports as 18.5 ± 0.5. We have taken repeated runs on this period using a 5 sec. bombardment which is sufficient to bring out this short period with no detectable presence of the longer ones. One such decay curve is shown in Fig. 5 and all runs give an average value of 17.4 min. with a computed probable deviation of 0.25 min.

Since the 79 and 81 isotopes of Se are not stable the above periods must be attributed to the reactions $Se^{80}(p\text{-}n)Br^{80}$ and $Se^{82}(p\text{-}n)Br^{82}$. One might expect to observe the 6.4-min. positron activity of Br^{78} formed from the abundant Se^{78}.

[13] A. H. Snell, Phys. Rev. **52**, 1007 (1937).

However, Snell finds the positron energy to be 2.3 Mev giving a predicted threshold of 4.1 Mev which is just over the limit of our beam.

The excitation functions (thick target) of the two Br^{80} periods are shown in Fig. 6. The cross section for the 17.4-min. period is about 0.6 $\times 10^{-26}$ cm^2 for a primary energy of 4 Mev. It is of interest that the thresholds for the two periods of Br^{80} differ by about 0.2 Mev. The inset curve showing the ratio of the two activities give evidence that this threshold difference is real. This "branching ratio" increases with decreasing energy, going to infinity at 3.2 Mev which is taken as the threshold for the 4.5-hr. period. At 4 Mev the branching ratio of short to long period, corrected for bombardment time, is about 15.

From Eq. (6) it is evident that since the initial and final isotopes (Se^{80} and Kr^{80}) are the same for the two periods of Br^{80}, there should exist a difference in β-ray (or γ-ray) energy of

TABLE I. *Summary of proton induced radioactivities.*

TARGET	OBS. PERIODS	EMITTED PARTICLES	ACTIVE ISOTOPE	REACTION	CHEM. SEP.	PREVIOUSLY OBS. PERIODS	PRODUCED BY	REF.
7 N	125 sec.	(+)	O^{15}	N^{14}-p-γ (N^{15}-p-n)		126 sec.	N-d-n O-γ-n O-n-$2n$	LB
8 O	74 sec.	+	F^{17}	O^{16}-p-γ		64–78 sec.	N^{14}-α-n O^{16}-d-n	7
	107 min.	+	F^{18}	O^{18}-p-n	Yes	112 min. 108 min.	Ne^{20}-d-α F^{19}-n-$2n$	8 9
20 Ca	~70 min. ~3.3 hr. >32 hr.	(+) (+) (+)	Sc^{41} $Sc^{42, 43}$ Sc^{44}?	Ca^{40}-p-γ Ca-p-n(?) Ca^{44}-p-n		53 min. 4.0 hr. 52 hr.		16 16 16
24 Cr	42 min.	(+)	Mn^{53}	Cr^{53}-p-n (Cr^{52}-p-γ)		46 min.	Cr^{52}-d-n	LB
27 Co	2.5 hr.		Ni(?)	Co-p-n		2 hr. (Ni^{57}?) 3 hr. (Ni^{59})	Ni^{58}-n-2n(?) Ni^{58}-n-γ	9 LB
30 Zn	18.2 min.	−	Ga^{70}	Zn^{70}-p-n	Yes	20 min.	Ga-n-γ Ga-γ-n	LB
	68 min.	+	Ga^{68}	Zn^{68}-p-n (Zn^{67}-p-γ)	Yes	68 min.	Cu-α-n	7
	82 hr.	−	?	?	Not Cu Zn, Ga			
34 Se	17.4 min.	−	Br^{80}	Se^{80}-p-n	Yes	18.5 min.	Br-d-p	11
	4.45 hr.	−	Br^{80}	Se^{80}-p-n	Yes	4.54 hr.	Br-d-p	11
	32.8 hr.	−	Br^{82}	Se^{82}-p-n	Yes	33.9 hr.	Br-d-p	11
42 Mo	30 sec.		?					
	31 min.		?					
46 Pd	2.41 min.	(−)	Ag^{108}	Pd^{108}-p-n		2.3 min.	Ag-n-γ	LB
	24.4 min.	(+)	Ag^{106}	Pd^{106}-p-n (Pd^{105}-p-γ)		24.5 min.	Ag-n-2n	14
48 Cd	70 sec. 6 min.? 37 min.? 128 min.		In^{112}? In^{117}?	(Cd^{112}-p-n) (Cd^{116}-p-γ)		72 sec. 138 min.	In-n-2n Cd-d-p	15 15
49 In	14 min.		Sn^{113}?	In^{113}-p-n		18 min.?	Sn-n-γ Sn-d-p	LB

[14] M. L. Pool, Phys. Rev. **52**, 380 (1937).
[15] J. M. Cork and R. L. Thornton, Phys. Rev. **51**, 608 (1937); **52**, 531 (1937).
[16] H. Walke, Phys. Rev. **51**, 439 (1937).

0.2 Mev. Such a difference has been found by Snell,[13] who gives 2.0 and 2.2 Mev for the β-ray energies for the long and short periods, respectively. However, *this is in the wrong direction* to account for the threshold difference, since it would predict a higher threshold for the short period. The situation is further complicated by Snell's observation that γ-rays accompany the 2.2 Mev electrons of the short period but there are no detectable long period γ-rays. These results are incompatible with the lower threshold for the short life activity unless an unusual isomerism in the excited states of the intermediate nucleus Br^{81} is assumed. Discussion of this possibility is best postponed until the experimental data are made more precise.

From Eqs. (5) and (6) one finds for the mass differences

$$Br^{80}-Se^{80}=2.2\pm0.2 \text{ Mev}$$

and $$Kr^{80}-Se^{80}=0.0\pm0.2 \text{ Mev}.$$

D. Other reactions

All the radioactive periods so far found with proton bombardment are listed in Table I. Periods obviously due to impurities have been eliminated but in many cases the activity is so weak that chemical tests have not been made and the reactions in some cases are doubtful (indicated by (?)). In other cases identification is possible by comparison with known periods. The results listed in the table supersede the preliminary values sent to Livingston and Bethe for inclusion in their article.[17] The weak 90–110-min. activity found in Mn and attributed in our first reports[1] to Fe^{55} has been traced to oxygen impurity (F^{18}), and we can now find no activity assignable to Fe^{55}. The 109-min. period in As listed in the table might also be due to F^{18} but the β-ray spectrum for the activated As seems to differ appreciably from the F^{18} spectrum and we assign this period tentatively to Se^{75}. The other listings are self-explanatory. Further work is now in progress.

Acknowledgments

The construction of the cyclotron and related equipment and its continued operation have been made possible by the generous cooperation of many individuals and corporations, to all of whom grateful acknowledgment is made. We wish particularly to express our indebtedness to the Rochester Gas and Electric Company, the Rochester Telephone Company, the Stromberg-Carlson Telephone Manufacturing Company, the Consolidated Machine Tool Corporation, the General Electric Company, the Bell Telephone Laboratories, the American Rolling Mill Company, and the Eastman Kodak Company for supplying equipment, materials, and services at reduced or no cost; to the Research Corporation for financial support; to Dr. A. G. Hill, Mr. George Valley, Mr. Tom Perry and Mr. Arthur Gibson, mechanician, for assistance in construction and operation. We are indebted to Drs. E. O. Lawrence, M. S. Livingston and Donald Cooksey for much valuable advice and assistance in planning and building the cyclotron.

Finally we wish to acknowledge the valuable assistance generously given by Professor E. O. Wiig of the chemistry department in planning and carrying out all chemical analyses.

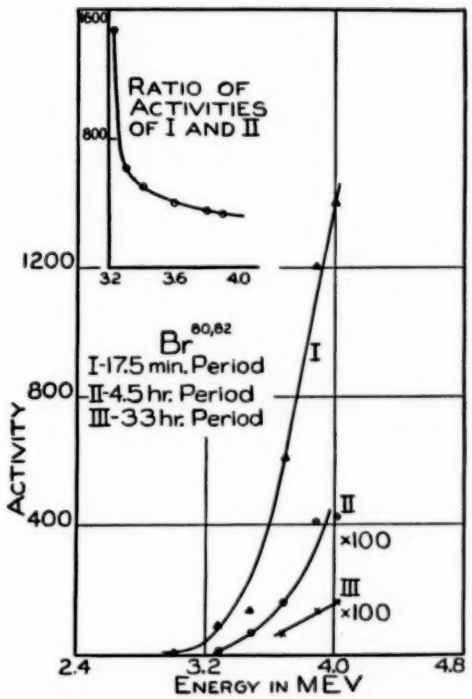

FIG. 6. Excitation functions of the two decay periods of Br^{80}.

[17] LB. p. 317.

Cloud Chamber Evidence Against the Existence of Heavy Beta-Particles

ARTHUR RUARK AND CREIGHTON C. JONES
Department of Physics, University of North Carolina, Chapel Hill, North Carolina

(Received January 20, 1938)

By studying collisions of Ra E beta-particles with electrons, photographed in the cloud chamber by Champion, it is shown that Jauncey's hypothesis of heavy beta-particles definitely disagrees with experiment.

RECENTLY the suggestion has often been made that beta-rays are not identical with electrons. Jauncey[1] has put forward a definite, and at first sight attractive hypothesis, to the effect that there is no neutrino; that the change in internal energy of a nucleus emitting beta-rays is always the same; and that the rest mass of every beta-particle is such that it carries away the same total energy. He reported to an informal discussion group at the December, 1937 meeting of the American Physical Society that he repeated the Bucherer experiment with Ra E beta-particles, obtaining results which appeared to support his hypothesis. Previously, Zahn and Spees[2] considered the possibility that for momenta below the upper limit of the beta-ray spectrum "some of the total energy is 'concealed' in a form other than kinetic," and described the results of a much improved modification of the Bucherer experiment. Their observations on Ra E showed a peak corresponding to the mass of the Lorentz electron within ten percent, on the side corresponding to greater mass. There were also small side peaks which will probably be explained as a consequence of the finite resolving power of the apparatus. The present writers accept the conclusion of Zahn and Spees, that their result definitely disproves the existence of the type of heavy electron described above.

Since, on the other hand, their principal result is not in perfect agreement with that to be expected on the basis of electrons of ordinary mass, the possibility still remains that beta-particles differ from ordinary electrons in some less drastic way, and it is of great interest to consider other available evidence from this point of view. On the occasion of the informal discussion mentioned above, one of us suggested reexamination of the cloud chamber experiments of Champion[3] on the conservation of momentum and energy in collisions of Ra E beta-particles with electrons. Champion obtained 30,000 beta-ray tracks and made a detailed study of 15 forked tracks of excellent quality. He discussed them by means of the usual relativistic relations. He believed that his velocity measurements were good to two percent, and his angular measurements to the order of one degree. His conclusion was that the conservation laws are verified, within the limits of his experimental errors, in 14 out of 15 cases. The other collision was definitely non-coplanar, and probably was a radiative collision. Even in this case, the deviation from the conservation laws was slight, so that the emitted quantum must have had small energy. We omit this collision from further consideration.

Suppose the quantities measured are the momenta of the particles and the angles between their paths. If the conservation laws are satisfied when the particles concerned are treated as ordinary electrons, then obviously the momentum relations are still satisfied on the assumption that one of the particles has a rest mass different from that of an electron; but by direct examination of the conservation equations we can see that the conservation of energy is violated by this assumption. We shall not give the simple algebraic proof, because it serves our purpose better to reexamine Champion's data numerically, showing that they definitely disagree with a prediction based on the type of heavy electron discussed by Jauncey.

Consider a collision in which a particle of rest mass Rm_0 collides with an electron of rest mass m_0. For a particle of velocity v, we write $\beta=v/c$,

[1] Jauncey, Phys. Rev. **52**, 1256 (1937); **53**, 106 (1938).
[2] Zahn and Spees, Phys. Rev. **52**, 524 (1937).
[3] Champion, Proc. Roy. Soc. **136**, 630 (1932).

and $\gamma=(1-\beta^2)^{-\frac{1}{2}}$. The relation

$$\beta\gamma=(\gamma^2-1)^{\frac{1}{2}} \tag{1}$$

will be used frequently. The β's and γ's existing before and after the collision are unprimed and primed, respectively, and the subscripts 1 and 2 are attached to quantities describing the incident particle and the electron, respectively.

Champion gives in his paper the fork-angle Ψ, shown in Fig. 1, one of the θ's, and the value of β for the incident particle, derived by measuring $H\rho$.[4] Since β was calculated on the assumption that the incident particle is an ordinary electron, we can recalculate $H\rho$ from it. Of course, when the collision partners are interpreted as ordinary electrons, the experimental values of the angles and of $H\rho$ do not *exactly* fulfill the requirements of the conservation laws; but if we assume that the incident particle is not an ordinary electron, and that the conservation laws *are* exactly satisfied, we can determine the value of R for each collision. The corresponding γ_1 can then be computed. $R\gamma_1$ is the energy of the incident particle in terms of the unit m_0c^2, and we can compare the computed value of $R\gamma_1$ with a value obtained from the heavy electron hypothesis.

Before doing this, we give a simple argument which indicates the order of magnitude of $R\gamma_1$ and makes it probable that the heavy electron hypothesis is incorrect. Let β_e denote the value of v/c for the incoming particle, as given by Champion on the assumption that it is an electron. Then $H\rho e=m_0c\beta_e\gamma_e$. If, however, we interpret this particle as a heavy electron, we have $H\rho e=Rm_0c\beta_1\gamma_1$ so that

$$R\beta_1\gamma_1=\beta_e\gamma_e. \tag{2}$$

Since Champion's collisions nearly satisfy the conservation laws on the assumption of ordinary electrons, it is certain that R will usually be close to unity, and β_1 close to β_e, so we have

$$R\gamma_1\sim\gamma_e. \tag{3}$$

On the heavy electron hypothesis, the beta-raying nucleus always loses the same internal

[4] The $H\rho$'s are not available for the arms of the fork, a circumstance which complicates the comparison with theory. Champion states that in a few cases they could be measured with the accuracy necessary to give useful information; in these cases the results agreed, within the experimental errors, with values calculated from β_1, θ_1, and Ψ.

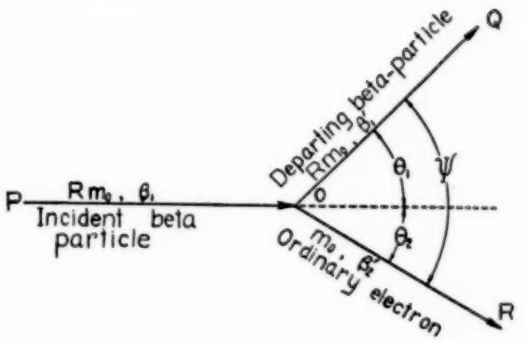

FIG. 1.

energy Q, and if one neglects the very small recoil energy,

$$Q=Rm_0c^2\gamma_1. \tag{4}$$

Let γ_m be the maximum value of γ_1, belonging to a beta-particle at the upper end of the velocity spectrum, for which $Q=m_0c^2\gamma_m$. Then

$$R\gamma_1=\gamma_m, \tag{5}$$

which is to be compared with (3). For radium E, $\gamma_m=3.44\pm0.06$,[5] while Champion's γ_e's are generally less than 2, and run from 1.75 to 2.72.

This is a large discrepancy, and further work might appear unnecessary. Nevertheless, since (3) is only an approximation, we have preferred to compute $R\gamma_1$ on the assumption that the conservation laws are exactly satisfied. The necessary relations are as follows:

Taking momentum components perpendicular to the line OQ in Fig. 1 we have

$$R\beta_1\gamma_1\sin\theta_1=\beta_2'\gamma_2'\sin\Psi \tag{6}$$

and Braunbek[6] has shown that

$$\gamma_2'=\frac{(R\gamma_1+1)^2+(R^2\gamma_1^2-1)\cos^2\theta_2}{(R\gamma_1+1)^2-(R^2\gamma_1^2-1)\cos^2\theta_2}. \tag{7}$$

In Eqs. (2), (6) and (7), the unknowns are R, γ_1, and γ_2'. Solving, we obtain

$$\gamma_2'^2=1+(\beta_e^2\gamma_e^2\sin^2\theta_1/\sin^2\Psi);$$

$$R^2=\left[\left(\frac{\gamma_2'+1}{\gamma_2'-1}\right)^{\frac{1}{2}}\beta_e\gamma_e\cos\theta_2-1\right]^2-\beta_e^2\gamma_e^2; \tag{8}$$

$$\gamma_1^2=1+(\gamma_e^2-1)/R^2.$$

[5] O'Conor, Phys. Rev. **52**, 303 (1937).
[6] Braunbek, Zeits. f. Physik **96**, 600 (1935).

In working out R and γ_1, it must be remembered that we do not know which of the final particles is to be taken as the "heavy" one. Therefore we have carried out the computations for both of the possible cases. First, the final particle whose track makes the smaller angle with the track of the incident one is assumed to have mass Rm_0; then the reverse assumption is made. The results from 14 collisions are as follows:

	Case 1	Case 2
Range of $R\gamma_1$:	1.65 to 2.74	1.73 to 2.74.

Value of $R\gamma_1$ required by Jauncey's hypothesis: 3.44 ± 0.06.

Indeed, the values of $R\gamma_1$ for ten of the collisions lie below 55 percent of γ_m. These results establish the validity of (3) and constitute conclusive evidence against Jauncey's proposal. This conclusion has no bearing on the possibility that the heavy particles reported in cosmic-ray experiments are electrons of exceptional rest mass; it deals only with nuclear beta-rays of Ra E.

In conclusion, it is of some interest to reconsider the extent to which Champion's data support the conservation laws, when the collision partners are treated as ordinary electrons. Study of the computed R values, which should be unity if there were no experimental errors, is not useful, for R is sensitive to experimental errors. (The values of R range from 0.62 to 1.07, and from 0.93 to 1.06, in the two cases mentioned above, the corresponding mean values being 0.923 and 0.994.) Using the customary relativistic mass formula, Champion computed values of Ψ from the observed values of θ_1 and of $H\rho$ for the incident particle, and compared these Ψ-values with the observed ones. The angle Ψ is rather insensitive to experimental errors, so it seems more instructive to proceed as follows. In the absence of $H\rho$ values for the tracks of the departing particles, we obtain the energy of the incident particle in units m_0c^2 from its $H\rho$ and call it $\gamma_1(H\rho)$. Another value of this energy, $\gamma_1(\theta)$, is obtained from the angles θ_1 and θ_2 alone by using the relation

$$2\cot\theta_1\cot\theta_2=\gamma_1+1. \tag{9}$$

Let $\Delta\gamma_1=\gamma_1(\theta)-\gamma_1(H\rho)$, and let us form the fractional error $\Delta\gamma_1/\gamma_1$, where in the denominator we employ the average of $\gamma_1(\theta)$ and $\gamma_1(H\rho)$. This quantity ranges from -0.106 to $+0.040$, and individual values tell us little, but the mean value of $\Delta\gamma_1/\gamma_1$ is -0.0207 ± 0.007. This is an easily understood index of the extent to which the conservation relations are satisfied by Champion's data, when the Lorentz formulas are employed.[7]

Note added in proof: Dr. Champion used his collision 11 in an attempt to discriminate between the Lorentz formula and the Abraham formula. From the data at his disposal he could calculate Ψ on the basis of both theories. It appeared that the value calculated from the Abraham formula was in definite disagreement with the observed angle. We could not check his result and in private communication he states that there was an error in the arithmetic. He requests that we give his revised results. On the Lorentz theory $\Psi=75.2°$ and on the Abraham theory 76°, while the experimental value is $75.2\pm0.5°$. The limits of error are such that this collision does not discriminate between the two theories.

[7] Unfortunately certain compensations which occur in applying the Lorentz and Abraham formulas to Champion's data prevent us from using the data to discriminate between the two theories. This difficulty would not exist if one had $H\rho$ measurements for all three branches of a forked track.

The Theory of the Continuous X-Ray Spectrum Near the Duane-Hunt Limit

EUGENE BRUNNER
California Institute of Technology, Pasadena, California

(Received January 24, 1938)

The effect on the distribution of energy in the continuous x-ray spectrum in the immediate vicinity of the Duane-Hunt limit of the extranuclear electrons in the atoms composing the target of the x-ray tube is considered. Resonance effects are found to occur which are capable of explaining the knee recently discovered by DuMond and Bollman in the isochromat very close to the threshold.

THE distribution of energy in the continuous x-ray spectrum in the immediate vicinity of the Duane-Hunt limit is of particular interest at the present time because of the discrepancy between the value of h/e found by recent measurements of the threshold voltage for x-ray isochromats,[1] the values of e and e/m, and the theoretical formula for the Rydberg constant;[2] and because of the knee recently discovered by DuMond and Bollman[1] in the isochromat very close to the threshold.

The effect of the extranuclear electrons in the atoms composing the target cannot be neglected in the theoretical treatment of this problem, because an electron which has been scattered with the radiation of a photon near the Duane-Hunt limit has very little energy; and its motion, and hence the probability of the transition producing it, is therefore greatly influenced by the field at a considerable distance from the nucleus of the scattering atom. For the production of high frequency x-rays near the Duane-Hunt limit only transitions leaving the electron in an S state are important; for high frequency x-rays must be produced in the region of large field near the nucleus, and the presence of the low energy scattered electron in the region inside the effective screening radius provided by the atomic electrons is inconsistent with its having an angular momentum different from zero. The problem may be reduced to a one-body problem by treating the incident electron as moving in the average field of the atom. The quantum theory of radiation then shows that the intensity per unit frequency range of the x-rays of frequency ν produced by the incidence on the atom of a beam of cathode rays of energy E_0 is proportional to

$$|A(E)|^2 \cdot \left| \int_0^\infty r^2 dr \psi_E^*(r) \cdot \frac{dV}{dr} \cdot \psi_{E_0}(r) \right|^2. \quad (1)$$

Here $V(r)$ is the average potential at the distance r from the nucleus, $\psi_E(r)$ is the radial wave function for an S electron of energy E in the field of the atom, $\psi_{E_0}(r)$ is the radial wave function for a P electron of energy E_0, and A is a normalizing constant such that the wave functions $A(E)\psi_E(r)$ are normalized on the energy scale. E is of course determined by the relation $E_0 - E = h\nu$.

Most of the value of the integral in (1) is contributed by small values of r. If, therefore, the wave function $\psi_E(r)$ be so normalized that its amplitude for small r is essentially independent of E—if, for example, it be required that the coefficient of the lowest power of r in the expansion of ψ_E as a power series be unity—the integral in (1) will be a slowly varying function of E; in particular, its behavior as a function of E will show no peculiarities for the value zero of E. But (1) as a whole must change rapidly from large values for $E>0$ to zero for $E<0$. Hence $A(E)$ must change rapidly with E for E near zero, and for sufficiently small values of E, (1) may be regarded as approximately proportional to $|A(E)|^2$.

$|A(E)|^2$ has been calculated using two different functions to represent the average potential V: namely,

$$V_1 = \begin{cases} -Ze^2(1/r - 1/a) & \text{for } r<a \\ 0 & \text{for } r>a \end{cases}$$

and

$$V_2 = -\frac{Ze^2}{a}\frac{e^{-r/a}}{1-e^{-r/a}}.$$

[1] J. W. M. DuMond and V. Bollman, Phys. Rev. **51**, 400 (1937); P. Kirkpatrick and P. A. Ross, Phys. Rev. **45**, 454 (1934); G. Schaitberger, Ann. d. Physik **24**, 84 (1935).
[2] J. W. M. DuMond, Phys. Rev. **52**, 1251 (1937); R. T. Birge, Phys. Rev. **52**, 241 (1937).

V_1 was treated with Langer's modification of the Wentzel-Kramers-Brillouin method.[3] If the potential be temporarily supposed to be given for all values of r by the analytic expression given above for V_1 for $r<a$, it will be found that for small values of E the kinetic energy of the electron will vanish for some value of r slightly greater than a. An approximate solution of Langer's type of the radial wave equation valid at the point at which the kinetic energy vanishes was matched in amplitude and phase at $r=a$ to a solution of the radial wave equation for a free electron and at a smaller value of r to the function given by Langer as an approximation to the radial wave function for an electron in a Coulomb field. In this way the amplitude for large values of r of the properly normalized wave function $\psi_E(r)$ was obtained, from which $|A(E)|^2$ was calculated. The potential V_2, which represents an approximately Coulomb field for small values of r, leads to a radial wave equation which is solvable in terms of the hypergeometric function.[4] A comparison of the asymptotic form of the wave function with the first term of its expansion as a power series in r leads immediately to the value of $|A(E)|^2$.

Both V_1 and V_2 lead to values of $|A(E)|^2$ which are nearly independent of E for large E. As E decreases, $|A(E)|^2$ may decrease more or less uniformly until it reaches the value zero for $E=0$; or, depending on the value of Za, it may rise to a maximum at a small value of E and then fall rapidly to zero. For certain values of Za, $|A(E)|^2$ may become infinite like $1/E^{\frac{1}{2}}$ as E approaches zero. This behavior is to be understood physically as an effect of resonance between the scattered electron and the virtual S levels of the atomic field somewhat analogous to the resonance effects observed in the scattering of slow electrons.[5] The result obtained from the potential V_2 is

$$|A(E)|^2=\frac{\sinh 2\pi k\alpha}{\cosh 2\pi k\alpha-\cos 2\pi(2Z\alpha-k^2\alpha^2)^{\frac{1}{2}}}, \quad (2)$$

where $k^2=2\hbar^2E/me^4$ and $\alpha=me^2a/\hbar^2$. m, e, and $\hbar$ have their usual significance.

It is, of course, necessary to choose different values of the parameters Z and a for the two potentials V_1 and V_2 in order to get rough agreement between the values of $|A(E)|^2$ which they respectively yield. V_2 was compared with the potential given by the Fermi-Thomas statistical model for the tungsten atom. With 74, the atomic number of tungsten, for Z it was found that values of α from about 0.09 to 0.18 give reasonable agreement between V_2 and the Fermi-Thomas potential. For V_1, values of about 36 for Z and 2 for α were thought to be suitable. With such values of the parameters, the maximum of $|A(E)|^2$ occurs, when it occurs at all, for values of E from about 5 to 25 electron volts, and $|A(E)|^2$ becomes sensibly constant for E larger than one or two hundred electron volts.

Thick target spectra were computed from (2) by the Thomas-Whiddington law for the loss of energy of the cathode rays as they penetrate the target and assuming the intensity of the x-rays to be inversely proportional to the energy of the incident electrons. From the transmission curve given by DuMond and Bollman[1] for the spectrometer used in their measurements, the total energy transmitted was calculated as a function of the setting of the spectrometer and the potential on the x-ray tube. The derivative of the transmitted energy with respect to the potential on the x-ray tube was plotted against this potential and the resulting curve compared with the corresponding experimental curve published by DuMond and Bollman. It was possible to get quite satisfactory agreement between the theoretical and experimental curves with values of Z and α which do not seem unreasonable for the tungsten atom. In particular, the sharp maximum by which the knee in the isochromat the nearer to the threshold manifests itself on this derived curve is well represented on the theoretical curve. In order to obtain the best possible agreement between the theoretical and experimental curves it was necessary to assume that the true threshold occurs at a potential of about 10 volts (0.05 percent) lower than the value chosen by DuMond and Bollman as the most probable. This shift in the position of the threshold is insignificant in amount; more-

[3] R. E. Langer, Phys. Rev. **51**, 669 (1937).
[4] M. F. Manning, Phys. Rev. **48**, 161 (1935).
[5] L. Nedelsky, Phys. Rev. **42**, 641 (1932), has shown that similar resonance effects are to be expected in the x-radiation from slow electrons.

over, it is in such a direction as to increase rather than to decrease, the discrepancy between the value of h/e obtained from this experiment and the other fundamental constants.

In conclusion it should be emphasized that the present theory can explain only the newly discovered knee in the isochromat in the immediate vicinity of the threshold—the well-known knee that appears at a hundred volts or so from the threshold must find another explanation; and that the theory is not sufficiently accurate to enable one to predict the presence or absence of this knee in the isochromat obtained from an x-ray tube with a target of a given material.

The author wishes to express his sincere appreciation to Professor W. V. Houston and Professor J. R. Oppenheimer for suggesting this work and for their helpful interest in its progress.

MARCH 15, 1938 PHYSICAL REVIEW VOLUME 53

The Fine Structure of the Nuclear Ground Level of Li^7

G. BREIT, *University of Wisconsin, Madison, Wisconsin*

AND

J. R. STEHN, *Harvard University, Cambridge, Massachusetts*

(Received January 27, 1938)

Calculations of the fine structure of the ground level of the Li^7 nucleus are made with the object of throwing light on the *form* of the interaction energy between pairs of nuclear particles. The requirements of relativistic covariance do not determine the spin-orbit interactions uniquely. Adjustable parameters, which are essentially coefficients of invariant additions to the Hamiltonian, are not fixed by considerations of covariance. The calculations reported show how, with approximate assumptions about the wave function, these parameters should be chosen in order to obtain agreement with the observed fine structure. A general rule simplifying the calculation of the spin-orbit interaction with a closed shell is developed for interactions between pairs of particles. The results are sensitive to the wave function used. The assumption of approximate symmetry of the nuclear Hamiltonian leads to an approximately symmetric coordinate function which is a linear combination of ^1S and ^1D states of the two neutrons in the p shell. For this function relatively large values of the adjustable parameters (~ 3) are needed. If, however, the ^1S state is supposed to be the predominant one, values of the parameters ~ 1 suffice. Present evidence favors the symmetric function and, therefore, the larger values of the parameters. These values do not correspond, even approximately, to the picture of a nuclear particle moving in a scalar field. An additional interaction having the transformation properties of an electromagnetic field is needed to obtain them. The sensitivity of the fine structure to perturbations suggests caution regarding the quantitative side of the calculations. Only qualitative significance can be attached to them.

INTRODUCTION

ACCORDING to Rumbaugh and Hafstad[1] there is an excited state of Li^7 about 400 kv above the normal level. Schuler,[2] Granath,[3] and Rabi[4] find the spin of this nucleus to be $\frac{3}{2}$. The normal state of Li^7 is expected to be ^2P according to the calculations of Feenberg and Wigner.[5] It is, therefore, logical to interpret the level found by Rumbaugh and Hafstad as the $^2P_{1/2}$ part of the ^2P state and the normal level of Li^7 as the $^2P_{3/2}$ condition of the same state. On this hypothesis an estimate was given by Inglis[6] for the magnitude of the expected energy difference between the two levels of the ^2P state, and it was pointed out by him that the spin-orbit coupling arising from the Thomas precession can be expected to be of special importance for nuclei. A similar estimate has been made by Rose and Bethe.[7] In both of these considerations

[1] L. H. Rumbaugh and L. R. Hafstad, Phys. Rev. **50**, 681 (1936).
[2] H. Schuler, Zeits. f. Physik **42**, 487 (1927).
[3] L. P. Granath, Phys. Rev. **42**, 44 (1932).
[4] M. Fox and I. I. Rabi, Phys. Rev. **48**, 746 (1935).
[5] E. Feenberg and E. Wigner, Phys. Rev. **51**, 95 (1937).
[6] D. R. Inglis, Phys. Rev. **50**, 783 (1936).
[7] M. E. Rose and H. A. Bethe, Phys. Rev. **51**, 205 (1936).

the valence particles in the p shell are pictured as moving in an attractive central field which has the transformation properties of a four-dimensional scalar. It is perhaps possible that in nuclei the elementary particles merge together in such a way as to lose their identity and to provide a scalar field of this character. Such a point of view would, however, be rather difficult to apply in a quantitative manner, at the present time, because of its extreme vagueness. Nuclear theories at present are developed using interactions between pairs of particles. Although they are not as yet completely quantitative, the success which they have met makes it unnecessary at present to abandon the simple point of view of interactions between pairs of particles. The possibility of a fundamental change in the description involving a merging of elementary particles is open, of course, but will not be investigated in the present note.

For forces between pairs of elementary particles one cannot make direct use of the Thomas precession or the scalar equation discussed in this connection by Furry.[8] A consideration of possible forms of wave equations for particles with spin determines[9] the interaction energies that may be used in these equations as

$$H^{\mathrm{W}}=\sum \mathbf{B}_{kl}[a^{\mathrm{W}}\boldsymbol{\sigma}_k+(a^{\mathrm{W}}-1)\boldsymbol{\sigma}_l]-\sum{}' J_{kl}, \tag{1}$$

$$\mathbf{B}_{kl}=-(\hbar/4M^2c^2)[\mathbf{p}_k\times\boldsymbol{\nabla}_k J_{kl}], \tag{1'}$$

$$H^{\mathrm{H}}=\sum \mathbf{B}_{kl}[a^{\mathrm{H}}\boldsymbol{\sigma}_k+(a^{\mathrm{H}}-1)\boldsymbol{\sigma}_l]P_{kl}{}^{\mathrm{H}} -\sum{}' J_{kl}P_{kl}{}^{\mathrm{H}}, \tag{2}$$

$$H^{\mathrm{M}}=\sum \mathbf{A}_{kl}[a^{\mathrm{M}}\boldsymbol{\sigma}_k+(a^{\mathrm{M}}-1)\boldsymbol{\sigma}_l]-\sum{}' J_{kl}P_{kl}{}^{\mathrm{M}}, \tag{3}$$

$$\mathbf{A}_{kl}=(i/4M^2c^2)[\mathbf{p}_k\times J_{kl}P_{kl}{}^{\mathrm{M}}\mathbf{p}_k]. \tag{3'}$$

The letters W, H, M, here, refer to Wigner, Heisenberg, and Majorana forces. The particles in the nucleus are referred to by subscripts k, l; the potential energy between two particles is $-J(r_{kl})$ for an ordinary force, $-J(r_{kl})P_{kl}$ for an exchange force, with r_{kl} standing for the distance between particles k and l; the momentum operators $\mathbf{p}_k=(\hbar/i)\boldsymbol{\nabla}_k$. $\sum'$ refers to sums over pairs of particles $(k>l)$; $\sum$ indicates sums over all values of k and l except $k=l$ (in other words, $k\gtrless l$). The interaction energies as written above do not include all the terms necessary[10] for invariance to order v^2/c^2. The parts omitted do not give rise to spin-orbit interactions and are of no interest for the present paper. The constants a^{W}, a^{H}, a^{M} are arbitrary and from considerations of invariance it is impossible to determine their value. For particles interacting through the electromagnetic field the value of a^{W} is -1. The picture of each particle producing a scalar field defined in the reference system moving instantaneously with it corresponds on the other hand to $a^{\mathrm{W}}=1$. By comparing calculation with experience one may hope to determine the constants a^{W}, a^{H}, a^{M} and to learn in this way a restricting condition for the interaction energy of the electron-neutrino field. Thus if it were found that $a^{\mathrm{W}}=-1$ the inference would be that the electron-neutrino field interacts with the heavy particles in a manner similar to the field of photons interacting with a charge.

A preliminary calculation of the energy splitting of the ground state of Li^7 has already been made[9] from Eq. (3) with $a^{\mathrm{M}}=1$. This calculation is incomplete because the two neutrons in the p shell were supposed to be coupled into a ^1S state, and because the influence of H^{W}, H^{H} as well as values of $a^{\mathrm{M}}\neq 1$ were not taken into account. In the present note the calculation will be made directly for a state having complete symmetry in the space coordinate wave function for the three particles in the p shell. On account of the approximate symmetry of the nuclear Hamiltonian, which appears probable in view of the scattering experiments of protons and neutrons in hydrogen,[11] this is expected[12] to be approximately the condition of the two neutrons and the one proton outside the alpha-particle shell in Li^7. On account of the Heisenberg force the symmetry of the space wave function is somewhat spoiled; this effect will be estimated as well.

[8] W. H. Furry, Phys. Rev. **50**, 784 (1936).
[9] G. Breit, Phys. Rev. **51**, 248 (1936).
[10] G. Breit, Phys. Rev. **53**, 153 (1938).
[11] M. A. Tuve, N. P. Heydenburg and L. R. Hafstad, Phys. Rev. **50**, 806 (1936); G. Breit, E. U. Condon and R. D. Present, Phys. Rev. **50**, 825 (1936); C. Cassen and E. U. Condon, Phys. Rev. **50**, 846 (1936); G. Breit and E. Feenberg, Phys. Rev. **50**, 850 (1936).
[12] E. Wigner, Phys. Rev. **51**, 947 (1937); E. Feenberg and M. Phillips, Phys. Rev. **51**, 597 (1937); F. Hund, Zeits. f. Physik **105**, 202 (1937).

General Relations

The interaction energies considered in Eqs. (1), (2), (3) consist of sums referring to pairs of particles. The evaluation of their expectation values is slightly more complicated than that of the expectation values of sums of single particle energies, such as are commonly used in approximate theories of spin-orbit interactions in atomic spectra. Nevertheless in these two cases there is a considerable similarity between the behaviors of that part of the energy which arises through interactions of the valence particles with a closed shell. The way in which this energy depends on the number of particles in the valence shell and on their coupling is the same for all kinds of interactions of the symmetric orbit-vector, spin-vector type and it is, furthermore, the same as for an interaction of the type $\sum \mathbf{A}(i)\boldsymbol{\sigma}_i$. This is a consequence of the spherical symmetry of a closed shell. Thus consider a closed shell with wave functions $u_1, u_2, \cdots, u_n$ and a set of three valence particles. Let u_a be the wave function corresponding to definite values of the orbital and spin magnetic quantum numbers of the states in the shell. Similarly let v_b stand for a wave function with definite orbital and spin magnetic quantum numbers in the incomplete shell. The states under consideration are then represented by the normalized determinants

$$\Psi = |u_1, u_2, \cdots, u_n; v_{b1}, v_{b2}, v_{b3}|,$$

having $n+3$ rows and columns, each row containing the functions with the coordinates of one of the particles. These determinants describe the "strong field" states of the system. The states b_1, b_2, b_3 may, in general, be any of the $2(2L+1)$ strong field states in the incomplete shell. Because of the exclusion principle only the possibilities $b_1 \neq b_2$, $b_1 \neq b_3$, $b_2 \neq b_3$ need be considered. The interaction energy is of the form $H' = \sum_{i>k} H(ik)$ with H_{ik} symmetric in the particles i and k. The matrix elements of H', $(\Psi', H'\Psi)$, are different from zero only if at most two of the states b are different for Ψ and Ψ'. If Ψ and Ψ' differ by two b's the matrix element contains only the functions v and will be said to contribute only to the interaction of the incomplete shell with itself. If Ψ and Ψ' differ by one b, or if they are identical, the matrix element $(\Psi', H'\Psi)$ is a sum containing matrix elements either with two v's or with one u and two v's (which may be identical). For $\Psi = \Psi'$ there is in addition a sum involving only u's. The latter vanishes in the present application since it is equal to the spin-orbit interaction of a closed shell with itself. The terms with one u and one v form the interaction of the valence particles with the closed shell. The terms with two v's give the interactions between the valence particles, which are readily seen to be the same as would be found if one worked with the normalized determinants

$$|v_{b1}v_{b2}v_{b3}|$$

so that the closed shell can be disregarded in this connection.

The interaction of the valence particles with the closed shell gives rise to matrix elements

$$(\Psi, H'\Psi) = \sum_{a=1}^{n} \sum_{b} (u_a(1)v_b(2), H(12)[u_a(1)v_b(2) - u_a(2)v_b(1)]),$$

$$(\Psi', H'\Psi) = \sum_{a=1}^{n} (u_a(1)v_b(2), H(12)[u_a(1)v_b(2) - u_a(2)v_b(1)]).$$

In the latter case the order of the functions v is supposed to be arranged in such a way as to have the last v different Ψ in and Ψ'. Let

$$H_{12} = \mathbf{A}_{12}\boldsymbol{\sigma}_1 + \mathbf{A}_{21}\boldsymbol{\sigma}_2$$

with $\mathbf{A}_{12}$, $\mathbf{A}_{21}$ independent of the $\boldsymbol{\sigma}$'s. For ordinary and Majorana interactions $H(12)$ is of this type. The typical matrix element $(\Psi', H'\Psi)$ is a sum of two parts obtained by inserting $\mathbf{A}_{12}\boldsymbol{\sigma}_1$ and $\mathbf{A}_{21}\boldsymbol{\sigma}_2$, respectively, for $H(12)$. Each of these is again a sum of two parts, one due to $u_a(1)v_b(2)$ and the other due to $-u_a(2)v_b(1)$. There are thus four parts in all. Since the wave functions u and v are products of

orbital and spin wave functions the matrix of $\mathbf{A}\boldsymbol{\sigma}$ for each of the terms in the sum over a is the direct product of the vector matrix $\mathbf{A}$ by the vector matrix $\boldsymbol{\sigma}$. Let

$$(u_a(1)v_\beta(2),\ \mathbf{A}u_a(1)v_b(2)) = (M_aM_\beta|\mathbf{A}|M_aM_b)\delta(m_am_\beta;\ m_am_b),$$
$$(u_a(1)v_\beta(2),\ \mathbf{A}u_a(2)v_b(1)) = [M_aM_\beta|\mathbf{A}|M_aM_b]\delta(m_am_\beta;\ m_bm_a),$$

with M and m standing, respectively, for orbital and spin magnetic quantum numbers. Similarly let

$$(u_a(1)v_\beta(2),\ \boldsymbol{\sigma}u_a(1)v_b(2)) = (m_am_\beta|\boldsymbol{\sigma}|m_am_b)\delta(M_aM_\beta;\ M_aM_b),$$
$$(u_a(1)v_\beta(2),\ \boldsymbol{\sigma}u_a(2)v_b(1)) = [m_am_\beta|\boldsymbol{\sigma}|m_am_b]\delta(M_aM_\beta;\ M_bM_a).$$

Then

$$\textstyle\sum_a(u_a(1)v_\beta(2),\ \mathbf{A}\boldsymbol{\sigma}u_a(1)v_b(2)) = \sum_{M_a}(M_aM_\beta|\mathbf{A}|M_aM_b)\sum_{m_a}(m_am_\beta|\boldsymbol{\sigma}|m_am_b),$$
$$\textstyle\sum_a(u_a(1)v_\beta(2),\ \mathbf{A}\boldsymbol{\sigma}u_a(2)v_b(1)) = \sum_{M_a}[M_aM_\beta|\mathbf{A}|M_aM_b]\sum_{m_a}[m_am_\beta|\boldsymbol{\sigma}|m_am_b].$$

Consider $\sum_{M_a}(M_aM_\beta|A^i|M_aM_b)$, where $i=1,2,3$ denotes a component of A. Under rotation of the coordinate system, the orbital wave functions corresponding to M_a, transform among themselves by linear formulas which form an irreducible representation of the group of rotations. Similarly the functions of the incomplete shell transform among themselves and the components of A^i do so as well, both according to irreducible representations. The orthogonality relations between the coefficients of the representations of the shell functions introduce $\delta(M_aM_a)$ in the summation over M_a and do not enter the result for the transformation of $\sum_{M_a}(M_aM_\beta|A^i|M_aM_b)$. This quantity thus transforms itself as though the M_a were not present. Since the representations for the A^i and M_b are irreducible, the sum of matrix elements of an A^i is determined as a function of β, b to within a constant factor.[13] It is seen that only the transformation properties of the sums of matrix elements are essential for the above and therefore, the discussion applies equally well to $[M_aM_\beta|\mathbf{A}|M_aM_b]$, the dependence on β, b being the same as before. The linear formulas determining the ratios of the sums of the matrix elements as functions of β, b are the same as for the matrix elements of a one-particle vector operator taken with respect to wave functions corresponding to M_b. Since all these functions correspond to the same operator $\mathbf{L}$, one can simply use the operator $\mathbf{L}$ to determine these ratios since its matrix elements do not vanish. In the same way $\sum_{m_a}(m_am_\beta|\boldsymbol{\sigma}|m_am_b)$ and $\sum_{m_a}(m_am_\beta|\boldsymbol{\sigma}|m_am_b)$ are determined to within a constant factor, the dependence on β and b being again the same in both cases. Hence also the combined dependence of the $\sum_a$ of $\mathbf{A}\boldsymbol{\sigma}$ on M_β, M_b, m_β, m_b is the same for all $\mathbf{A}$. The matrix $(\Psi', H'\Psi)$ is, therefore, also determined to within a constant factor and the ratios of the matrix elements corresponding to different strong field states are thus seen to depend only on the azimuthal quantum number of the incomplete shell as well as the functions v_b entering Ψ, Ψ'. They are the same as though one were calculating the spin orbit interaction of the particles in the incomplete shell in a central field.

The above discussion applies only to those cases in which $\mathbf{A}$ is an operator diagonal in the spin. For the Heisenberg operator an additional consideration is necessary. For identical particles the operator $P^H=-1$. According to Eq. (2) it thus reduces to an ordinary interaction. If the particles are not identical, as in the interaction of an incomplete shell of protons with a complete shell of neutrons, the relations are still true because they are true for the four parts corresponding to combinations of $\mathbf{A}_{12}\boldsymbol{\sigma}_1$, $\mathbf{A}_{21}\boldsymbol{\sigma}_2$ with direct and exchange terms, the proportionality also holds for the Heisenberg operator of Eq. (2).

It thus suffices, in the calculation of an interaction with a complete shell, to determine the diagonal matrix elements of the operator $\sum\mathbf{L}_i\boldsymbol{\sigma}_i$ taken over the incomplete shell for the states of coupling that correspond to fixed total angular momenta. The product of these elements and the ratio of the diagonal element of $\frac{1}{2}\sum H(ik)$ for a single particle outside a complete shell to the value of $\mathbf{L}_1\boldsymbol{\sigma}_1$ for a single particle in the same state gives the change in energy due to the spin orbit interaction.

[13] E. Wigner, *Gruppentheorie* (Braunschweig, 1931).

INTERACTION WITH s SHELL (ALPHA-PARTICLE)

The state of the p shell can be conveniently described as a linear combination of the state in which the two neutrons are coupled into a ^1S state with the state in which they are in a ^1D condition. Thus

$$\psi = U[(+-+)-(-++)], \tag{4}$$

where $$U = cU_S + sU_D; \quad c^2+s^2=1. \tag{4.1}$$

Here the symbols $(+-+)$ etc. denote the spin function of the three particles, indicating in order, the sign of the projection along the z axis of the spins of the particles 1, 2, 3. Particles 1, 2 are the neutrons while 3 is the proton. The function U contains the space coordinates of 1, 2, 3 and is subject to the normalizing condition

$$(\psi, \psi) = 2(U, U) = 1. \tag{4.2}$$

The functions U_S, U are the orbital functions with the above normalization for S and D states respectively. For the maximum orbital magnetic quantum number one may take

$$U_S = (3/2)(4\pi)^{-\frac{1}{2}} Q_1 Q_2 Q_3 (\mathbf{r}_1\mathbf{r}_2)\xi_3, \tag{4.3}$$

$$U_D = (81/80)^{\frac{1}{2}}(4\pi)^{-\frac{1}{2}} Q_1 Q_2 Q_3 [\xi_1(\mathbf{r}_2\mathbf{r}_3) + \xi_2(\mathbf{r}_3\mathbf{r}_1) - \tfrac{2}{3}\xi_3(\mathbf{r}_1\mathbf{r}_2)] \tag{4.4}$$

with $$\xi = x + iy. \tag{4.5}$$

Here $Q_i = Q(r_i)$ is the radial function of the ith particle normalized so that

$$\int_0^\infty Q^2(r) r^4 dr = 1. \tag{4.6}$$

The values of ψ corresponding to U_S, U_D will be written as ψ_S, ψ_D. One has

$$(\psi_S, \textstyle\sum \mathbf{L}_i\boldsymbol{\sigma}_i\psi_S) = 2(U_S, L_3^z U_S) = 2(U_S, U_S) = 1,$$

$$(\psi_D, \textstyle\sum \mathbf{L}_i\boldsymbol{\sigma}_i\psi_D) = \dfrac{L(L+1)+L_3(L_3+1)-(L_1+L_2)[(L_1+L_2)+1]}{2L(L+1)} = -\tfrac{1}{2},$$

$$(\psi_D, \textstyle\sum \mathbf{L}_i\boldsymbol{\sigma}_i\psi_S) = 0.$$

The last equation is true because $L_3^z U_S = U_S$ and U_S is orthogonal to U_D. Thus for the general equation (4)

$$(\psi, \textstyle\sum \mathbf{L}_i\boldsymbol{\sigma}_i\psi) = \tfrac{3}{2}c^2 - \tfrac{1}{2} = P_2(c). \tag{4.7}$$

For $c = 5^{\frac{1}{2}}/3$, $s = \frac{2}{3}$ one obtains a state symmetric in the Cartesian coordinates of the three particles

$$U' = 3(20)^{-\frac{1}{2}}(4\pi)^{-\frac{1}{2}} Q_1 Q_2 Q_3 \mathfrak{S} \tag{4.8}$$

with $$\mathfrak{S} = (\mathbf{r}_1\mathbf{r}_2)\xi_3 + (\mathbf{r}_2\mathbf{r}_3)\xi_1 + (\mathbf{r}_3\mathbf{r}_1)\xi_2. \tag{4.9}$$

It is this state that should be close to the actual one according to the considerations of Wigner, Hund, Feenberg and Phillips.[13] It will be noted that according to Eq. (4.7) the splitting of the level due to interaction of the p shell with the alpha-particle is in the ratios of $1 : (1/3) : (-1/2)$ for the states U_S, U', U_D, respectively. According to the previous estimate[9] the interaction corresponding to $a^{\mathrm{M}} = 1$ was sufficient, for the state U_S, to account for the observed splitting and the principal contribution came from the interaction of the p shell with the alpha-particle. Since for U' this energy is decreased to $\frac{1}{3}$ of its previous value it becomes necessary to consider other values of a^{M}, a^{H}, a^{W}. According to the preceding section the energy splitting due to the interaction with the s shell is obtained simply by calculating it for a single particle in the p shell and multiplying it by the factor, $P_2(c)$. The alpha-particle will be supposed to be a complete shell of two neutrons and two protons,

both in s states. The orbital functions of these particles will be called $R(r)$ normalized so that

$$\int_0^\infty R^2 r^2 dr = 1. \tag{5}$$

The energy splitting for a single p proton due to its spin orbit interaction with the s shell of neutrons will be called $(\Delta E)_{sv}$ and the splitting due to the interaction with the s shell of protons will be written as $(\Delta E)_{s\pi}$. In all cases $\Delta E = E_{3/2} - E_{\frac{1}{2}}$ where $E_{3/2}$, $E_{\frac{1}{2}}$ are respectively the energies for $^2P_{3/2}$ and $^2P_{\frac{1}{2}}$. The values of ΔE will be listed below in terms of integrals involving Q, R as well as the special values that one obtains for

$$Q = N_Q e^{-\nu r^2/2}, \qquad R = N_R e^{-\mu r^2/2} \tag{5.1}$$

$$N_Q^2 = 8\nu^{5/2}/3\pi^{\frac{1}{2}}, \quad N_R^2 = 4\mu^{\frac{1}{2}}/\pi^{\frac{1}{2}} \tag{5.2}$$

with
$$J = Ae^{-\alpha r^2}. \tag{5.3}$$

The abbreviations

$$\beta^2 = \tfrac{1}{4}(\mu+\nu)^2 + \alpha(\mu+\nu); \quad \gamma^2 = \mu\nu + \alpha(\mu+\nu) \tag{5.4}$$

and
$$\lambda = \hbar/Mc \tag{5.5}$$

will be used. One finds

$$(\Delta E)_{sv}^{M1} = -(3/64\pi^2)\lambda^2 \int J\{6Q_1Q_2 + 2r_1Q_1'Q_2 + 2r_2Q_1Q_2' + r_1r_2 \sin^2\theta Q_1'Q_2'\}R_1R_2 d\tau_1 d\tau_2$$
$$= -(3/4)\lambda^2\nu^{5/2}\mu^{5/2}A(\mu+4\alpha)\beta^{-5} \tag{6}$$

$$(\Delta E)_{s\pi}^{M1} - (\Delta E)_{sv}^{M1} = (3/32\pi^2)\lambda^2 \int Jr_2 \cos\theta Q_2^2 R_1 R_1' d\tau_1 d\tau_2 = -(3/2)\lambda^2\nu^{5/2}\mu^{5/2}A\alpha\gamma^{-5} \tag{6.1}$$

where the superscripts M1 indicate that quantities are taken for $a^M = 1$. These formulas are in agreement with the previous calculation.[9]

$$(\Delta E)_{sv}^{M0} = -(3/64\pi^2)\lambda^2 \int Jr_1r_2 \sin^2\theta Q_1Q_2R_1'R_2' d\tau_1 d\tau_2 = -(3/4)\lambda^2\nu^{5/2}\mu^{7/2}A\beta^{-5} \tag{6.2}$$

$$(\Delta E)_{s\pi}^{M0} - (\Delta E)_{sv}^{M0} = -[(\Delta E)_{s\pi}^{M1} - (\Delta E)_{sv}^{M1}] \tag{6.3}$$

$$(\Delta E)_{sv}^{H1} = -(3/128\pi^2)\lambda^2 \int R_1Q_2(J'/r)\{(2r_2^2 - 2\mathbf{r}_1\mathbf{r}_2)R_2Q_1$$
$$+ [Q_1'R_2/r_1 - Q_1R_2'/r_2]r_1^2r_2^2 \sin^2\theta\} d\tau_1 d\tau_2 = (3/2)\lambda^2\nu^{5/2}\mu^{5/2}\alpha A\beta^{-5} \tag{6.4}$$

$$(\Delta E)_{s\pi}^{H1} - (\Delta E)_{sv}^{H1} = 2[(\Delta E)_{s\pi}^{M0} - (\Delta E)_{sv}^{M0}]; \tag{6.5}$$

$$(\Delta E)_{sv}^{H0} = -(\Delta E)_{sv}^{H1}; \quad (\Delta E)_{s\pi}^{H0} = (\Delta E)_{sv}^{H0}; \tag{6.6}$$

$$(\Delta E)_{sv}^{W1} = -(\Delta E)_{s\pi}^{H1} + (\Delta E)_{sv}^{H1}; \quad (\Delta E)_{s\pi}^{W1} - (\Delta E)_{sv}^{W1} = -(\Delta E)_{sv}^{H1}; \tag{6.7}$$

$$(\Delta E)_{sv}^{W0} = 0; \quad (\Delta E)_{s\pi}^{W0} - (\Delta E)_{sv}^{W0} = (\Delta E)_{sv}^{H1}. \tag{6.8}$$

The order of the above equations is such as to give in succession the values of the needed quantities for $a^M = 1$, $a^M = 0$, $a^H = 1$, $a^H = 0$, $a^W = 1$, $a^W = 0$. For $a^M = 1$ and $a^M = 0$ it is supposed that there are no spin orbit interactions of the Heisenberg and Wigner types and similarly in Eqs. (6.5), (6.6) only the Heisenberg and in Eqs. (6.7), (6.8) only the Wigner spin orbit interactions are considered. An equation such as (6.5) is, of course, not supposed to hold for the actual contributions due to the Heisenberg and Majorana forces but rather for the expressions on the two sides of the equation using the same function $J(r)$ in Eqs. (1), (2). The relations between quantities for different a^M, a^H, a^W are expressed

TABLE I. *Values of* $\Delta E = E_{3/2} - E_{1/2}$ *for the symmetric state due to interactions in the p shell.*

$a^M=1$	$a^M=0$	$a^H=1$	$a^H=0$	$a^W=1$	$a^W=0$
W	$-W$	$-W$	W	$-W$	W

simply in terms of $(\Delta E)_{sv}$ and $(\Delta E)_{s\tau} - (\Delta E)_{sv}$. For this reason Eqs. (6.3), (6.5), (6.6), (6.7), (6.8) were written in terms of them. For practical applications one needs, however, $(\Delta E)_{sv} + (\Delta E)_{s\tau}$ since this gives the result due to the whole alpha-particle.

INTERACTION WITH THE *p* SHELL

For the symmetric state represented by U' of Eq. (4.8) the relations are particularly simple. One obtains a contribution to the energy difference $E_{3/2} - E_{\frac{1}{2}}$ the values in Table I with

$$W = -\frac{3\lambda^2}{16\pi^2}\int [\tfrac{1}{2}(\mathbf{r}_1\mathbf{r}_2) J Q_1^2 Q_2^2 + \tfrac{2}{5} r_2 (\mathbf{r}_1\mathbf{r}_2) J Q_1^2 Q_2 Q_2'] d\tau_1 d\tau_2$$
$$= +\frac{9\lambda^2}{320\pi^2}\int Q_1^2 Q_2^2 \frac{J'}{r} [\tfrac{2}{3}(r_1^2 + r_2^2)\mathbf{r}_1\mathbf{r}_2 - r_1^2 r_2^2 - \tfrac{1}{3}(\mathbf{r}_1\mathbf{r}_2)^2] d\tau_1 d\tau_2. \tag{7}$$

For the special forms of Eqs. (5.1), (5.2), (5.3)

$$W = \lambda^2 A \alpha (1 + 2\alpha/\nu)^{-7/2}. \tag{7.1}$$

The relations between the values of ΔE given in Table I may be seen from the symmetry of U'. Thus one finds $\Delta E/3 = 4(U', A_{21}{}^Z U')$ for $a^M = 1$. The change to $a^M = 0$ is made by changing $\mathbf{A}_{kl}$ into $-\mathbf{A}_{lk}$. Since U' is completely symmetric $(U', A_{21}{}^Z U') = (U', A_{12}{}^Z U')$ and therefore ΔE for $a^M = 0$ is just the negative of that for $a^M = 1$. For $a^H = 1$

$$\Delta E = 3\lambda^2 i \left(U', \frac{dJ}{r dr}\left[(y_1 - y_2)\frac{\partial}{\partial x_1} - (x_1 - x_2)\frac{\partial}{\partial y_1}\right] U' \right)$$
$$= 3\lambda^2 i \left(U', J\left[\frac{\partial^2}{\partial y_2 \partial x_1} - \frac{\partial^2}{\partial x_2 \partial y_1}\right] U' \right) + 3\lambda^2 i \int J \left[\frac{\partial U'^*}{\partial y_2}\frac{\partial U'}{\partial x_1} - \frac{\partial U'^*}{\partial x_2}\frac{\partial U'}{\partial y_1}\right] d\tau_1 d\tau_2 d\tau_3.$$

The first term of this expression is zero since on interchanging 1 and 2 the square brackets change sign while U' does not. The last term is, on the other hand, just the negative of ΔE for $a^M = 1$. The relations between $(\Delta E)^{H0}$ and $(\Delta E)^{H1}$ and between $(\Delta E)^{W0}$ and $(\Delta E)^{W1}$ are the same as between $(\Delta E)^{M0}$ and $(\Delta E)^{M1}$. For

$$a^H = 1, \quad (\psi, Q_0{}^H \psi) = (U', [B_{23}{}^Z + B_{32}{}^Z + B_{31}{}^Z + B_{13}{}^Z] U')$$

for
$$a^W = 1, \quad (\psi, Q_0{}^W \psi) = 2(U', [B_{31}{}^Z + B_{32}{}^Z] U').$$

On account of the symmetry of U' these expressions are equal.

Using Eqs. (6), Table I and Eq. (7) one obtains the general result for ΔE for the state U' in the case of the most general interaction of the type in which the potential energy is

$$-(1 - g - g_1) J^M P^M - g J^H P^H - g_1 J^W \cdot 1$$

TABLE II. *Values of* $\Delta E/mc^2$.

μ/α	$a^M = -a^H = a^W = 1$	$a^M = -a^H = a^W = 2$	$a^M = -a^H = a^W = 3$
2	−0.32	−0.60	−0.87
1.5	−0.21	−0.41	−0.60
1	−0.11	−0.22	−0.33

with corresponding correction terms in a^{M}, a^{H}, a^{W}. The general result being lengthy, it suffices to write it down for $J^{\mathrm{M}}=J^{\mathrm{H}}=J^{\mathrm{W}}$ and the special forms of Eqs. (5):

$$\begin{aligned}\Delta E=\lambda^2 A\{&(1-g-g_1)a^{\mathrm{M}}[-\nu^{5/2}\mu^{5/2}(\mu+4\alpha)/2\beta^5-\nu^{5/2}\mu^{5/2}\alpha/2\gamma^5+\alpha(1+2\alpha/\nu)^{-7/2}]\\&+(1-g-g_1)(1-a^{\mathrm{M}})[-\nu^{5/2}\mu^{7/2}/2\beta^5+\nu^{5/2}\mu^{5/2}\alpha/2\gamma^5-\alpha(1+2\alpha/\nu)^{-7/2}]\\&+ga^{\mathrm{H}}[\nu^{5/2}\mu^{5/2}\alpha/\beta^5+\nu^{5/2}\mu^{5/2}\alpha/\gamma^5-\alpha(1+2\alpha/\nu)^{-7/2}]+g(1-a^{\mathrm{H}})[-\nu^{5/2}\mu^{5/2}\alpha/\beta^5+\alpha(1+2\alpha/\nu)^{-7/2}]\\&+g_1a^{\mathrm{W}}[-2\nu^{5/2}\mu^{5/2}\alpha/\gamma^5-\nu^{5/2}\mu^{5/2}\alpha/2\beta^5-\alpha(1+2\alpha/\nu)^{-7/2}]\\&+g_1(1-a^{\mathrm{W}})[\nu^{5/2}\mu^{5/2}\alpha/2\beta^5+\alpha(1+2\alpha/\nu)^{-7/2}]. \quad (8)\end{aligned}$$

For $\mu=\nu$, $\beta=\gamma$ and the formula simplifies:

$$\begin{aligned}\Delta E=\lambda^2 A\alpha\Big\{&(1-g-g_1)a^{\mathrm{M}}\left[-\frac{(5\alpha+\mu)\mu^5}{2\alpha\beta^5}+\frac{\mu^7}{\beta^7}\right]+(1-g-g_1)(1-a^{\mathrm{M}})\left[\frac{(\alpha-\mu)\mu^5}{2\alpha\beta^5}-\frac{\mu^7}{\beta^7}\right]+ga^{\mathrm{H}}\left[\frac{2\mu^5}{\beta^5}-\frac{\mu^7}{\beta^7}\right]\\&+g(1-a^{\mathrm{H}})\left[-\frac{\mu^5}{\beta^5}+\frac{\mu^7}{\beta^7}\right]+g_1a^{\mathrm{W}}\left[-\frac{5\mu^5}{2\beta^5}-\frac{\mu^7}{\beta^7}\right]+g_1(1-a^{\mathrm{W}})\left[\frac{\mu^5}{2\beta^5}+\frac{\mu^7}{\beta^7}\right]\Big\}. \quad (8.1)\end{aligned}$$

For $\alpha=16Mmc^2/\hbar^2$, $A=72mc^2$, $\lambda^2 A\alpha=0.627mc^2$. Substituting numbers into the last equation one obtains for $g=\frac{1}{4}$, $g_1=\frac{1}{4}$

$$\begin{aligned}&\mu/\alpha=2, \quad \Delta E=\lambda^2 A\alpha[-0.066-0.177a^{\mathrm{M}}+0.088a^{\mathrm{H}}-0.177a^{\mathrm{W}}],\\&\mu/\alpha=1.5, \quad \Delta E=\lambda^2 A\alpha[-0.030-0.129a^{\mathrm{M}}+0.064a^{\mathrm{H}}-0.116a^{\mathrm{W}}].\end{aligned} \quad (8.2)$$

According to Feenberg and Wigner,[5] μ/α is between 1.6 and 2.0. In order to account for the experimental value $-0.78\ mc^2$ one needs rather high values of a^{M}, a^{H}, a^{W} as is seen from Table II. The result is sensitive to μ/α. For the larger $\mu/\alpha=2$ one needs values of a^{M}, $-a^{\mathrm{H}}$, a^{W} in the vicinity of 3; for $\mu/\alpha=1.5$ these values have to be about 4. The result is not sensitive to reasonably small changes of g and g_1. The presence of an ordinary interaction (g_1) is favorable for getting a large absolute value of ΔE without using excessive values of a^{W}, a^{H}, a^{M}. If A and α are changed so as to remain in agreement with the binding energy of the deuteron the factor $A\alpha$ changes approximately as α^2. Due to this cause alone it is difficult to have a sufficiently large change in ΔE to make an important difference in the results without using values of α in bad contradiction with Feenberg and Knipp's and Feenberg and Share's[14] determination of α. This cause might change $a^{\mathrm{M}}=4$ into $a^{\mathrm{M}}=3$ for $\mu/\alpha=1.5$ since this would require using $\alpha=18\ mc^2/\hbar^2$.

The values of a^{M}, etc. in the neighborhood of 3 appear to be so high that one might discredit them on the grounds that they indicate the theory to be forced, since it appears to give the experimental value as a difference of two large numbers. This, however, is a false argument in several respects. The contributions to $\Delta E/mc^2$ for $\mu/\alpha=2$, for example are $-0.33(1-g-g_1)a^{\mathrm{M}}$, $-0.11(1-g-g_1)(1-a^{\mathrm{M}})$ for the Majorana interaction. For $a^{\mathrm{M}}=3$ these contributions are in the ratio of $-0.99:+0.22$. Although the signs of these contributions are different, one of them is less than $\frac{1}{4}$ of the other. For the Heisenberg interaction the terms in ga^{H} and $g(1-a^{\mathrm{H}})$ are of opposite signs for $a^{\mathrm{H}}=-3$ but one of them is about twice the other; for the Wigner interaction the signs of the contributions of g_1a^{W} and $g_1(1-a^{\mathrm{W}})$ are the same. It should also be remembered that although the absolute value of a^{W} for electromagnetic interactions is small ($a^{\mathrm{W}}=-1$) yet the coefficients that occur in the interaction energy [Eq. (1)] are as in

$$\mathbf{B}_{kl}(-\boldsymbol{\sigma}_k-2\boldsymbol{\sigma}_l),$$

which gives rise to combinations $2\mathbf{p}_2-\mathbf{p}_1$ when terms in one spin vector are collected. The occurrence

[14] E. Feenberg and J. K. Knipp, Phys. Rev. **50**, 253 (1936); E. Feenberg and S. Share, Phys. Rev. **50**, 253 (1936).

of large numbers in the electromagnetic interaction is not much more plausible than that suggested by the experimental fine structure *viz.*

$$\mathbf{B}_{kl}(3\boldsymbol{\sigma}_k+2\boldsymbol{\sigma}_l).$$

Departure from the Most Symmetric Wave Function

When account is taken of the ^1S and the ^1D condition of the neutrons the interaction energy as used for the calculation of the spin orbit splitting does not correspond exactly to the wave function U' on account of the presence of the Heisenberg interaction. In terms of L and K of Feenberg and Wigner one finds for the matrices of the potential energy[15]

	Majorana	Heisenberg	Ordinary
ψ'	$\begin{pmatrix} 3L+2K, & 0 \\ 0, & 5K \end{pmatrix}$	$\begin{pmatrix} 0, & 5^{\frac{1}{2}}K \\ 5^{\frac{1}{2}}K, & -3L/2+2K \end{pmatrix}$	$\begin{pmatrix} 3L+2K, & 0 \\ 0, & 3L-4K \end{pmatrix}$
ψ''			

Here the rows and columns are referred to the wave functions

$$\psi'=(5^{\frac{1}{2}}/3)\psi_S+(2/3)\psi_D, \quad \psi''=-(2/3)\psi_S+(5^{\frac{1}{2}}/3)\psi_D.$$

The Heisenberg interaction mixes a small amount of ψ'' into ψ'. From the values of K, L obtained by Feenberg and Wigner and by Feenberg and Phillips, the ratio K/L is seen to be so small that K may be neglected in the diagonal elements of the above matrices for purposes of estimating the coefficient of ψ''. This coefficient is according to a simple perturbation calculation

$$\bar{s}\leqq\frac{5^{\frac{1}{2}}gK}{3(1-g/2-g_1)L}$$

and correspondingly the change in c of Eqs. (4.1) and (4.7) is $-\frac{2}{3}$ of this. Hence

$$c=\frac{5^{\frac{1}{2}}}{3}-\frac{2(5^{\frac{1}{2}})gK}{9(1-g/2-g_1)L}=0.7454-0.497\frac{gK/L}{1-g/2-g_1}. \tag{9}$$

According to Eq. (9) positive K/L gives smaller c than that corresponding to the most symmetric function ψ'. The wave function thus contains slightly more ^1D than is the case for ψ'. The factor $(3c^2-1)/2$ of Eq. (4.8) is decreased, so that the expected splitting due to the interaction with the alpha-particle is also decreased. For $g=g_1=\frac{1}{4}$ the change in c is -0.021 and $(3c^2-1)/2$ changes due to this from 0.333 to 0.288 or about 14 percent. The uncertainty in the theoretical value of ΔE due to the uncertainty in μ/α is greater than this. There appears to be no point, therefore, in estimating the effect of the departure of c from $5^{\frac{1}{2}}/3$ more closely for the s shell. The spin-orbit interaction of the p shell with itself is smaller than that with the s shell for the symmetric state ψ' as well as the ^1S state of neutrons. It is to be expected that the effect of the small change in c on the contribution to ΔE due to the interaction within the p shell is also slight and it will not be considered in detail here.

An approximate idea of the magnitude of the effect of the p shell can be obtained by calculating the spin orbit interaction in the S condition of neutrons. The interaction with the s shell is taken care of by Eq. (4.7) (6.0), (6.1)$\cdots$(6.8). The interactions within the p shell give

$$(\Delta E)^{M1}=-(3/64\pi^2)\lambda^2\int J_{12}Q_1Q_2(\boldsymbol{\tau}_1\boldsymbol{\tau}_2)[6Q_1Q_2+2r_1Q_1'Q_2+2r_2Q_1Q_2'+r_1r_2\sin^2\theta Q_1'Q_2']d\tau_1d\tau_2$$

$$=-\frac{\lambda^2A\alpha(4\alpha/\nu-3)}{4(1+2\alpha/\nu)^{7/2}}. \tag{10}$$

[15] Since the main part of the potential energy is $-(1-g-g_1)JP^M-gJP^H-g_1J$, the J of this paper is opposite in sign to that of Feenberg and Wigner. This should be remembered in using their integrals for L and K.

This formula is in agreement with the one previously found.[9]

$$(\Delta E)^{M0}=-(3/64\pi^2)\lambda^2\int J_{12}Q_1Q_2Q_1'Q_2'r_1^2r_2^2\cos\theta\sin^2\theta d\tau_1 d\tau_2$$

$$=\frac{-5\lambda^2 A\alpha}{4(1+2\alpha/\nu)^{7/2}}, \tag{10.1}$$

$$(\Delta E)^{H1}=-(3/128\pi^2)\lambda^2\int Q_1^2Q_2^2(J'/r)[-r_1^2r_2^2\sin^2\theta+2r_1r_2^3\cos\theta-2r_1^2r_2^2\cos^2\theta]d\tau_1 d\tau_2$$

$$=\frac{\lambda^2 A\alpha(\alpha/\nu-2)}{2(1+2\alpha/\nu)^{7/2}}. \tag{10.2}$$

There is a general relation

$$2(\Delta E)^{H1}=(\Delta E)^{M0}-(\Delta E)^{M1}, \tag{10.3}$$

which follows from the identity

$$\mathbf{A}_{kl}+\mathbf{A}_{lk}=-(\mathbf{B}_{kl}+\mathbf{B}_{lk})P_{kl}^{M}.$$

One has also

$$(\Delta E)^{H0}=-(\Delta E)^{H1}, \tag{10.4}$$

$$(\Delta E)^{W1}=-(3/32\pi^2)\lambda^2\int Q_1^2Q_2^2r_1^2(J'/r)(r_1r_2\cos\theta-r_3^2)d\tau_1 d\tau_2$$

$$=-\frac{\lambda^2 A\alpha(3+\alpha/\nu)}{(1+2\alpha/\nu)^{7/2}}, \tag{10.5}$$

$$(\Delta E)^{W0}=0. \tag{10.6}$$

Collecting the contributions for the s and p shell one obtains a formula of the type of Eq. (8). For $\mu=\nu$ the equation simplifies and becomes

$$\Delta E=\lambda^2 A\alpha\Big\{a^{M}(1-g-g_1)\Big[-\frac{3\mu^5}{2\beta^5}\Big(5+\frac{\mu}{\alpha}\Big)-\Big(\frac{\alpha}{\mu}-\frac{3}{4}\Big)\frac{\mu^7}{\beta^7}\Big]+(1-g-g_1)(1-a^{M})\Big[\frac{3\mu^5}{2\beta^5}\Big(1-\frac{\mu}{\alpha}\Big)-\frac{5\mu^7}{4\beta^7}\Big]$$
$$+ga^{H}\Big[\frac{6\mu^5}{\beta^5}+\Big(\frac{\alpha}{2\mu}-1\Big)\frac{\mu^7}{\beta^7}\Big]+g(1-a^{H})\Big[-\frac{3\mu^5}{\beta^5}-\Big(\frac{\alpha}{2\mu}-1\Big)\frac{\mu^7}{\beta^7}\Big]$$
$$+g_1a^{W}\Big[-\frac{15\mu^5}{2\beta^5}-\Big(3+\frac{\alpha}{\mu}\Big)\frac{\mu^7}{\beta^7}\Big]+g_1(1-a^{W})\frac{3\mu^5}{2\beta^5}\Big\}. \tag{10.7}$$

The contributions of the p shell are here represented by the last term within each of the square brackets. For $g_1(1-a^{W})$ the p shell contributes nothing. For $g=g_1=\frac{1}{4}$, $A=72\,mc^2$, $\alpha=16M\,mc^2/\hbar^2$. and $\mu/\alpha=2$, Eq. (10.7) gives

$$\Delta E/mc^2=-0.150-0.457a^{M}+0.229a^{H}-0.298a^{W}$$

The experimental value is then accounted for without difficulty by letting $a^{M}=-a^{H}=a^{W}=1$ giving $\Delta E=-1.134\,mc^2$. With somewhat smaller values of μ/α or with different a^{M}, a^{H}, a^{W} the absolute value of ΔE is easily decreased. The contributions to ΔE due to the p shell are relatively insignificant in this case, the main contributions arising from the interaction with the s shell. Thus with the above numbers the ratios of the p shell interaction to that with the s shell are for $a^{M}=1$, -0.012; for $a^{M}=0$, 0.42; for

$a^H=1, -0.063$; for $a^H=-1, -0.093$; for $a^H=0, -0.13$; for $a^W=1, 0.23$, for $a^W=0, 0$. The largest of these ratios, 0.42 for $a^M=0$, does not enter the result at all if one uses $a^M=1$ as has been done above. The net effect of the p shell for the ^1S condition of neutrons is only $-0.011\ mc^2$. For the symmetric state Eq. (8.1) gives values for the interaction with the p shell which are about $-\frac{1}{5}$ of the whole for $\mu/\alpha=2$.

It should be noted that the ^1S condition of neutrons does not represent the actual coupling, even approximately, if the interaction energy is of the form $-(1-g-g_1)JP^M-gJ^HP^H-g_1J^W\cdot 1$ with values of the constants such as were used above. The object of calculations with Eq. (10) with such constants is to see how sensitive the splitting is to a change in the wave function for a fixed form of spin-orbit interaction energy.

Experiments of Bothe and Maier-Leibnitz and of Maier-Leibnitz and Maurer[16] indicate the presence of a state of C^{13} at about 0.8 Mev above the ground level. According to Feenberg and Wigner, Feenberg and Phillips as well as Hund[13] the lowest state of C^{13} may be a ^2P arising out of two missing p protons and one missing p neutron similarly to the way in which the ground state of Li^7 arises out of one p proton and two p neutrons. The possibility that the two lowest levels of C^{13} in the level scheme of Bothe and Maier-Leibnitz are to be indentified with this ^2P level is open but it does not fit in a simple way the large ratio of intensities of the 80 cm and 90 cm groups of protons emitted in the reaction $B^{10}+He^4=C^{13}+H^1$. This interpretation appears to be doubtful but if correct it would indicate a fine structure splitting of 0.8 Mev with an error of possibly ± 0.2 Mev. Even though this splitting is larger than that in Li^7 there is no contradiction involved since with spin orbit interactions between pairs of particles the simple relationship between holes and particles does not hold. If the splitting of the normal state of C^{13} is of the order of 0.4 or 0.2 Mev it could remain unobserved in $B^{10}+He^4=C^{13}+H^1$. The 80 cm proton group would have to be interpreted then as being due to a level with a different angular momentum from that of the ground state. This interpretation is apparently not in contradiction with observations of Cockcroft and Lewis[17] on $C^{12}+H^2=C^{13}+H^1$. The ejected protons, according to their Fig. 1 on p. 264, show a number-energy distribution that is not quite symmetric about the maximum, judging by their "protons D+D" curve. The experimental point for the range 11.9 cm and the part of the curve for ranges between 9 and 11 cm are suggestive of fine structure. It would be interesting to see a more detailed experimental curve with more points for ranges between 11 cm and 14 cm with thin carbon targets and a monochromatic proton beam of nearly the same energy used for comparison.

It is a pleasure to record our indebtedness to the Alumni Research Foundation of the University of Wisconsin for its support of this work.

[16] W. Bothe and H. Maier-Leibnitz, Zeits. f. Physik **107**, 513 (1937); H. Maier-Leibnitz and W. Maurer, Zeits. f. Physik **107**, 509 (1937).

[17] J. D. Cockcroft and W. B. Lewis, Proc. Roy. Soc. **154**, 261 (1936).

On Nuclear Magnetic Moments

D. R. INGLIS
Palmer Physical Laboratory, Princeton University, Princeton, New Jersey*
(Received January 11, 1938)

The general regularity of observed nuclear magnetic moments confirms the theoretical expectation that the total spin angular momentum should be one-half or zero, and suggests further that the orbital and spin moments of protons and neutrons separately are approximately constants of the motion in most nuclei. The possibility is discussed that this separability of the orbital moments (as well as the spin moments) should be expected as a result of the customary exchange nature of the binding forces. The separability seems to be due to neutron excess and to a vestige of the shell structure of the Hartree model, in which the contributing neutrons are loosely coupled to the protons by exchange forces because of being in quite different states. The moments of potassium are singled out as having exceptionally simple structure.

THE observed magnetic moments μ_I of nuclei composed of an odd number of protons n_π and an even number of neutrons n_ν (and also of nuclei with even n_π and odd n_ν)[1] have been rather roughly correlated by supposing that each μ_I is simply due to one proton (or neutron) with a spin magnetic moment $\mu_{s\pi}$ (or $\mu_{s\nu}$) slightly less than observed.[2] Schmidt has pointed out,[3] more exactly, that these μ_I all lie between the limits given by the one-particle model with correct spin moments (Fig. 1). That the μ_I are not larger than this, and also that they lie in two quite well-defined groups (Fig. 1, and reference 3, Fig. 4) which seem to correspond to two possible orientations of the spin relative to the orbital moment, indicates that the total spin moment is one-half, which is not surprising. But it is rather striking that the magnitudes of μ_I indicate, as we shall see, that the orbital moment seems to be due almost entirely to protons (or, in the odd-neutron case, to neutrons). This apparent simplicity is here discussed from the point of view of our present tentative conception of nuclear binding forces.

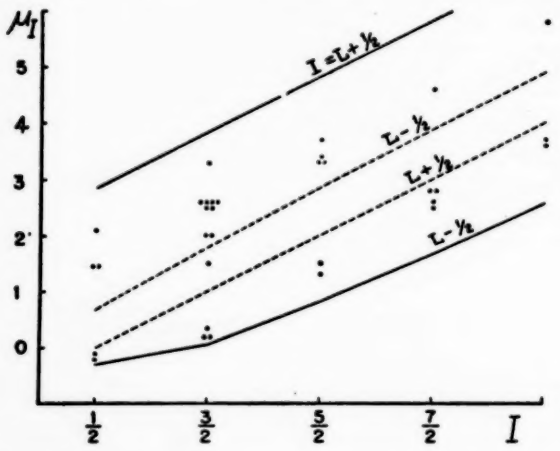

FIG. 1. Observed magnetic moments μ_I (in heavy magnetons) for various angular momenta I (in units $\hbar$) of nuclei with an odd proton. The solid lines are calculated values for $S=\frac{1}{2}$, $\mu_S=2.85$, $g_L=1$ (as for a single proton). To Schmidt's[3] Fig. 3, the dotted lines (calculated orbital contributions, with $g_L=1$) have been added.

I

The spin-orbit coupling being small,[4] we have (LS) or Russell-Saunders coupling.[5] If we treat (compare Section III) the spin-spin dependence of the binding forces as a small correction, as in current "nuclear spectroscopy,"[5] we have further what we might call ($LS_\pi S_\nu$) coupling. The like-

* On leave of absence from the University of Pittsburgh.

[1] These two cases comprise all known μ_I but three with $n_\pi=n_\nu$ odd.

[2] (a) A. Lande, Phys. Rev. **46**, 477 (1934); (b) Estermann, Simpson and Stern, Phys. Rev. **52**, 535 (1937); (c) Kellogg, Rabi and Zacharias, Phys. Rev. **50**, 472 (1936). The slight disagreement of (b) and (c) is unimportant here, the other μ_I being more uncertain. For hyperfine structure (reference 3) data, compare (d) Bethe and Bacher, Rev. Mod. Phys. **8**, 82 (1936).

[3] Th. Schmidt, Zeits. f. Physik **106**, 358 (1937).

[4] D. R. Inglis, Phys. Rev. **50**, 783 (1936). Here $E(\mathbf{l}\cdot\mathbf{s}) \approx \omega_T \cdot \mathbf{s}\hbar \approx (v/c)^2(\hbar^2/2r^2) \approx (v/c)^2$ (*kinetic energy*). Even very rough validity of the "raindrop" model would suggest that this estimate errs by giving too large spin-orbit coupling for heavy nuclei. That paper and $S=\frac{1}{2}$, discussed below, annul the earlier suggestions on correlating nuclear moments of Inglis, Nature **135**, 998 (1935); Phys. Rev. **47**, 84 (1935).

[5] (a) Feenberg and Wigner, Phys. Rev. **51**, 95 (1937); (b) E. Wigner, Phys. Rev. **51**, 106, 947 (1937); (c) F. Hund, Zeits. f. Physik **105**, 202 (1937); (d) Rose and Bethe, Phys. Rev. **51**, 205 (1937) (magnetic moments in the p shell); (e) Bohr and Kalckar, Kgl. Danske Selskab. **14**, 10 (1937).

particle interactions, even if independent of spin, give rise to a like-particle spin coupling, analogous to the familiar "exchange" coupling of electron spins, because of the Pauli antisymmetry. This rather strong like-particle spin coupling tends in general to make the total proton spin S_π and the total neutron spin S_ν as small as possible in the ground state (the inversion of the usual atomic situation arises from the attractive interactions). With even numbers of particles, n_π and n_ν, the spin is thus zero. With n_π odd and n_ν even,[6] we should have $S_\pi=\frac{1}{2}$ and $S_\nu=0$, so that the total spin, $S=\frac{1}{2}$, would have as its magnetic moment μ_S the magnetic moment of a proton spin, $\mu_{s\pi}$, in first approximation. The spin dependence of the unlike-particle interactions would introduce an admixture of the properties of higher states, such as $S_\pi=\frac{1}{2}$, $S_\nu=1$, $S=\frac{1}{2}$, in an amount roughly equal to the square of the ratio of the spin dependence of the unlike-particle interaction to the like-particle spin coupling.[7]

The determination of the expected values of the total orbital angular momentum L and its gyromagnetic ratio g_L would in most cases be very involved. Let us instead accept them empirically. For each nuclear angular momentum, I, there are, with $S=\frac{1}{2}$, two possible L's, which would give two possible values of the nuclear magnetic moment, μ_I, (with the same vector addition as for a single particle) if we should know μ_S and g_L. Taking $\mu_S=\mu_{s\pi}$, as if for a single proton, we have the solid curves of Fig. 1. The orbital contribution alone (reckoned with $\mu_S=0$, $g_L=1$) is given by the dotted curves, so that one can visualize the effect of altering μ_S and g_L, which enter linearly. The expectation of $S=\frac{1}{2}$ is beautifully confirmed[6] by the division of the experimental points into two groups, and by the lack of any points above the upper curve. While it remains possible that the division of the points into two groups is a result of chance and the uncertainty of the data, this is unlikely[6] and one may assume that the lower group does in general correspond to $I=L-\frac{1}{2}$ and the upper group to $I=L+\frac{1}{2}$. Assuming further that the degree of admixture of neutrons and protons within each of the loosely-coupled[4] moments L and S is independent of their relative orientation,[8] one sees that the experimental points indicate a range of values of μ_S and g_L, averaging around $\mu_S\approx(2/3)\mu_{s\pi}$, $g_L\approx 7/8$.

The orbital moment seems thus[9] to be due almost entirely to protons, as though L_π and L_ν were approximately constants of the motion, and $L_\nu=0$. This is somewhat surprising, since the Pauli antisymmetry does not in general introduce a like-particle orbit coupling as it does a like-particle spin coupling, to overshadow the unlike-particle coupling. This enigma should be associated with another striking experimental regularity which is most simply ascribed to a tendency for an even number of like particles to have a vanishing orbital, as well as spin, moment: that nuclei with n_π even and n_ν even have $I=0$, without exception, as is well known. We raise the question, whether the observed semblance of $(L_\pi L_\nu S_\pi S_\nu)$ coupling corresponds to a result which would be expected theoretically on the basis of interactions of an exchange nature. Since heavy nuclei are too complicated to submit to exact calculation, we may at least consider them rather vaguely as being in a condition between the Hartree extreme of independent particles in a central field and the opposite extreme, a description in terms of alpha-particles, in which the individual particles influence one anothers' motion very much. If it could be carried out, the lowest states might thus be described by a partial transformation from one representation to the other, and might be expected to retain some of the properties of the

[6] The following discussion is confined to the more prevalent odd-proton case, explicitly, the odd-neutron case being closely analogous with $g_L=0$—see Fig. 4 of reference 3. Note that the same degree of admixture of spins which below gives $\mu_S=(\frac{2}{3})\mu_{s\pi}$ would in the odd-neutron case give $\mu_S\approx(\frac{1}{2})\mu_{s\nu}$, and likewise $g_L\approx\frac{1}{8}$, corresponding nicely with the data.

[7] This ratio would then have to be 4/9 for the admixture of a state with $S_\pi=\frac{1}{2}$, $S_\nu=1$, $S=\frac{1}{2}$ (which has positive $\mu_{s\pi}$ pointing backwards and negative $\mu_{s\nu}$ pointing forwards along S) to reduce μ_S to $(\frac{2}{3})\mu_{s\pi}$, as required below. Smaller ratios would give it if several states contribute, as seems likely. The final S remains $\frac{1}{2}$.

[8] It is possible, on the other hand, that the remnant of shell-structure which causes a negative sign of the spin-orbit coupling in some nuclei also enhances their g_L, thus elevating the lower group of points and exaggerating the semblance of $(L\,L\,S\,S)$ coupling in Fig. 1. But this effect would not account for the approximate symmetry of Fig. 4 of reference 3.

[9] If L were due about equally to protons and neutrons, as one might expect on the average, we would have $g_L\approx\frac{1}{2}$ and the points would lie lower in Fig. 1; for pure protons, $g_L=1$.

low states in those representations. In Section II it appears that nuclei in the alpha-particle representation would have a semblance of $(L_\pi L_\nu S_\pi S_\nu)$ coupling, which, however, would not be expected to persist in the intermediate case. The discussion of Section III makes it seem likely that the Hartree scheme would give only $(LS_\pi S_\nu)$ coupling for nuclei with small neutron excess. For them this consideration of the two extremes thus merely corroborates the simpler conclusion from a "raindrop" picture,[5e] in which L is due about equally to protons and neutrons. But for larger neutron excess the Hartree scheme yields a possible explanation of the $(L_\pi L_\nu S_\pi S_\nu)$ coupling, as is shown in Section IV. Neither the discussion nor the data on which it is based can at this stage claim sufficient finality to test the adequacy of any special form of heavy-particle interaction, perhaps involving several opposing types of exchange operator.[10]

II

An alpha-particle representation would describe a nucleus as a collection of alpha-particles cemented together by extra neutrons (and perhaps one proton) which would resemble conduction electrons in a metal. In this rather unsymmetrical clump of alpha-particles (considered at first to be at rest), the states for such "conduction neutrons" would lack the degeneracy of states in a central field, and would be filled by pairs of neutrons as far as possible, making $L_\nu=0$ and $S_\nu=0$ for even n_ν. An extra proton would be in the lowest of these states and would with exchange forces, interact strongly with the neutrons in that state, weakly with the rest. If there are many "conduction neutrons," as for most nuclei in this representation, excitation of one in the lowest state requires a large energy jump. Compared to this, the unlike-particle spin coupling and orbit coupling are apt to be small, giving only small admixtures of the high states to the ground state. In the zero rotational states of the alpha-particle representation, the vectors L_π, L_ν, S_π, and S_ν would thus be quite independent, each being either zero or due to only one particle. There are, however, slightly higher states in this representation in which the clump of alpha-particles rotates so that $g_L \neq 1$ (or 0). In this extreme it seems likely that the different rotational states would not be badly mixed for much the same reason that makes the rotational and electronic moments good quantum numbers in molecules, and one would have $(L_\pi L_\nu S_\pi S_\nu)$ coupling. But deviations from the extreme would be expected to mix the different rotational states in such a way that the coupling scheme would not persist in the intermediate case.[11]

III

Calculations to determine the type of coupling to be expected from simple interactions in the Hartree extreme have been carried out[5a] only for the p shell (up to oxygen). In the more complicated nuclei beyond that, the main feature of exchange interactions, the enhanced like-particle spin coupling used in Section I above, is known to be preserved.[5b] The calculations beyond oxygen have, however, by assuming certain integrals to be smooth functions of the atomic number and the same for all terms, neglected a great deal of the detail which would presumably be important in determining the extent to which L_π and L_ν are intermixed. Groups of terms are left degenerate[5b] which would be separated in the Hartree approximation, the separations involving several integrals in the more complicated configurations. One is led to believe that the splitting is relatively small, up to atomic number 50 (where the unsymmetrical Coulomb force seems to upset the scheme), by the success of Wigner in neglecting it.[5b] If instead the splitting were large but the maximum depression of the terms of maximum scope T were the same, for example, in each degenerate group, his results

[10] A simple symmetrical interaction involving only one spin operator is adequate for many purposes (reference 5). That it is not adequate for all purposes (and *a fortiori* if it contains no nonexchange term to satisfy the saturation requirement (21) of (a)), without marked modification of the usual radial functions, is at least strongly suggested by calculations of (a) D. R. Inglis, Phys. Rev. **51**, 531 (1937); (b) Rarita and Present, Phys. Rev. **51**, 788 (1937). These agree in giving He^4 too much binding relative to its less compact neighbors Li^6 and H^3. In comparing critically the apparent convergence of the deuteron calculation, as discussed by Margenau and Warren, Phys. Rev. **52**, 790, 1027 (1937), with Li^6, for example, one should bear in mind that a halting progression seems much less likely where many more terms are involved.

[11] A property of the alpha-particle representation, some trace of which does seem to persist in the intermediate case, is relative stability: W. Wefelmeier, Zeits. f. Physik **107**, 332 (1937).

concerning isobars would have been the same. With smoothly varying integrals, he obtains from symmetry properties an uneven variation of binding which exhibits a four structure, preference of even n_τ and n_ν, etc., results quite suggestive of alpha-particle formation. If the clustering into incipient alpha-particles discussed in Section II should spoil the smooth variation of his integrals, it would thus be expected to do so in such a way as merely to accentuate his principal results, at the same time possibly bringing about a tendency toward $(L_\tau L_\nu S_\tau S_\nu)$ coupling within his scheme.

It would be interesting to know whether the greater detail given by the formal Hartree model of heavy nuclei would contain a tendency toward $(L_\tau L_\nu S_\tau S_\nu)$ coupling without the effect of Section II. The calculations having been carried only through the p shell, one is tempted to seek some help in answering the question by comparison with atomic calculations.[12] The analogy is, however, rather remote, and can perhaps only serve to indicate the need for caution in generalizing results known in simple cases. The highest state of an atomic configuration corresponds to a low nuclear state, the interactions being of opposite sign. The question of most interest is whether or not the lowest state of an even number of equivalent like-particles with attractive interactions (predominantly space-exchange) is always a ^1S far separated from other singlets and triplets. It is rather striking that in the atomic configuration d^2 (and f^2) the calculated highest state is indeed a surprisingly high[13] ^1S. If the analogous separation were as large in nuclei, we would have approximately $(L_\tau L_\nu S_\tau S_\nu)$ coupling on the Hartree model, since the other smaller separations would serve as a measure of the ordinary (and so, unlike-particle) orbit coupling. This isolation of the highest atomic ^1S is, however, no longer uniquely large in the more complicated[12e] configuration d^4. It is thus even somewhat doubtful whether the highest atomic state would be a ^1S in such complicated configurations as, say, i^8, which occur in the formal Hartree model of heavy nuclei and introduce enormous numbers of terms[12d] and secular determinants of high order. Modification of the Coulomb interaction by introduction of a space-exchange operator reduces the isolation of the ^1S in the known cases, but this result of the Coulomb calculation does not hold even qualitatively for the exponential interactions assumed in nuclei, judging by the p shell where both calculations are available: Specializing Table III of Feenberg and Wigner[5a] (p^2 $^1S=L+2K$, $^1D=L-K$, $^3P=\pm(L-3K)$ with $+$ for nonexchange, $-$ for space-exchange, interaction) to the Coulomb interaction,[12a] we have $K=(3/4)L$, whereas for exponential interactions they estimate $K\approx L/7$. The space-exchange operator thus greatly increases the separation between the ^1S and the ^3P of p^2 (the $^1S-^1D$ separation remaining small) with an exponential interaction, contrary to the Coulomb case. The impracticability of judging by atomic analogy is here especially apparent. Without, then, being able to extrapolate beyond the p shell, we do at least know that there is no trace of $(L_\tau L_\nu S_\tau S_\nu)$ coupling in the p shell with the Hartree model, and the complexity of several protons and neutrons in a shell beyond the p shell makes any regularity there seem unlikely.

The only case from the p shell considered above is Li^7. It fits the general scheme of Fig. 1 without having $(L_\tau L_\nu S_\tau S_\nu)$ coupling[5d] because an excess of μ_S (which $=0.99\mu_{s\tau}$) compensates a defect of g_L (which $=0.3$). It is exceptional among the cases considered in being so light that the Hartree scheme may be expected to hold for it moderately well, unmodified by incipient alpha-particle formation.

IV

Perhaps the most essential difference between heavier nuclei and the nuclei up to oxygen is their neutron excess. In the Hartree model of most nuclei with fairly large neutron excess, the shells partly filled with protons and with neutrons are not the same shell. The important saturation property of exchange interactions is associated

[12] (a) J. C. Slater, Phys. Rev. **34**, 1293 (1929); (b) Condon and Shortley, *Theory of Atomic Spectra;* (c) M. Ostrofsky, Phys. Rev. **46**, 604 (1934); (d) C. Shudeman, J. Frank. Inst. **224**, 501 (1937).

[13] Far off the diagrams in reference 12(b), page 204. That the observed levels are not so high seems to indicate that high states perturb the ^1S more than the other terms. This suggests another possible but very intricate source of $(L_\tau L_\nu S_\tau S_\nu)$ coupling in nuclei. On page 543 of reference 10(a) it is estimated that the ground state of Li^6 is depressed considerably more than others by second-order perturbations.

with the fact that their average between particles in very different states (different shells) is relatively small. The coupling between unlike particles in different shells is then expected to be weak compared to the like-particle interaction within a shell, giving $(L_\pi L_\nu S_\pi S_\nu)$ coupling. Since two-thirds of the known μ_I correspond to neutron excess greater than ten, one may tentatively ascribe the observed regularity to this effect. The frequent occurrence of negative spin-orbit coupling (making $I=L-\frac{1}{2}$) is also plausibly ascribed to a remnant of shell structure in actual nuclei.

V

Since the Hartree model has more meaning for the lighter nuclei,[10a] its shell structure might be expected to make the moments of a few light nuclei much simpler than the more general case considered above. The nucleus $_{19}K^{39}$ seems to be quite simple. Its position on Fig. 1 ($I=3/2$, $\mu_I=0.36$) indicates that it has the sign of spin-orbit coupling[4] corresponding to an almost-closed shell. This is explicable on the basis of a zero-order (fictitious!) potential[10a] somewhat narrower toward the bottom than a harmonic oscillator potential (as is reasonable for so light a nucleus), making[14] the order of single-particle states $1s$, $2p$, $2s$, $3d$, $3p$. We have then the configuration $(3d^9\ ^2D)_\pi(3d^{10}\ ^1S)_\nu$, $^2D_{3/2}$. The two additional neutrons in the isotopic nucleus $_{19}K^{41}$ would be $3p^2$ with $^1S_0$ lowest,[5a] leaving the ground state unaltered except for the admixture of new higher states. The lowest of these admixed states is $(^2D)_\pi(3p^2\ ^1D)_\nu\ ^2D_{3/2}$, which would reduce g_L (by polluting L with neutrons) and hence would reduce the total magnetic moment, as is observed: for $_{19}K^{41}$ one has $\mu_I=0.20$. (It would also reduce the doublet splitting slightly, but this has not yet been observed.) The other new state of interest is $(^2D)_\pi(3p^2\ ^3P)_\nu\ ^2D_{3/2}$, which would tend to increase μ_I, but only slightly since it is quite high and is only admixed by unlike-particle spin coupling. It may be regretted that the interesting isotopic pairs Cu, Re, and Tl, each having $\mu_I\sim$(mass) quite exactly,[15] may not be treated so simply.

Discussion with Dr. Feenberg has been appreciated.

[14] Compare the term orders for square, parabolic (reference 2(d), page 173) and Coulomb potentials.
[15] Schüler and Korsching, Zeits. f. Physik **105**, 168, 495 (1937).

MARCH 15, 1938 PHYSICAL REVIEW VOLUME 53

The First Spark Spectrum of Manganese

C. W. CURTIS
*Princeton University, Princeton, New Jersey**
(Received January 3, 1938)

The analysis of the Mn II spectrum has been extended to include a classification of over seven hundred lines arising from combinations between terms belonging to the quintet and septet systems. From four members of the $3d^5(^6S)nf\ ^7f$ series an ionization potential of 126,147 wave numbers has been calculated by means of a Ritz formula. Pictures have been taken and measurements made covering the range from approximately 800A to 6000A. A hollow cathode discharge was used as a source, with each of the three gases, helium, argon and neon, as conducting media.

HISTORY

IT was in the manganese spectra, arc and first spark, that Catalan first noted groups of lines of a more complicated structure than could be attributed to triplet-triplet combinations.[1] Among the enhanced lines he called attention to the groups which were later identified independently by Russell[2] and by Black and Duffendack[3] as being $3d^54s\ ^7S-3d^54p\ ^7P$, $3d^54s\ ^5S-3d^54p\ ^5P$, $3d^6\ ^5D-3d^54p\ ^5P$ and $3d^54p\ ^7P-3d^54d\ ^7D$, all based on the ^6S ion. Intersystem lines were found

* Now located at Western Reserve University, Cleveland, Ohio.
[1] Catalan, Phil. Trans. Roy. Soc. **A223**, 127 (1922).
[2] Russell, Astrophys. J. **66**, 233 (1927).
[3] Black and Duffendack, Science **66**, 402 (1927).

connecting the septet and quintet systems. Russell added the second member of the ^7S series, and Catalan[4] later located the corresponding ^5S. This completed the analysis as far as it had been carried until the present investigation was undertaken.

Apparatus and Observations

A Schuler tube, similar in design to that used by A. G. Shenstone for the production of the Cu II spectrum[5] has proved quite satisfactory as a source for the manganese ion. The lines obtained are extremely sharp. The degree of excitation of the once ionized atom can be controlled to a considerable extent by the use of different noble gases; and, provided helium or neon is used, lines originating in high energy levels, which are either extremely diffuse or absent entirely in the spark, are here present with considerable intensity.

Since helium alone of the noble gases has an ionization potential sufficient to excite the complete Mn II spectrum, it was used to cover the complete range of wave-lengths from 800A to 6200A. Pictures of certain regions were also taken with argon and with neon in the tube, and wherever feasible, arc and spark pictures were also obtained.

In the region above 2250A the Princeton 21-foot concave grating (ruled by Professor R. W. Wood) was used. For wave-lengths between 2000A and 2400A only the strongest lines were obtainable with reasonable exposures with this grating, so supplementary measurements were made from plates taken on an Hilger E1 quartz prism instrument. Through the kindness of Professor J. C. Boyce, the author was permitted to use the two-meter normal incidence vacuum spectrograph of the Carnegie Institution of Washington, which is located in the Spectroscopy Laboratory of the Massachusetts Institute of Technology.[6] The plates taken with this spectrograph extended the observations to about 800A. Later the vacuum region was retaken on the two meter spectrograph at Princeton with neon and argon in the tube instead of helium.

[4] Catalan, An. Soc. Espan. **26**, 67 (1928).
[5] Shenstone, Phil. Trans. Roy. Soc. **235**, 195 (1936).
[6] Compton and Boyce, Rev. Sci. Inst. **5**, 218 (1934).

The Analysis

Positions of the low configurations

To the closed shell completed in argon, one must add six electrons to obtain the structure of once-ionized manganese. The possible low electron configurations are thus $3d^6$, $3d^5 4s$, and $3d^4 4s^2$. Series limits of Mn I determine the relative positions of the high multiplicity terms of $3d^6$ and $3d^5 4s$—the former limit being predicted higher by about 14,300 wave numbers.[2] From the height of $3d^4 4s$ above $3d^5$ in Mn III,[7] and from homologous terms of the neighboring first spark spectra, the $3d^4 4s^2$ configuration should be found rather high in the spectrum—between 55,000 and 60,000 wave numbers above the normal state. The positions (centers of gravity) of the lowest terms of these configurations are actually

$$3d^5 4s\ {}^7S - 0$$
$$3d^6\ {}^5D - 14550$$
$$3d^4 4s^2\ {}^5D - 55364.$$

Details of the configurations

$3d^5 4s$.—Consider the possible terms in the doubly ionized atom which form limits of the first spark spectrum. Because of Pauli's exclusion principle, $3d^5$ can give rise to only one sextet, ^6S, but there are many allowable quartet terms.

Upon the addition of a $4s$ electron one obtains $^{7,5}S$ from the sextet, the septet being the normal state. Based upon each quartet are metastable quintet and triplet terms. The arc spectra of Mn and Cr indicate that the lowest of these should be ^5G, ^5P, and ^5D. These have been located in Mn II and their term values (centers of gravity) compare with the corresponding terms of Mn I and Cr I as follows:

$3d^5 4s$	Mn II	$3d^5 4s^2$	Mn I	$3d^5 4s$	Cr I
^5G	27571.3	^4G	25278.4	^5G	20521.3
^5P	29911.6	^4P	27230.4	^5P	21846.3
^5D	32828.3	^4D	30397.0	^5D	24292.1

The remaining quintet term of this configuration is ^5F. This has not been found, probably because of its weak inter limit combinations.

$3d^6$ and $3d^4 4s^2$.—The only quintet terms possible from these configurations are the ^5D terms previously mentioned.

[7] Gilroy, Phys. Rev. **38**, 2217 (1931).

$3d^54p$.—The expected $^{7,5}P$ terms, based upon ^6S, are those found earlier by other investigators.

Associated with each of the even terms ^5G, ^5P, and ^5D should be a triad of odd ones. It is thought that all of these nine terms have been located; however, there is some doubt as to whether those assigned to $3d^5(^4P)4p\ ^5D$ and ^5S have been correctly named. The assignment is here made difficult because these levels undoubtedly mix characteristics with those of $3d^5(4G)4p\ ^5F$. All three terms occur quite close together and are the only terms that have been found which show strong transitions which involve a change in L other than ±1 or 0. The z^5F combines with a^5P, and the terms designated as z^5S and z^5D both combine with ^5G terms. Of the levels with the same j values in the three terms, the ones with the lowest j values are closest together. One might then expect that the transfer of characteristics would be greatest in these cases. This is borne out by the fact that the strongest combinations in the anomalous multiplets are between levels of low j values, while the intensities in the proper multiplets drop off more rapidly than might ordinarily be expected. The intensities of the lines in the a^5P-z^5D and a^5P-z^5S multiplets are not at all what would be predicted by theory. However, if one calculates the sums of the intensities for these two multiplets and compares them with the sums of the actual intensities of the lines to the a^5P term the agreement is quite good considering that only visual estimates of the lines have been made.

$3d^44sp$.—This configuration should give rise to a septet and a quintet triad based on ^6D and a quintet and triplet triad based on ^4D. Terms w^5F and w^5D have been allotted to the ^4D ion structure. Probably either w^5P or v^5P is the remaining member of this triad. It is suggested that the x^5P belongs to the group based on the sextet term. The separations of its levels are comparatively large as one would expect, and it falls in the right region. However, it exhibits two rather peculiar features. Its combinations with the b^5D are extremely weak and it shows marked enhancements when helium is used in the Schuler tube. Such enhancements do not occur with neighboring terms and cannot be explained as due to a metastable state of helium. Unfortunately, the normal state is the only low state with which septets may combine without intersystem combinations. Thus one would expect only the ^7P to be apparent. z^7P has been tentatively assigned to this configuration instead of $5p^7P$ since the latter shows combinations with $7s^7S$. Either assignment indicates a perturbation.

$3d^54d$.—The $^{7,5}D$ based on ^6S are known, and ^5I and ^5H based on ^4G have been found.

Series members and ionization potential

Certain higher members of the low terms discussed in the foregoing paragraphs have been found. These are listed below.

Configuration	Term	Total quantum number of excited electron.
$3d^5(^6S)ns$	^7S	$n=4, 5, 6, 7, 8, 9, 10.$
$3d^5(^6S)ns$	^5S	$n=4, 5, 6, 7, 8.$
$3d^5(^6S)np$	^7P	$n=4, 5.$
$3d^5(^6S)np$	^5P	$n=4, 5.$
$3d^5(^6S)nd$	^7D	$n=4, 5, 6, 7.$
$3d^5(^6S)nd$	^5D	$n=4, 5, 7.$
$3d^5(^6S)nf$	^7F	$n=4, 5, 6, 7.$
$3d^5(^6S)nf$	^5F	$n=4, 5, 6, 7, 8.$
$3d^5(^4G)ns$	^5G	$n=4, 5.$

The levels of the fourth member of the nd^5D series are slightly perturbed but otherwise show the correct characteristics for this assignment. $6f^5F$ is also slightly perturbed by t^5F.

The best value of the ionization potential can be obtained from the nf^7F series. These terms are fixed by combinations with $4d^7D$, which in turn depends upon $4p^7P$. All of the lines used to place these levels occur in the region above 2400A where the measurements are most reliable. The series shows no perturbations and the last member is within 9000 wave numbers of the limit. A Ritz formula adequately represents the series and gives an ionization potential of 126,147 wave numbers. This value is substantiated by a value of 126,148 obtained from the last five members of the ns^7S series.

Term Values

In Table I the values of the terms are listed. Their absolute values are given with respect to the normal state, $4s^7S$. Although the levels belonging to configurations $3d^54s$ and $3d^54p$ and based on quartet ion structures are consistent among themselves to within a few hundredths of a wave number, their absolute values with

TABLE I. *Absolute term values in the first spark spectrum of manganese with respect to the normal state. Column 1, discoverer (R, Russell; D, Duffendack and Black; C, Catalan; A, Curtis). Column 2, electron configuration. Column 3, term designation. Column 4, term value.*

1	2	3	4
	Even Terms		
C, R, D	$3d^5(^6S)4s$	$4s^7S_3$	0.00
"	$3d^5(^6S)4s$	$4s^5S_2$	9472.86
"	$3d^6$	$3d^5D_4$	14325.64
"	"	$3d^5D_3$	14593.62
"	"	$3d^5D_2$	14781.03
"	"	$3d^5D_1$	14901.06
"	"	$3d^5D_0$	14959.68
A	$3d^5(^4G)4s$	a^5G_6	27546.90*
"	"	a^5G_5	27570.95*
"	"	a^5G_4	27583.30*
"	"	a^5G_3	27588.23*
"	"	a^5G_2	27589.03*
"	$3d^5(^4P)4s$	a^5P_3	29889.31*
"	"	a^5P_2	29919.22*
"	"	a^5P_1	29951.12*
"	$3d^5(^4D)4s$	a^5D_4	32787.60*
"	"	a^5D_0	32818.10*
"	"	a^5D_1	32836.40*
"	"	a^5D_2	32856.95*
"	"	a^5D_2	32858.84*
"	$3d^54s^2$	b^5D_0	54846.0
"	"	b^5D_1	54938.1
"	"	b^5D_2	55115.8
"	"	b^5D_3	55371.3
"	"	b^5D_4	55696.5
R	$3d^5(^6S)5s$	$5s^7S_3$	74559.91
C	$3d^5(^6S)5s$	$5s^5S_2$	76374.56
C, R, D	$3d^5(^6S)4d$	$4d^7D_1$	79540.76
"	"	$4d^7D_2$	79544.51
"	"	$4d^7D_3$	79550.28
"	"	$4d^7D_4$	79558.38
"	"	$4d^7D_5$	79561.10
A	$3d^5(^6S)4d$	$4d^5D_4$	82136.30
"	"	$4d^5D_3$	82144.34
"	"	$4d^5D_2$	82151.07
"	"	$4d^5D_1$	82155.72
"	"	$4d^5D_0$	82158.16
"	$3d^5(^6S)6s$	$6s^7S_3$	97728.0
"	$3d^5(^6S)6s$	$6s^5S_2$	98410.1
"	$3d^5(^6S)5d$	$5d^7D_2$	99892.5
"	"	$5d^7D_3$	99894.8
"	"	$5d^7D_4$	99898.6
"	"	$5d^7D_5$	99903.1
"	"	$5d^5D_4$	100682.3
"	"	$5d^5D_3$	100688.1
"	"	$5d^5D_2$	100692.6
"	"	$5d^5D_1$	100695.3
"	$3d^5(^4G)5s$	e^5G_6	101467.58*
"	"	e^5G_5	101489.31*
"	"	e^5G_4	101499.03*
"	"	e^5G_2	101499.84*
"	"	e^5G_3	101501.30*
"	$3d^5(^4G)4d$	e^5H_3	106157.4
"	"	e^5H_4	106164.2
"	"	e^5H_7	106167.7
"	"	e^5H_5	106168.9
"	"	e^5H_6	106169.9
"	$3d^5(^4G)4d$	e^5I_8	106508.1
"	"	e^5I_4	106512.1
"	"	e^5I_5	106519.1
"	"	e^5I_7	106519.8
"	"	e^5I_6	106522.5
"	$3d^5(^6S)7s$	$7s^7S_3$	108126.2
"	$3d^5(^6S)7s$	$7s^5S_2$	108447.6
"	$3d^5(^6S)6d$	$6d^7D_2$	109242.3
"	"	$6d^7D_4$	109244.4
"	"	$6d^7D_5$	109248.2
"	$3d^5(^6S)8s$	$8s^7S_3$	113697.0
"	$3d^5(^6S)8s$	$8s^5S_2$	113895.2
"	$3d^5(^6S)7d$	$7d^7D$	114347.0
"	$3d^5(^6S)7d$	$7d^5D_4$	114932.2
"	"	$7d^5D_3$	114943.9
"	"	$7d^5D_2$	114951.9
"	"	$7d^5D_1$	114956.5
"	"	$7d^5D_0$	114958.1
	Even Terms		
A	$3d^5(^6S)9s$	$9s^7S_3$	117031.1
"	$3d^5(^6S)10s$	$10s^7S_3$	119185.6
	Odd Terms		
C, R, D	$3d^5(^6S)4p$	$4p^7P_2$	38366.07
"	"	$4p^7P_3$	38542.96
"	"	$4p^7P_4$	38806.53
"	$3d^5(^6S)4p$	$4p^5P_3$	43370.37
"	"	$4p^5P_2$	43484.50
"	"	$4p^5P_1$	43557.03
A	$3d^5(^4G)4p$	z^5G_2	64456.33*
"	"	z^5G_3	64473.13*
"	"	z^5G_4	64493.83*
"	"	z^5G_5	64518.57*
"	"	z^5G_6	64549.72*
"	$3d^5(^4G)4p$	z^5H_3	65482.66*
"	"	z^5H_4	65565.68*
"	"	z^5H_5	65658.30*
"	"	z^5H_6	65754.61*
"	"	z^5H_7	65846.61*
"	$3d^5(^4G)4p$	z^5F_5	66542.26*
"	"	z^5F_4	66643.01*
"	"	z^5F_1	66644.78*
"	"	z^5F_2	66676.56*
"	"	z^5F_3	66686.45*
"	$3d^5(^4P)4p$	z^5D_1	66893.79*
"	"	z^5D_2	66901.14*
"	$3d^5(^4P)4p$	z^5S_2?	66929.22*
"	$3d^5(^4P)4p$	z^5D_3	67008.93*
"	"	z^5D_4	67295.16*
"	$3d^5(^4P)4p$	z^5P_3	68284.38*
"	"	z^5P_2	68417.34*
"	"	z^5P_1	68496.37*
"	$3d^5(^4D)4p$	y^5F_1	70150.39*
"	"	y^5F_2	70231.07*
"	"	y^5F_3	70342.58*
"	"	y^5F_4	70497.44*
"	"	y^5F_5	70657.18*
"	$3d^5(^4D)4p$	y^5P_1	71263.92*
"	"	y^5P_2	71323.15*
"	"	y^5P_3	71390.14*
"	$3d^5(^4D)4p$	y^5D_4	72010.75*
"	"	y^5D_3	72247.38*
"	"	y^5D_2	72306.81*
"	"	y^5D_1	72320.62*
"	"	y^5D_0	72322.07*
"	$3d^54s(^6D)4p$?	z^7P_2	83255.1
"	"	z^7P_3	83375.9
"	"	z^7P_4	83529.6
"	$3d^5(^6S)5p$?	$5p^7P_2$	85895.1
"	"	$5p^7P_3$	85960.6
"	"	$5p^7P_4$	86057.4
"	$3d^5(^6S)5p$	$5p^5P_3$	86897.7
"	"	$5p^5P_2$	86936.9
"	"	$5p^5P_1$	86960.8
"	$3d^54s(^6D)4p$?	x^5P_1	88839.6
"	"	x^5P_2	89078.9
"	"	x^5P_3	89428.8
"	$3d^5(^6S)4f$	$4f^7F_6$	98423.5
"	"	$4f^7F_5$	98423.7
"	"	$4f^7F_4$	98423.8
"	"	$4f^7F_3$	98424.0
"	"	$4f^7F_2$	98424.1
"	$3d^5(^6S)4f$	$4f^5F_1$	98461.76
"	"	$4f^5F_2$	98462.34
"	"	$4f^5F_3$	98463.16
"	"	$4f^5F_4$	98464.14
"	"	$4f^5F_5$	98465.15
"	$3d^54s(^4D)4p$	w^5F_1	106265.3
"	"	w^5F_2	106373.7
"		w^5P_1	106479.2
"	$3d^54s(^4D)4p$	w^5F_3	106525.8
"	"	w^5F_4	106707.3
"		w^5P_2	106750.0
	Odd Terms		
A	$3d^54s(^4D)4p$	w^5F_5	106893.8
"		w^5P_3	107172.8
"	$3d^5(^6S)5f$	$5f^7F_{6,5}$	108409.8
"	"	$5f^7F_4$	108410.1
"	"	$5f^7F_3$	108410.2
"	"	$5f^7F_2$	108410.3
"	$3d^5(^6S)5f$	$5f^5F_1$	108435.6
"	"	$5f^5F_2$	108437.2
"	"	$5f^5F_3$	108439.0
"	"	$5f^5F_4$	108441.4
"	"	$5f^5F_5$	108443.0
"		v^5G_2	108485.4
"		v^5G_3	108503.0
"		v^5G_4	108524.7
"		v^5G_5	108550.7
"		v^5G_6	108587.9
"		v^5P_1	108726.4
"		v^5P_2	108974.7
"		v^5F_1	108994.0
"		v^5F_2	109045.7
"		v^5F_3	109122.4
"		w^5D_0	109167.7
"		v^5F_4	109221.1
"		w^5D_1	109235.3
"		v^5F_5	109327.1
"		w^5D_2	109343.7
"		v^5P_3	109378.9
"		w^5D_3	109476.3
"		w^5D_4	109607.8
"	$3d^54s(^4D)4p$	v^5D_0	109958.0
"	"	v^5D_1	109994.3
"	"	v^5D_2	110068.5
"	"	v^5D_3	110204.9
"	"	v^5D_4	110428.7
"		v^5H_3	110547.5
"		v^5H_4	110602.0
"		v^5H_5	110692.2
"		v^5H_6	110795.0
"		v^5H_7	110926.0
"		u^5F_1	111017.5
"		u^5F_2	111060.5
"		u^5F_3	111115.4
"		u^5F_4	111159.2
"		u^5F_5	111160.5
"		u^5P_1	111162.3
"		u^5P_2	111178.8
"		u^5P_3	111212.8
"		u^5G_4	113181.7
"		u^5G_5	113250.8
"		u^5G_6	113323.0
"		t^5F_2	113641.4
"		t^5F_2	113645.0
"		t^5F_1	113645.5
"		t^5F_4	113646.7
"		t^5F_5	113658.0
"	$3d^5(^6S)6f$	$6f^7F_6$	113840.0
"	"	$6f^7F_5$	113840.1
"	"	$6f^7F_4$	113840.2
"	"	$6f^7F_3$	113840.3
"	$3d^5(^6S)6f$	$6f^5F_1$	114024.5
"	"	$6f^5F_2$	114025.5
"	"	$6f^5F_3$	114026.4
"	"	$6f^5F_5$	114027.8
"	"	$6f^5F_4$	114026.9
"	$3d^5(^6S)7f$	$7f^7F_6$	117112.9
"	"	$7f^7F_5$	117113.0
"	"	$7f^7F_{4,3}$	117113.1
"	$3d^5(^6S)7f$	$7f^5F_1$	117148.3
"	"	$7f^5F_4$	117137.8
"		s^5F_1	117164.7
"		s^5F_2	117231.7
"		s^5F_3	117314.6
"		s^5F_4	117399.3
"		s^5F_5	117483.2
"	$3d^5(^6S)8f$	$8f^5F$	119253.

respect to $4s^7S$ may be incorrect by several tenths. This is because the only lines connecting this group with levels fixed accurately with respect to the normal state fall in the region below 2000A where measurements cannot be relied upon to better than a few tenths of a wave number. Levels of this type are listed to hundredths and followed by an asterisk.

CLASSIFIED LINES

Table IIA contains the classified lines from 2000A to 6200A. All lines were observed with the

TABLE IIA. *Classified lines from 2000A to 6200A. Lines whose wave-lengths are followed by an asterisk were photographed with a quartz prism instrument. Columns 1, 2, and 3, visual estimates of intensities in spark, helium Schuler tube, and arc. Column 4, wave-length in air. Column 5, wave number. Column 6, classification.*

1	2	3	4	5	6	1	2	3	4	5	6
	5		6131.917	16303.61	$4d^5D_0-4f^5F_1$		0		2870.665	34824.94	$z^5F_2-e^5G_3$
	5		6131.005	16306.04	$4d^5D_1-4f^5F_1$		4u		2868.887	34846.52	$z^5F_4-e^5G_5$
	15		6130.794	16306.59	$4d^5D_1-4f^5F_2$						also Mn I
	10		6129.022	16311.31	$4d^5D_2-4f^5F_2$		0		2868.098	34856.10	$z^5F_4-e^5G_4$
	20		6128.725	16312.10	$4d^5D_2-4f^5F_3$	1u	5		2862.410	34925.36	$z^5F_5-e^5G_6$
	10		6126.210	16318.80	$4d^5D_3-4f^5F_3$		1		2860.629	34947.11	$z^5F_5-e^5G_5$
	25		6125.855	16319.74	$4d^5D_3-4f^5F_4$	2	1u		2821.840	35427.46	$a^5D_3-z^5P_3$
	8		6122.799	16327.89	$4d^5D_4-4f^5F_4$	20	10	4	2816.329	35496.79	$a^5D_4-z^5P_3$
	40		6122.438	16328.85	$4d^5D_4-4f^5F_5$	3	3	1	2811.438	35558.53	$a^5D_2-z^5P_2$
	30		5302.320	18854.44	$4d^7D_5-4f^7F_{6,5,4}$	7	6	2	2811.290	35560.40	$a^5D_3-z^5P_2$
	25		5299.278	18865.26	$4d^7D_4-4f^7F_{5,4,3}$	0	0		2809.661	35581.02	$a^5D_1-z^5P_2$
	20		5296.968	18873.49	$4d^7D_3-4f^7F_{4,3,2}$		5		2806.513	35620.93	$z^5H_7-e^5G_6$
	15		5295.292	18879.46	$4d^7D_2-4f^7F_{3,2,1}$	3	3u	1	2805.207	35637.52	$a^5D_2-z^5P_1$
	10		5294.216	18883.30	$4d^7D_1-4f^7F_{2,1,0}$	2	2u		2803.442	35659.95	$a^5D_1-z^5P_1$
	1		4652.816	21486.36	$5p^5P_1-7s^5S_2$		5		2797.580	35734.67	$z^5H_6-e^5G_5$
	2		4647.585	21510.55	$5p^5P_2-7s^5S_2$	5u	50	2	2796.113	35753.42	$4p^7P_4-5s^7S_3$
	3		4639.150	21549.66	$5p^5P_3-7s^5S_2$		5		2789.306	35840.66	$z^5H_5-e^5G_4$
	5		4530.034	22068.72	$5p^7P_4-7s^7S_3$		6		2781.935	35935.62	$z^5H_4-e^5G_3$
	3		4510.210	22165.72	$5p^7P_3-7s^7S_3$	5u	50	2	2775.654	36016.94	$4p^7P_3-5s^7S_3$,
	2		4496.989	22230.89	$5p^7P_2-7s^7S_3$						$z^5H_3-e^5G_2$
	0		3804.476	26277.40	$4d^5D_0-5f^5F_1$	2	1u		2763.165	36179.71	$4p^5P_3-4p^7D_3$
	0		3803.881	26281.51	$4d^5D_1-5f^5F_2$	2	2	1	2762.548	36187.80	$4p^5P_3-4d^7D_4$
	0		3802.958	26287.89	$4d^5D_2-5f^5F_3$	5u	50	1	2762.090	36193.80	$4p^7P_2-5s^7S_3$
	3		3801.633	26297.05	$4d^5D_3-5f^5F_4$	12	8	2	2724.461	36693.66	$a^5P_1-z^5F_1$
					blend?	10	10	2	2722.097	36725.52	$a^5P_1-z^5F_2$,
	2		3800.240	26306.69	$4d^5D_4-5f^5F_5$						$a^5P_2-z^5F_1$
40	25	25	3497.536	28583.41	$3d^5D_1-4p^5P_2$	?	3	0	2720.013	36753.66	$a^5P_3-z^5F_4$
30	20	20	3496.814	28589.31	$3d^5D_2-4p^5P_3$	10	10	2	2719.739	36757.36	$a^5P_2-z^5F_2$
60	40	35	3495.831	28597.35	$3d^5D_0-4p^5P_1$	?	8	2	2719.018	36767.11	$a^5P_2-z^5F_3$
75	40	40	3488.676	28656.00	$3d^5D_1-4p^5P_1$						also Fe
80	40	40	3482.905	28703.48	$3d^5D_2-4p^5P_2$	8	4	1	2717.531	36787.23	$a^5P_3-z^5F_2$
()	40	35	3474.124	28776.03	$3d^5D_2-4p^5P_1$	8	8	1	2716.800	36797.12	$a^5P_3-z^5F_3$
100						15	8	4	2711.630	36867.28	$a^5G_2-z^5G_2$
()	50	50	3474.037	28776.75	$3d^5D_3-4p^5P_3$	()					
	9		3466.336	28840.68	$4d^7D_5-5f^7F_{6,5,4}$	?	6	2	2711.568	36868.12	$a^5G_3-z^5G_2$
	8		3465.037	28851.41	$4d^7D_4-5f^7F_{5,4,3}$	?	2	0	2710.392	36884.11	$a^5G_2-z^5G_3$
	7		3464.043	28859.77	$4d^7D_3-5f^7F_{4,3,2}$	()					
	6		3463.330	28865.71	$4d^7D_2-5f^7F_{3,2,1}$	18	8	4	2710.335	36884.89	$a^5G_3-z^5G_3$
	5		3462.878	28869.48	$4d^7D_1-5f^7F_{2,1,0}$	9	8	3	2709.973	36889.82	$a^5G_4-z^5G_3$
100	75	75	3460.312	28890.88	$3d^5D_3-4p^5P_2$	5	4	1	2708.813	36905.61	$a^5G_3-z^5G_4$
()						20	20	5	2708.454	36910.52	$a^5G_4-z^5G_4$
	8	10	3460.039	28893.16	$4s^5S_2-4p^7P_2$		5		2707.915	36917.85	$z^5G_6-e^5G_6$
150	100	100	3441.983	29044.73	$3d^5D_4-4p^5P_3$	10	10	2	2707.546	36922.88	$a^5G_5-z^5G_4$
10	20	15	3438.978	29070.10	$4s^5S_2-4p^7P_3$	6	4	1	2706.639	36935.26	$a^5G_4-z^5G_5$
	0		3136.315	31875.35	$4d^5D_2-6f^5F_3$	1	1		2706.094	36942.69	$a^5P_1-z^5D_1$
	0		3135.507	31883.56	$4d^5D_3-6f^5F_4$	25	25	5	2705.734	36947.61	$a^5G_5-z^5G_5$
	1		3134.819	31890.56	$4d^5D_4-6f^5F_5$	10	5	2	2705.561	36949.97	$a^5P_1-z^5D_2$
4u	30	1	3046.266	32817.55	$4p^5P_1-5s^5S_2$		4		2704.043	36970.70	$z^5G_6-e^5G_5$
4u	40	1	3039.551	32890.06	$4p^5P_2-5s^5S_2$	15	7		2703.972	36971.68	$a^5G_6-z^5G_5$
4u	50	2	3029.041	33004.17	$4p^5P_3-5s^5S_2$	1			2703.74	36974.6	$a^5P_2-z^5D_1$
	1		2965.801	33707.89	$b^5D_3-x^5P_2$	?	2		2703.508	36978.03	$a^5P_1-z^5S_2$
	0		2963.633	33732.55	$b^5D_4-x^5P_3$	()					
5	3	1	2961.694	33754.63	$a^5D_4-z^5F_5$	3	1	1	2703.455	36978.75	$a^5G_5-z^5G_6$
5	0	1	2958.944	33786.00	$a^5D_3-z^5F_4$,		1		2702.240	36995.48	$z^5G_4-e^5G_5$
					$a^5D_3-z^5F_1$	30	20	8	2701.696	37002.83	$a^5G_6-z^5G_6$
1	1	1?	2956.984	33808.39	$a^5D_1-z^5F_1$		4		2701.528	37005.13	$z^5G_4-e^5G_4$
4	0	0	2956.168	33817.73	$a^5D_2-z^5F_2$		0		2701.351	37007.55	$z^5G_4-e^5G_3$
2	0	0	2956.005	33819.59	$a^5D_3-z^5F_3$	12	12	4	2701.171	37010.02	$a^5P_2-z^5S_2$
1			2955.37	33826.9	$a^5D_0-z^5F_1$	10	10	4	2701.035	37011.88	$a^5P_3-z^5D_2$
6	3u	1	2955.110	33829.83	$a^5D_3-z^5F_3$		1		2700.011	37025.92	$z^5G_3-e^5G_4$
					double?		2		2699.853	37028.09	$z^5G_3-e^5G_3$
0			2954.20	33840.2	$a^5D_1-z^5F_2$	8	5	2	2698.989	37039.94	$a^5P_3-z^5S_2$
3			2952.87	33855.5	$a^5D_4-z^5F_4$		3		2698.729	37043.51	$z^5G_2-e^5G_2$
200	75	75	2949.209	33897.52	$4s^5S_2-4p^5P_2$,		0		2698.623	37044.96	$z^5G_2-e^5G_3$
					$a^5D_4-z^5F_3$	5	8	3	2695.366	37089.72	$a^5P_2-z^5D_3$
150	60	60	2939.309	34011.68	$4s^5S_2-4p^5P_2$	15	10	4	2693.191	37119.67	$a^5P_3-z^5D_3$
1			2936.51	34044.1	$a^5D_3-z^5D_2$		0		2680.776	37291.47	$a^5D_2-y^5F_1$
1			2935.35	34057.6	$a^5D_1-z^5D_1$	6	5	1	2679.165	37313.99	$a^5D_1-y^5F_1$
3			2934.71	34065.0	$a^5D_1-z^5D_2$	7	5	1	2677.853	37332.29	$a^5D_0-y^5F_1$
1	0	0	2933.784	34075.73	$a^5D_0-z^5D_1$	5	5	1	2674.990	37372.22	$a^5D_2-y^5F_2$
100	50	50	2933.057	34084.18	$4s^5S_2-4p^5P_1$		0		2674.861	37374.03	$a^5D_3-y^5F_2$
1			2932.32	34092.6	$a^5D_1-z^5S_2$	12	6	2	2673.384	37394.68	$a^5D_1-y^5F_2$
5	1	1	2927.394	34150.11	$a^5D_2-z^5D_3$	20	20	5	2672.588	37405.81	$a^5P_3-z^5D_4$
4	0	0	2927.221	34152.13	$a^5D_3-z^5D_3$	12	6	3	2667.033	37483.72	$a^5D_2-y^5F_3$
	0		2923.630	34194.07	$z^5D_4-e^5G_5$	?	2	1	2666.895	37485.66	$a^5D_3-y^5F_3$
2	1		2921.320	34221.11	$a^5D_4-z^5D_3$		1		2662.764	37543.81	$4d^7D_5-7f^7F_{6,5,4}$
					also ghost?		0		2661.994	37554.67	$4d^7D_4-7f^7F_{5,4,3}$
	4		2917.076	34270.90	$4d^7D_5-6f^7F_{6,5,4}$		0		2661.420	37562.77	$4d^7D_3-7f^7F_{4,3,2}$
	4		2916.155	34281.72	$4d^7D_4-6f^7F_{5,4,3}$		0		2661.005	37568.62	$4d^7D_2-7f^7F_{3,2,1}$
	3		2915.458	34289.91	$4d^7D_3-6f^7F_{4,3,2}$	10	6	2	2655.925	37640.48	$a^5D_3-y^5F_4$
	2		2914.956	34295.82	$4d^7D_2-6f^7F_{3,2,1}$	1	2	0	2651.039	37709.85	$a^5D_4-y^5F_4$
10	4	1	2902.902	34438.22	$a^5D_3-z^5D_4$	20	7	4	2639.857	37869.58	$a^5D_4-y^5F_5$
	1		2898.531	34490.15	$z^5D_3-e^5G_4$	20	20	5	2638.179	37893.66	$a^5G_2-z^5H_3$
15	10	2	2897.066	34507.59	$a^5D_4-z^5D_4$	()					
	0		2889.424	34598.85	$z^5D_2-e^5G_2$	?	3	0	2638.127	37894.40	$a^5G_3-z^5H_3$
	0		2889.311	34600.21	$z^5D_2-e^5G_3$	25	20	6	2632.358	37977.45	$a^5G_3-z^5H_4$
	2		2888.809	34606.22	$z^5D_1-e^5G_2$	8	4	1	2632.016	37982.38	$a^5G_4-z^5H_4$
	1		2871.679	34812.64	$z^5F_3-e^5G_4$	25	20	9	2625.607	38075.09	$a^5G_4-z^5H_5$
	0		2871.489	34814.95	$z^5F_3-e^5G_3$	4	5	1	2624.768	38087.25	$a^5G_5-z^5H_5$

21-foot grating except those whose wave-lengths are followed by an asterisk. The latter were taken from plates photographed with the quartz prism instrument. All wave-lengths are air wave-lengths.

The lines below 2000A are given in Table IIB. The vacuum spectrographs were necessarily employed for this region, and only vacuum wave-lengths are recorded.

It is perhaps worth noting that the number of lines in this list which originate in levels near 114,000 wave numbers, and which occur in the neon but not in the helium Schuler tube pictures, illustrates the enhancements that are obtained by the use of different noble gases.

Conclusion

Although most of the strong lines have been classified, there remain many unidentified. Large numbers of these are undoubtedly due to triplet-triplet combinations. There are, however, striking omissions among the quintet terms, of which the most notable are the $3d^5(^4F)4s\ ^5F$ and its triad of odd terms, and the two remaining terms of $3d^4(^6D)4sp$.

A few of the triplet terms have been dis-

Table IIA.—*Continued.*

1	2	3	4	5	6	1	2	3	4	5	6
28	30	10	2618.144	38183.61	$a^5G_6-z^5H_6$	5	3		2531.804	39485.67	$a^5D_1-y^5D_0$
4	2*u*	1	2616.489	38207.76	$a^5G_6-z^5H_6$	7	4	0	2530.725	39502.50	$a^5D_0-y^5D_1$
30	30	10	2610.207	38299.71	$a^5G_6-z^5H_7$	1			2517.39	39711.9	$a^5G_4-z^5D_4$
75	30	30	2605.696	38366.01	$4s^7S_3-4p^7P_2$, $a^5P_3-z^5P_2$	4	2*u*		2516.600	39724.20	$a^5G_5-z^5D_4$
						1*uu*	5		2479.346	40321.04	$z^5H_7-e^5H_7$
15	4	3	2603.727	38395.02	$a^5P_2-z^5P_3$		1		2473.64*	40414.1	$z^5H_6-e^5H_5$
3	3	2	2603.045	38405.08	$a^5D_2-y^5P_1$		3		2473.560	40415.35	$z^5H_6-e^5H_6$
5	2	1	2601.526	38427.50	$a^5D_1-y^5P_1$		2		2467.753	40510.45	$z^5H_5-e^5H_5$
4	1	0	2600.285	38445.85	$a^5D_0-y^5P_1$		2		2462.407	40598.39	$z^5H_4-e^5H_4$
6	1	1	2599.036	38464.32	$a^5D_2-y^5P_2$		0		2462.12*	40603.1	$z^5H_4-e^5H_5$
15	6	3	2598.910	38466.18	$a^5P_1-z^5P_2$, $a^5D_3-y^5P_2$	2*uu*	10		2458.583	40661.52	$z^5H_7-e^5I_8$
							0		2457.885	40673.07	$z^5H_7-e^5I_7$
2*u*			2597.56	38486.2	$a^5D_1-y^5P_2$		1		2457.785	40674.74	$z^5H_3-e^5H_3$
3			2596.76	38498.1	$a^5P_2-z^5P_2$	1*uu*	8	0	2453.620	40743.76	$4p^7P_4-4d^7D_3$
6	3	2	2594.736	38528.06	$a^5P_3-z^5P_2$	3*uu*	15	1	2453.133	40751.85	$4p^7P_4-4d^7D_4$
0	0		2594.404	38532.98	$a^5D_3-y^5P_3$	7*uu*	25	2	2452.488	40762.57	$4p^7P_4-4d^7D_5$
90	50	50	2593.731	38542.98	$4s^7S_3-4p^7P_3$, $a^5P_1-z^5P_1$		5		2452.323	40765.31	$z^5H_6-e^5I_7$
							0		2452.172	40767.72	$z^5H_6-e^5I_6$
7	3	2	2591.432	38577.17	$a^5P_2-z^5P_1$		1		2446.592	40860.79	$z^5H_5-e^5I_5$
	3		2590.229	38594.05	$4p^5P_1-4d^5D_2$		6		2446.385	40864.25	$z^5H_5-e^5I_6$
5	4	1	2589.987	38598.70	$4p^5P_1-4d^5D_1$ blend?		0		2441.475	40946.42	$z^5H_4-e^5I_4$
							5		2441.059	40953.40	$z^5H_4-e^5I_5$
	2		2589.824	38601.13	$4p^5P_1-4d^5D_0$	3*uu*	10	0	2438.192	41001.56	$4p^7P_3-4d^7D_2$
10	5	2	2589.729	38602.54	$a^5D_4-y^5P_3$	4*uu*	15	1	2437.848	41007.34	$4p^7P_3-4d^7D_3$
3*uu*	5	2	2585.889	38659.86	$4p^5P_2-4d^5D_3$	5*uu*	20	1	2437.368	41015.42	$4p^7P_3-4d^7D_4$
2*uu*	4	1	2585.440	38666.57	$4p^5P_2-4d^5D_2$	1*uu*	5		2436.539	41029.37	$z^5H_3-e^5I_4$
1*uu*	2	0	2585.130	38671.21	$4p^5P_2-4d^5D_1$	4*uu*	10	1	2427.939	41174.69	$4p^7P_2-4d^7D_3$
4*uu*	10	3	2578.813	38765.93	$4p^5P_3-4d^5D_4$	4*uu*	8	1	2427.719	41178.42	$4p^7P_3-4d^7D_2$
2*uu*	4	1	2578.280	38773.95	$4p^5P_3-4d^5D_3$	3*uu*	7	1	2427.379	41184.18	$4p^7P_2-4d^7D_2$
2*uu*	?		2577.84	38780.6	$4p^5P_3-4d^5D_2$		1		2419.81	41313.0	$a^5P_1-y^5P_1$
100	50	50	2576.113	38806.56	$4s^7S_3-4p^7P_4$		1		2417.94	41344.9	$a^5P_2-y^5P_1$
2	1		2566.035	38958.96	$a^5G_4-z^5F_5$	2	4		2416.35	41372.2	$a^5P_1-y^5P_2$
10	20	2	2565.219	38971.35	$a^5G_5-z^5F_5$	1	2		2412.74	41434.1	$a^5P_3-y^5P_2$
30	50	6	2563.641	38995.34	$a^5G_6-z^5F_5$	3	4		2410.57	41471.1	$a^5P_2-y^5P_3$
1	1		2559.737	39054.81	$a^5G_3-z^5F_4$	0	1		2408.85	41501.0	$a^5P_3-y^5P_3$
2	2		2559.676	39055.73	$a^5G_2-z^5F_1$		5		2402.071	41618.07	$z^5G_6-e^5H_7$
10	10	3	2559.413	39059.75	$a^5G_4-z^5F_4$		1		2401.946	41620.23	$z^5G_6-e^5H_6$
25	20	5	2558.607	39072.05	$a^5G_5-z^5F_4$		0		2400.211	41650.31	$z^5G_5-e^5H_5$
?	2		2557.595	39087.51	$a^5G_2-z^5F_2$		4		2400.150	41651.37	$z^5G_5-e^5H_6$
()							0		2399.050	41670.47	$z^5G_4-e^5H_4$
15	6	2	2557.540	39088.35	$a^5G_3-z^5F_2$		3		2398.789	41675.00	$z^5G_4-e^5H_5$
?	0		2556.942	39097.49	$a^5G_2-z^5F_3$		0		2398.23*	41684.7	$z^5G_3-e^5H_3$
()							2		2397.866	41691.04	$z^5G_3-e^5H_4$
12	8	2	2556.893	39098.24	$a^5G_2-z^5F_3$		2		2397.286	41701.13	$z^5G_2-e^5H_3$
20	15	4	2556.571	39103.17	$a^5G_4-z^5F_3$	3	4		2373.36	42121.5	$a^5P_3-y^5D_4$
5	5	0	2553.263	39153.83	$a^5D_3-y^5D_4$	2	1		2361.76	42328.4	$a^5P_2-y^5D_3$
15	15	3	2548.752	39223.12	$a^5D_4-y^5D_4$	1	2		2360.24*	42355.5	$a^5P_1-y^5D_2$
13	15	3	2543.461	39304.70	$a^5G_2-z^5D_1$	1	1		2360.10	42358.1	$a^5P_3-y^5D_3$
?	4		2542.984	39312.08	$a^5G_2-z^5D_2$		2		2359.44*	42369.9	$a^5P_1-y^5D_1$
()							0		2359.37*	42371.1	$a^5P_1-y^5D_0$
12	10	3	2542.928	39312.94	$a^5G_2-z^5D_2$		0		2358.46	42387.6	$a^5P_2-y^5D_2$
?	2		2541.168	39340.17	$a^5G_2-z^5S_2$		0		2357.65*	42402.1	$a^5P_2-y^5D_1$
()							0		2356.78*	42417.7	$a^5P_3-y^5D_2$
8	6	1	2541.115	39340.99	$a^5G_2-z^5S_2$		2		2348.82*	42561.5	$a^5G_2-y^5F_1$
8	6	1	2538.047	39388.54	$a^5D_2-y^5D_3$		3		2344.32*	42643.2	$a^5G_3-y^5F_2$
10	10	1	2537.926	39390.42	$a^5D_3-y^5D_3$		0		2338.21*	42754.6	$a^5G_2-y^5F_2$
5	3		2535.980	39420.65	$a^5G_3-z^5D_3$		1*u*		2337.96*	42759.2	$a^5G_4-y^5F_3$ also Fe
7	5		2535.660	39425.62	$a^5G_4-z^5D_3$						
7	8	1	2534.223	39447.97	$a^5D_2-y^5D_2$		0		2329.50*	42914.5	$a^5G_4-y^5F_4$
7	4	0	2534.102	39449.86	$a^5D_3-y^5D_2$		2		2328.83*	42926.9	$a^5G_5-y^5F_4$
1	0*u*		2533.463	39459.79	$a^5D_4-y^5D_3$		0		2320.20*	43086.4	$a^5G_5-y^5F_5$
7	5	0	2533.336	39461.80	$a^5D_2-y^5D_1$		2		2318.89*	43110.8	$a^5G_6-y^5F_5$
8	6	0	2532.782	39470.42	$a^5D_1-y^5D_2$		8		2305.010	43370.40	$4s^7S_3-4p^5P_3$
4	1		2531.897	39484.21	$a^5D_1-y^5D_1$		3		2298.95	43484.6	$4s^7S_3-4p^5P_2$

TABLE IIB. *Classified lines below 2000A. Columns 1 and 2, intensities due to neon and helium Schuler tube, respectively. Column 3, wave-length in vacuum. Column 4, wave number. Column 5, designation.*

1	2	3	4	5	1	2	3	4	5	1	2	3	4	5
5	11	1960.358	51011.1	$b^5D_4-w^5F_4$	10	10	1816.866	55039.8	$4p^5P_3-6s^5S_2$	10		1692.457	59085.7	$b^5D_1-6f^5F_{2,1}$
0	1	1955.060	51149.3	$b^5D_2-w^5F_1$	20	7	1816.287	55057.4	$b^5D_2-v^5D_4$,	0	8	1691.246	59128.0	$a^5P_1-x^5P_2$
7	12	1954.855	51154.7	$b^5D_3-w^5F_3$					$b^5D_1-v^5D_1$	4		1689.845	59177.0	$b^5D_0-6f^5F_1$
30	40	1953.233	51197.2	$b^5D_4-w^5F_5$	20	6	1815.243	55089.0	$b^5D_2-v^5D_3$	15	15	1689.614	59185.1	$4p^7P_3-6s^7S_3$
7	15	1950.919	51257.9	$b^5D_2-w^5F_2$	15	6	1813.863	55130.8	$b^5D_1-v^5D_2$	1	15	1689.489	59189.5	$a^5P_3-x^5P_2$
6	10	1948.277	51327.4	$b^5D_1-w^5F_1$	10	0	1813.287	55148.5	$b^5D_0-v^5D_1$	10	10	1684.576	59362.1	$4p^7P_2-6s^7S_3$
20	40	1947.945	51336.2	$b^5D_3-w^5F_4$	−1		1811.904	55190.7	$3d^5D_0-y^5F_1$	0	10	1680.401	59509.6	$a^5P_2-x^5P_1$
5	4	1946.919	51363.2	$b^5D_2-w^5P_1$	−1		1809.983	55249.1	$3d^5D_1-y^5F_1$	2	15	1679.564	59539.3	$a^5P_3-x^5P_2$
9	10	1946.335	51378.6	$b^5D_3-w^5P_2$	0		1807.347	55329.7	$3d^5D_1-y^5F_2$	6	?	1636.964	61088.7	$4p^7P_4-5d^7D_3$
12	25	1945.150	51409.9	$b^5D_2-w^5F_3$	−1		1804.446	55418.7	$b^5D_4-u^5F_5$		()			
5	12	1944.794	51419.3	$b^5D_0-w^5F_1$	8		1803.023	55462.4	$b^5D_4-u^5F_4$	15	?	1636.869	61092.2	$4p^7P_4-5d^7D_4$
10	15	1944.168	51435.9	$b^5D_1-w^5F_2$	()						()			
20	12	1942.645	51476.2	$b^5D_4-w^5P_3$	12		1802.979	55463.8	$b^5D_4-u^5F_5$	25	40	1636.751	61096.6	$4p^7P_4-5d^7D_5$
6	8	1940.191	51541.3	$b^5D_1-w^5P_1$	50	10	1801.272	55516.3	$b^5D_4-u^5P_3$	7	?	1630.004	61349.5	$4p^7P_3-5d^7D_2$
10	10	1936.717	51633.8	$b^5D_2-w^5P_2$,	2	5	1799.792	55561.9	$3d^5D_2-y^5F_3$		()			
				$b^5D_0-w^5P_1$	4		1793.903	55744.4	$b^5D_3-u^5F_3$	10	?	1629.940	61351.9	$4p^7P_3-5d^7D_3$
2		1934.790	51685.2	$3d^5D_0-z^5F_1$	0		1793.755	55749.0	$3d^5D_3-y^5F_3$		()			
1		1932.600	51743.8	$3d^5D_1-z^5F_1$	3		1792.519	55787.4	$b^5D_3-u^5F_4$	20	30	1629.845	61355.5	$4p^7P_3-5d^7D_4$
10	5	1931.408	51775.7	$3d^5D_1-z^5F_2$	25	4	1791.884	55807.2	$b^5D_3-u^5P_2$	20	()	1625.353	61525.1	$4p^7P_2-5d^7D_{2,1}$
8	7	1930.437	51801.7	$b^5D_3-w^5P_3$	20		1790.788	55841.3	$b^5D_3-u^5P_3$		20			
1		1928.121	51864.0	$3d^5D_2-z^5F_1$	1		1788.783	55903.9	$3d^5D_3-y^5F_4$	10	()	1625.278	61527.9	$4p^7P_2-5d^7D_3$
9	2	1926.939	51895.8	$3d^5D_2-z^5F_2$	2		1787.477	55944.8	$b^5D_2-u^5F_2$	1		1618.366	61790.7	$4s^5S_2-y^5P_1$
15	10	1926.579	51905.5	$3d^5D_2-z^5F_3$		1	1786.322	55980.9	$a^5D_2-x^5P_1$	1		1616.806	61850.3	$4s^5S_2-y^5P_2$
10	5	1925.506	51934.4	$3d^5D_0-z^5D_1$	1		1785.733	55999.4	$b^5D_2-u^5F_3$	1		1615.046	61917.7	$4s^5S_2-y^5P_3$
10	5	1923.341	51992.9	$3d^5D_1-z^5D_1$	−1	1	1785.026	56021.6	$a^5D_0-x^5P_1$	4		1541.059	64890.4	$4p^5P_1-7s^5S_2$
10	5	1923.060	52000.4	$3d^5D_1-z^5D_2$	15		1784.245	56046.1	$b^5D_3-u^5P_1$	5		1539.335	64963.1	$4p^5P_2-7s^5S_2$
5	2	1922.036	52028.2	$3d^5D_1-z^5S_2$	20	−1	1783.718	56062.7	$b^5D_2-u^5P_2$	7	1	1536.632	65077.4	$4p^5P_3-7s^5S_2$
25	15	1921.245	52049.6	$3d^5D_3-z^5F_4$	0		1783.184	56079.5	$b^5D_1-u^5F_1$	25	4	1442.594	69319.6	$4p^7P_4-7s^7S_3$
2		1920.959	52057.3	$b^5D_2-w^5P_3$	5		1782.626	56097.0	$b^5D_3-u^5F_3$	15	1	1437.126	69583.3	$4p^7P_3-7s^7S_3$
3	−1	1920.018	52082.8	$3d^5D_3-z^5F_2$	0		1781.816	56122.5	$b^5D_1-u^5F_2$	15	1	1433.481	69760.2	$4p^7P_2-7s^7S_3$
7	8	1919.639	52093.1	$3d^5D_3-z^5F_3$	−1		1780.248	56171.9	$3d^5D_4-y^5F_4$	5		1421.713	70337.7	$4p^5P_1-8s^5S_2$
2		1918.908	52113.0	$3d^5D_2-z^5D_1$		12	1778.686	56221.3	$a^5D_3-x^5P_2$,	8		1420.239	70410.7	$4p^5P_2-8s^5S_2$
6	5	1918.637	52120.3	$3d^5D_2-z^5D_2$					$a^5D_2-x^5P_2$	40	6	1419.612	70441.8	$4p^7P_4-6d^7D_{5,4,3}$
4		1917.599	52148.5	$3d^5D_2-z^5S_2$	20		1778.595	56224.1	$a^5D_1-u^5P_1$	10		1417.945	70524.6	$4p^5P_3-8s^5S_2$
30	20	1915.095	52216.7	$3d^5D_4-z^5F_5$	6		1778.090	56240.1	$a^5D_1-u^5P_2$	30	6	1414.398	70701.4	$4p^7P_3-6d^7D_{4,3,2}$
12	5	1914.677	52228.1	$3d^5D_2-z^5D_3$		0	1778.024	56242.2	$a^5D_1-x^5P_2$	25	5	1410.910	70876.2	$4p^7P_2-6d^7D_{2,1}$
12	10	1911.395	52317.8	$3d^5D_4-z^5F_4$	3		1776.057	56304.5	$3d^5D_0-y^5P_1$	2		1400.659	71394.9	$4p^5P_1-7d^5D_2$
5	0	1909.830	52360.7	$3d^5D_4-z^5F_3$	6		1775.693	56316.0	$a^5D_0-u^5P_1$	3		1400.568	71399.6	$4p^5P_1-7d^5D_1$
8	2	1907.839	52415.3	$3d^5D_3-z^5D_3$	2		1775.194	56331.9	$3d^5D_4-y^5F_5$	2		1400.538	71401.1	$4p^5P_1-7d^5D_0$
1		1898.134	52683.3	$3d^5D_4-z^5D_2$	5	0	1774.202	56363.4	$3d^5D_1-y^5P_1$	4		1399.395	71459.4	$4p^5P_2-7d^5D_3$
5	0	1897.464	52701.9	$3d^5D_3-z^5D_4$	5		1772.349	56422.3	$3d^5D_1-y^5P_2$	3		1399.244	71467.2	$4p^5P_2-7d^5D_2$
2		1869.042	53503.3	$3d^5D_2-z^5P_3$	1		1770.441	56483.1	$3d^5D_2-y^5P_1$	2		1399.153	71471.8	$4p^5P_2-7d^5D_1$
4	1	1868.588	53516.3	$3d^5D_1-z^5P_2$	7	1	1768.591	56542.2	$3d^5D_2-y^5P_2$	6	2	1397.394	71561.8	$4p^5P_3-7d^5D_4$
0		1868.312	53524.2	$b^5D_4-v^5F_4$	1	7	1767.665	56571.8	$a^5D_3-x^5P_2$	3		1397.170	71573.3	$4p^5P_3-7d^5D_3$
5	2	1867.872	53536.8	$3d^5D_0-z^5P_1$	5		1766.498	56609.2	$3d^5D_2-y^5P_3$	2	3	1388.877	72000.6	$3d^5D_0-5p^5P_1$
10	8	1865.831	53595.4	$3d^5D_1-z^5P_1$	3	10	1765.495	56641.3	$a^5D_4-x^5P_3$	2	3	1388.206	72035.4	$3d^5D_1-5p^5P_2$
12	8	1865.547	53603.6	$b^5D_3-v^5P_2$	1		1762.754	56729.4	$3d^5D_3-y^5P_2$	6	5	1387.749	72059.1	$3d^5D_1-5p^5P_1$
8	5	1865.296	53610.8	$b^5D_2-v^5P_1$	10		1760.680	56796.2	$3d^5D_3-y^5P_3$	10	7	1385.892	72155.7	$3d^5D_2-5p^5P_2$
15	10	1864.617	53630.3	$b^5D_4-v^5F_5$	−1		1755.073	56977.7	$a^5P_2-5p^5P_3$	4	4	1385.431	72179.7	$3d^5D_2-5p^5P_1$
10	8	1864.403	53636.5	$3d^5D_2-z^5P_2$	−1		1754.847	56985.0	$a^5P_1-5p^5P_2$	4	6	1383.049	72304.0	$3d^5D_3-5p^5P_3$
20	15	1862.816	53682.2	$b^5D_4-v^5P_3$	1		1754.136	57008.1	$a^5P_3-5p^5P_3$	10	10	1382.298	72343.3	$3d^5D_3-5p^5P_2$
10	6	1862.518	53690.7	$3d^5D_3-z^5P_3$	−1		1752.932	57047.3	$a^5P_3-5p^5P_2$	15	12	1377.938	72572.2	$3d^5D_4-5p^5P_3$
10	8	1861.663	53715.4	$3d^5D_2-z^5P_1$	0		1752.412	57064.2	$3d^5D_4-y^5P_3$		0	1360.236	73516.7	$a^5D_2-w^5F_2$
3	0	1860.425	53751.1	$b^5D_3-v^5F_3$	6	()	1750.202	57136.3	$4p^5P_1-5d^5D_2$		2	1359.861	73536.9	$a^5D_1-w^5F_2$
8	8	1859.444	53779.5	$b^5D_4-w^5D_3$		5u				1	0	1358.323	73620.2	$a^5D_2-w^5P_1$
10	8	1859.119	53788.9	$b^5D_1-v^5P_1$	8	()	1750.115	57139.1	$4p^5P_1-5d^5D_{1,0}$	1	0	1357.915	73642.3	$a^5D_1-w^5P_1$
20	12	1857.918	53823.7	$3d^5D_3-z^5P_2$	12	6	1748.137	57203.7	$4p^5P_2-5d^5D_3$		5	1357.451	73667.5	$a^5D_3-w^5F_3$,
10	10	1857.018	53849.8	$b^5D_3-v^5F_4$	10	5	1748.000	57208.2	$4p^5P_2-5d^5D_2$					$a^5D_3-w^5F_3$
12	10	1856.700	53859.0	$v^5D_2-v^5P_2$	3		174791.9	57210.9	$4p^5P_2-5d^5D_1$		5	1354.084	73850.7	$a^5D_3-w^5F_4$
9	5	1855.942	53881.0	$b^5D_0-v^5P_1$	15	10	1744.836	57312.0	$4p^5P_3-5d^5D_4$	6	5	1553.326	73892.0	$a^5D_3-w^5P_2$,
20	12	1854.902	53911.2	$b^5D_4-w^5D_4$	5	3	1744.659	57317.8	$4p^5P_3-5d^5D_3$					$a^5D_3-w^5P_2$
3		1854.268	53929.6	$b^5D_2-v^5F_2$	2		1744.537	57321.8	$4p^5P_3-5d^5D_2$	1	0	1352.828	73919.2	$a^5D_4-w^5F_4$
25	20	1853.271	53958.6	$3d^5D_4-z^5P_3$	4	0	1743.349	57360.9	$3d^5D_0-y^5D_1$	2	5	1349.408	74106.6	$a^5D_4-w^5F_5$
10	10	1852.810	53972.1	$b^5D_3-w^5D_2$	6		1741.983	57405.8	$3d^5D_1-y^5D_2$		2	1345.619	74315.2	$a^5D_3-w^5P_2$,
15	12	1851.597	54007.4	$b^5D_3-v^5P_2$,	5		1741.651	57416.8	$3d^5D_3-y^5D_4$					$a^5D_2-w^5P_2$
				$b^5D_2-v^5F_3$	4		1741.535	57420.6	$3d^5D_1-y^5D_{1,0}$	5	6	1344.352	74385.3	$a^5D_4-w^5P_3$
5	8	1850.602	54036.5	$b^5D_1-v^5P_2$	6	3	1740.155	57466.1	$3d^5D_2-y^5D_3$	25		1335.271	74891.2	$4p^7P_4-8s^7S_3$
3	0	1849.937	54055.9	$b^5D_1-v^5F_1$	4	1	1738.349	57525.8	$3d^5D_2-y^5D_2$	12		1330.606	75153.7	$4p^7P_3-8s^7S_3$
20	15	1848.266	54104.8	$b^5D_3-w^5D_3$	5	2	1737.930	57539.7	$3d^5D_2-y^5D_1$	12		1327.476	75330.9	$4p^7P_2-8s^7S_3$
10	8	1848.161	54107.8	$b^5D_3-v^5F_2$	12	7	1734.491	57653.8	$3d^5D_3-y^5D_3$	15		1323.784	75541.0	$4p^7P_4-7d^7D_{5,4,3}$
10	10	1847.780	54119.0	$b^5D_2-w^5D_1$	15	10	1733.556	57684.9	$3d^5D_4-y^5D_4$	10		1319.209	75803.0	$4p^7P_3-7d^7D_{4,3,2}$
4	2	1846.790	54148.0	$b^5D_0-v^5F_1$	6	5	1732.707	57713.2	$3d^5D_3-y^5D_2$	3	1	1318.086	75867.6	$a^5D_2-v^5P_1$
5	()	1844.080	54227.6	$b^5D_2-w^5D_2$	5	3	1726.481	57921.3	$3d^5D_4-y^5D_3$	4	2	1317.703	75889.6	$a^5D_1-v^5P_1$
	15				3		1725.621	57950.1	$b^5D_3-t^5F_4$	3	0	1317.392	75907.5	$a^5D_0-v^5P_1$
6	()	1844.027	54229.1	$b^5D_1-w^5D_0$	15	2	1725.295	57961.1	$b^5D_4-t^5F_5$	9		1316.161	75978.5	$4p^7P_2-7d^7D_{3,2,1}$
1		1843.784	54236.3	$b^5D_3-w^5D_4$	8		1716.138	58270.4	$b^5D_3-t^5F_3$	10	10	1313.766	76117.0	$a^5D_3-v^5P_2$,
5	2	1842.871	54263.1	$b^5D_2-v^5P_3$	12	0	1715.984	58275.6	$b^5D_3-t^5F_4$					$a^5D_2-v^5P_2$
3		1841.718	54297.1	$b^5D_1-w^5D_1$	20		1714.403	58329.3	$b^5D_4-6f^5F_{5,4,3}$	2	0	1313.407	76137.9	$a^5D_1-v^5P_2$
5	1	1839.595	54359.8	$b^5D_2-w^5D_3$	6	0	1708.652	58525.7	$b^5D_2-t^5F_3$	1		1309.293	76377.1	$a^5D_3-w^5D_1$
3	2	1838.607	54389.0	$b^5D_0-w^5D_1$	4		1708.553	58529.0	$b^5D_2-t^5F_2$	1		1307.409	76487.1	$a^5D_3-w^5D_2$
4	2	1838.050	54405.5	$b^5D_1-w^5D_2$	15	0	1704.866	58655.6	$b^5D_3-6f^5F_{4,3,2}$	10	6	1306.814	76522.0	$a^5D_2-v^5P_3$
25	6	1834.572	54508.6	$b^5D_4-v^5D_3$	5		1703.366	58707.3	$b^5D_1-t^5F_2$	5	4	1306.168	76559.8	$a^5P_2-w^5P_1$
20	4	1828.250	54697.1	$b^5D_3-v^5D_2$	3		1700.692	58799.6	$b^5D_0-t^5F_1$	15	12	1305.628	76591.5	$a^5D_4-v^5P_3$
50	15	1827.078	54732.2	$b^5D_4-v^5D_4$	4	2	1700.355	58811.2	$4s^5S_2-z^5P_3$	1		1302.117	76798.0	$a^5P_1-w^5P_2$
30	8	1823.697	54833.7	$b^5D_3-v^5D_3$		2	1698.132	58888.2	$a^5P_1-x^5P_1$	3	4	1301.061	76860.3	$a^5P_3-w^5P_2$
8	5	1823.049	54853.2	$4p^5P_1-6s^5S_2$	12		1697.526	58909.2	$b^5D_2-6f^5F_{3,2,1}$	5		1296.669	77120.7	$a^5D_1-v^5D_0$
10	2	1822.212	54878.3	$b^5D_2-v^5D_1$	15	20	1697.181	58921.2	$4p^5P_4-6s^5S_2$,	6	1	1296.429	77134.9	$a^5D_2-v^5D_1$
9	8	1820.648	54925.5	$4p^5P_2-6s^5S_2$					$a^5P_2-x^5P_1$	3		1296.031	77158.6	$a^5D_1-v^5D_1$
9	0	1819.751	54952.6	$b^5D_3-v^5D_2$	4	1	1696.516	58944.3	$4s^5S_2-z^5P_2$	6	1	1295.736	77176.2	$a^5D_0-v^5D_1$
6	2	1817.493	55020.8	$b^5D_1-v^5D_0$	3		1694.252	59023.1	$4s^5S_2-z^5P_1$					

TABLE IIB.—*Continued.*

1	2	3	4	5	1	2	3	4	5	1	2	3	4	5
10	3	1295.150	77211.1	$a^5D_3-v^5D_2$,	20		1236.770	80855.8	$a^5G_4-5f^5F_3$	25		1156.658	86456.0	$a^5G_5-6f^5F_4$
				$a^5D_2-v^5D_2$	15		1236.545	80870.5	$a^5G_3-5f^5F_4$,	30		1156.345	86479.4	$a^5G_6-6f^5F_5$
10	2	1294.803	77231.8	$a^5D_1-v^5D_2$					$a^5D_4-t^5F_5$	6		1116.374	89575.7	$a^5G_2-s^5F_1$
2	2	1294.437	77253.7	$a^5P_2-w^5P_3$	25	3	1236.148	80896.5	$a^5G_2-v^5G_2$,	6		1115.529	89643.6	$a^5G_3-s^5F_2$
1	0	1293.932	77283.8	$a^5P_3-w^5P_3$					$a^5G_6-5f^5F_5$	0		1114.500	89726.3	$a^5G_3-s^5F_3$
15	7	1292.877	77346.9	$a^5D_3-v^5D_3$,	25	4	1235.869	80914.7	$a^5G_3-v^5G_3$	8		1114.437	89731.4	$a^5G_4-s^5F_4$
				$a^5D_2-v^5D_3$	10		1235.793	80919.7	$a^5G_4-v^5G_3$	0		1113.389	89815.9	$a^5G_4-s^5F_4$
10	()	1291.702	77417.2	$a^5D_4-v^5D_3$	25		1235.463	80941.3	$a^5G_4-v^5G_4$	9		1113.232	89828.5	$a^5G_5-s^5F_4$
	15				10	0	1235.273	80953.8	$a^5G_3-v^5G_4$	0		1112.195	89912.3	$a^5G_5-s^5F_5$
10	()	1291.584	77424.3	$4s^5S_2-5p^5P_2$	8	−2	1235.060	80967.7	$a^5G_4-v^5G_5$	10		1111.898	89936.3	$a^5G_6-s^5F_5$
10	5	1290.926	77463.8	$4s^5S_2-5p^5P_2$	25	5	1234.871	80980.1	$a^5G_5-v^5G_5$	−1		1093.218	91473.1	$3d^5D_1-w^5F_2$
8	2	1290.524	77487.9	$4s^5S_2-5p^5P_1$	8	−1	1234.507	81004.0	$a^5G_6-v^5G_5$	1		1089.981	91744.7	$3d^5D_2-w^5F_2$
15	4	1289.132	77571.6	$a^5D_3-v^5D_4$	5		1234.301	81017.5	$a^5G_5-v^5G_6$	2		1085.619	92113.3	$3d^5D_3-w^5F_4$
15	6	1287.978	77641.1	$a^5D_4-v^5D_4$	30	5	1233.952	81040.4	$a^5G_6-v^5G_6$	5	2	1080.288	92567.9	$3d^5D_4-w^5F_5$
2		1279.443	78159.0	$a^5D_2-u^5F_1$	5		1231.346	81211.9	$a^5P_1-u^5P_1$	3		1077.017	92849.0	$3d^5D_4-w^5P_3$
10		1279.089	78180.6	$a^5D_1-u^5F_1$	8		1231.101	81228.1	$a^5P_1-u^5P_2$	10		1069.775	93477.6	$3d^5D_0-5f^5F_1$
15	1	1278.749	78201.4	$a^5D_2-u^5F_2$	10		1230.873	81243.1	$a^5P_2-u^5P_1$	20	1	1069.110	93535.7	$3d^5D_1-5f^5F_2$
10	0	1278.369	78224.7	$4p^7P_4-9s^7S_3$,	1		1230.622	81259.7	$a^5P_2-u^5P_2$	23	3	1067.729	93656.7	$3d^5D_2-5f^5F_3$
				$a^5D_1-u^5P_1$	1		1230.457	81270.6	$a^5P_3-u^5F_4$	25	4	1065.564	93847.0	$3d^5D_3-5f^5F_4$
20	4	1277.817	78258.5	$a^5D_3-u^5F_3$,	15		1230.152	81290.8	$a^5P_3-u^5P_2$	1		1063.430	94035.3	$3d^5D_0-v^5F_1$
				$a^5D_2-u^5F_3$	20		1230.106	81293.8	$a^5P_2-u^5P_3$	30		1062.507	94117.0	$3d^5D_4-5f^5F_5$
20	4	1277.119	78301.2	$a^5D_2-u^5P_1$,	25		1229.653	81323.7	$a^5P_3-u^5P_3$	1		1061.640	94193.9	$3d^5D_2-v^5P_2$
				$a^5D_3-u^5F_4$	20	3	1228.423	81405.2	$a^5G_2-v^5F_1$	1		1059.980	94341.4	$3d^5D_2-v^5F_2$
10		1276.772	78322.5	$a^5D_3-u^5P_2$,	23	3	1227.638	81457.2	$a^5G_3-v^5F_2$	1		1059.530	94381.5	$3d^5D_3-v^5P_2$
				$a^5D_2-u^5P_2$	25	4	1226.396	81539.7	$a^5G_4-v^5F_3$	4		1056.802	94625.1	$3d^5D_3-v^5F_4$
8		1276.450	78342.3	$a^5D_1-u^5P_2$,	6	0	1224.928	81637.4	$a^5G_4-v^5F_4$	5		1052.599	95002.9	$3d^5D_4-v^5F_5$
				$a^5D_0-u^5P_1$	28	5	1224.733	81650.4	$a^5G_5-v^5F_4$	5		1052.037	95053.7	$3d^5D_4-v^5P_2$
20		1276.238	78355.3	$a^5D_3-u^5P_3$,	8	0	1223.152	81756.0	$a^5G_5-v^5F_5$	2u		1050.782	95167.2	$3d^5D_1-v^5D_2$
				$a^5D_2-u^5P_3$	30	6	1222.785	81780.5	$a^5G_6-v^5F_5$	4		1047.952	95424.2	$3d^5D_2-v^5D_3$
40	7	1275.973	78371.6	$a^5D_4-u^5F_5$,	20		1205.423	82958.4	$a^5G_3-v^5H_3$	1		1047.401	95474.4	$3d^5D_2-v^5D_2$
				$a^5D_4-u^5F_4$	25		1204.619	83013.8	$a^5G_3-v^5H_4$	4		1045.887	95612.6	$3d^5D_3-v^5D_3$
20		1275.102	78425.1	$a^5D_4-u^5P_3$	30		1203.252	83108.2	$a^5G_4-v^5H_5$	3		1043.456	95835.4	$3d^5D_3-v^5D_4$
2		1274.077	78488.2	$4p^7P_3-9s^7S_3$	8		1203.068	83120.8	$a^5G_5-v^5H_5$	3		1042.979	95879.2	$3d^5D_4-v^5D_3$
2		1271.217	78664.8	$4p^7P_2-9s^7S_3$	40		1201.570	83224.4	$a^5G_5-v^5H_6$	8		1040.538	96104.1	$3d^5D_4-v^5D_4$
5	1	1269.417	78776.3	$a^5P_1-v^5P_1$	5		1201.233	83247.8	$a^5G_6-v^5H_6$	2		1032.687	96834.8	$3d^5D_4-w^5F_5$
10	5	1268.905	78808.1	$a^5P_2-v^5P_1$	20	10	1201.124	83255.3	$4s^7S_3-z^7P_2$	10	5	1030.866	97005.8	$4s^5S_2-w^5P_1$
10	4	1265.383	79027.4	$a^5P_1-v^5P_2$	25	11	1199.388	83375.9	$4s^7S_3-z^7P_3$	18	4	1027.995	97276.7	$4s^5S_2-w^5P_2$
				blend	40		1199.341	83379.1	$a^5G_6-v^5H_7$	20	10	1023.546	97699.6	$4s^5S_2-w^5P_3$
12	6	1264.447	79085.9	$a^5P_3-v^5P_3$	10		1198.630	83428.6	$a^5G_2-u^5F_1$	0u		1013.349	98682.7	$3d^5D_0-t^5F_1$
1		1263.794	79126.8	$a^5P_2-v^5F_2$	10		1197.996	83472.7	$a^5G_3-u^5F_2$	4		1012.713	98744.6	$3d^5D_1-t^5F_2$
4		1262.566	79203.8	$a^5P_2-v^5F_3$	10		1197.565	83502.8	$3d^5D_0-4f^5F_1$	5		1011.506	98862.5	$3d^5D_2-t^5F_3$
4	0	1262.353	79217.1	$a^5P_1-w^5D_0$	40	13	1197.172	83530.2	$4s^7S_3-z^7P_4$	6		1009.562	99052.8	$3d^5D_3-t^5F_4$
8	2	1261.282	79284.4	$a^5P_1-w^5D_1$	25	6	1196.724	83561.4	$3d^5D_1-4f^5F_2$	10		1009.448	99064.1	$3d^5D_0-6f^5F_1$
1	0	1260.768	79316.7	$a^5P_2-w^5D_1$	20		1196.517	83575.9	$a^5G_4-u^5F_4$	12		1008.848	99123.0	$3d^5D_1-6f^5F_2$
1		1260.523	79332.1	$a^5P_3-v^5F_4$	25		1196.333	83588.8	$a^5G_5-u^5F_5$, 4	15		1007.612	99244.5	$3d^5D_2-6f^5F_3$
6	6	1259.967	79367.1	$4s^5S_2-x^5P_2$	30		1195.973	83613.9	$a^5G_6-u^5F_5$	15	5	1007.530	99252.6	$4s^5S_2-v^5P_1$
8	1	1259.561	79392.7	$a^5P_1-w^5D_2$	30	8	1194.998	83682.1	$3d^5D_2-4f^5F_3$	7		1006.721	99332.4	$3d^5D_4-t^5F_5$
12	1	1259.049	79425.0	$a^5P_2-w^5D_2$	40	10	1192.313	83870.6	$3d^5D_3-4f^5F_4$	22		1005.702	99433.0	$3d^5D_3-6f^5F_4$
15	5	1258.513	79458.8	$a^5P_2-v^5P_3$	50	12	1188.502	84139.5	$3d^5D_4-4f^5F_5$	20	4	1005.019	99500.6	$4s^5S_2-v^5P_2$
15	3	1258.028	79489.5	$a^5P_3-v^5P_3$	1		1180.693	84696.0	$a^5D_4-t^5F_5$	22		1003.000	99700.9	$3d^5D_4-6f^5F_5$
10	2	1256.957	79557.2	$a^5P_2-w^5D_3$	15		1168.254	85597.8	$a^5G_4-u^5G_4$	25	6	1000.956	99904.5	$4s^5S_2-v^5P_3$
8	2	1256.474	79587.8	$a^5P_3-w^5D_3$	5		1168.069	85611.4	$a^5G_5-u^5G_4$	15		983.403	101687.7	$4s^5S_2-u^5P_1$
6	7	1256.175	79606.7	$4s^5S_2-x^5P_2$	9		1167.306	85667.3	$a^5G_4-u^5G_5$	20		983.240	101704.5	$4s^5S_2-u^5P_2$
15	6	1254.407	79718.9	$a^5P_3-w^5D_4$	20		1167.130	85680.2	$a^5G_5-u^5G_5$	25		982.901	101739.6	$4s^5S_2-u^5P_3$
7	10	1250.681	79956.4	$4s^5S_2-x^5P_3$	8		1166.810	85703.7	$a^5G_6-u^5G_5$	0		978.703	102176.0	$3d^5D_0-7f^5F_1$
6		1249.315	80043.9	$a^5P_1-v^5D_1$	10		1166.157	85751.7	$a^5G_5-u^5G_6$	5		978.115	102237.5	$3d^5D_1-7f^5F_2$
4		1248.827	80075.1	$a^5P_2-v^5D_1$	25		1165.823	85776.3	$a^5G_6-u^5G_6$	7		976.964	102357.9	$3d^5D_2-7f^5F_3$
5		1248.149	80118.6	$a^5P_1-v^5D_2$	30	12	1164.211	85895.1	$4s^7S_3-5p^7P_2$	8		975.189	102544.2	$3d^5D_3-7f^5F_4$
15		1247.650	80150.1	$a^5P_2-v^5D_2$	40	14	1163.324	85960.6	$4s^7S_3-5p^7P_3$	10		972.547	102822.8	$3d^5D_4-7f^5F_5$
15		1245.551	80285.7	$a^5P_2-v^5D_3$	50	16	1162.017	86057.3	$4s^7S_3-5p^7P_4$,	−1		957.205	104470.8	$3d^5D_2-8f^5F_3$
0		1244.105	80379.1	$4p^7P_4-10s^7S_3$					$a^5G_4-t^5F_3$	0		955.481	104659.3	$3d^5D_3-8f^5F_4$
10		1241.626	80539.5	$a^5P_3-v^5D_4$	20		1161.764	86076.0	$a^5G_5-t^5F_4$	1		953.039	104927.5	$3d^5D_4-8f^5F_5$
0		1240.037	80642.7	$4p^7P_3-10s^7S_3$	3		1161.612	86087.3	$a^5G_5-t^5F_5$					
1		1237.784	80789.5	$a^5D_3-t^5F_4$	20	0	1161.295	86110.8	$a^5G_6-t^5F_5$					
20		1236.873	80849.0	$a^5G_3-5f^5F_2$,	20		1156.919	86436.5	$a^5G_3-6f^5F_2$					
				$a^5G_2-5f^5F_1$	20		1156.834	86442.8	$a^5G_4-6f^5F_3$					

covered, but inasmuch as they represent a mere fragment of the system and have not as yet been connected by intersystem lines to the normal state, it was thought best not to include them in this report.

I am greatly indebted to Professor A. G. Shenstone. Not only were his suggestions invaluable, but some of the identifications were made by him. I wish also to thank Professor H. N. Russell for his suggestions and Professor J. C. Boyce for permitting me to use the vacuum spectrograph at the Massachusetts Institute of Technology. Many discussions with Dr. L. Green have been most helpful.

Domain Theory of Ferromagnetics Under Stress

Part II. Magnetostriction of Polycrystalline Material*

WILLIAM FULLER BROWN, JR.
Columbia University, New York, New York

(Received January 7, 1938)

From the general formulas of Part I, expressions are derived for the magnetostriction of polycrystalline iron and nickel when the domains are isotropic, and when they are crystalline and have [111] or [100] as the direction of easy magnetization. The effect of assuming uniform strain rather than uniform stress is discussed. For iron at room temperature the experimental data fit the theoretical curve over a limited range; the deviations at high and low magnetizations can be explained qualitatively. For nickel at temperatures from 6°C to the Curie point, excellent agreement is found between theory and experiment. The analysis indicates that for the specimen studied, the domains are polycrystalline at low temperatures, but become smaller than the crystals at a little below 200°C, where the direction of easy magnetization becomes [100]. From the measurements at the higher temperatures, values are obtained for the saturation magnetostriction of nickel crystals magnetized in the [100] direction; from these and the saturation magnetostriction of polycrystalline nickel, values for the [111] direction are calculated.

THE magnetostriction of single crystals of nickel and iron has been calculated theoretically as a function of magnetization by Heisenberg, Gans and v. Harlem and Fowler.[1] The theory assumes that magnetization occurs in two separate stages: at low fields, a change in the magnetization of individual domains from one "easy magnetization" direction to another, without appreciable rotation out of these directions, until finally all the domains are magnetized as nearly parallel to the field direction as this permits; at higher fields, a rotation of the magnetization vector toward the field direction. The theoretical curves agree well with experiment except in the transition region where, actually, there is appreciable overlapping of the two processes.

In Part I under the present title,[2] the theory for the first stage of magnetization was developed in a general form capable of application to any ferromagnetic. The general formulas will now be used to calculate the longitudinal magnetostriction of polycrystalline nickel or iron under various assumptions in regard to its structure. An analysis will then be made of data obtained by the writer on Armco iron at room temperature, and by Kirkham on nickel at various temperatures.

PRELIMINARY FORMULAS

We assume first that all components of stress are uniform and equal to zero. We shall later consider the alternative assumption that the strains are uniform and such as to make the average stresses zero.

In polycrystalline material the crystals may be larger or smaller than the domains; the size of the latter, according to the measurements of Bozorth and Dillinger,[3] is from 10^{-9} to 5×10^{-8} cm³ and depends very little on the crystalline structure of the material. If the crystals are large, the domains must be regarded as crystalline and grouped into classes in accordance with the orientation of their crystal axes in space. It is more convenient, however, to consider the orientation of fixed axes (Ox_1', Ox_2', Ox_3') with respect to the crystal axes (Ox_1, Ox_2, Ox_3) of a domain. We shall take Ox_3' to be the direction of the field **H**. The arbitrary assignment of labels 1, 2, 3 to three properly related tetragonal axes of each domain is to be carried out in a completely random manner. The directions of the field with respect to these different sets of domain axes, if plotted as different directions in a single $x_1x_2x_3$-system, will then be distributed uniformly over the unit sphere. For present purposes we may

* Publication assisted by the Ernest Kempton Adams Fund for Physical Research of Columbia University.

[1] W. Heisenberg, Zeits. f. Physik **69**, 287 (1931); R. Gans and J. v. Harlem, Ann. d. Physik **16**, 162 (1933); R. H. Fowler, *Statistical Mechanics*, second edition (1936), p. 520.

[2] W. F. Brown, Phys. Rev. **52**, 325 (1937): hereafter cited as I.

[3] R. M. Bozorth and J. F. Dillinger, Phys. Rev. **35**, 733 (1930).

group together, as a single class, all domains for which this direction (l_1, l_2, l_3) or (φ, ϑ) is within a solid angle $d\omega$, and the number of domains in this class will be $d\omega/4\pi$. In the analysis of transverse effects it is necessary to consider also different orientations of the Ox_1'- and Ox_2'-axes about the direction (l_1, l_2, l_3), for instance by introducing the third Eulerian angle ψ.

If all the domains are of a single class (l_1, l_2, l_3), as is the case in a crystal, the contribution of any domain to the magnetostriction $\lambda(l)$[4] will depend on the particular "easy magnetization" direction in which the domain happens to be magnetized. If this contribution is $\lambda_\sigma(l)$ when the domain is magnetized in the σth easy-magnetization direction, the resultant magnetostriction is a weighted average of $\lambda_\sigma(l)$ over all values of σ. The weighting factors, which of course are proportional to the number of domains in the various states σ, are given according to the theory by formulas very similar to those of statistical mechanics. There is this difference, however: the quantity analogous to $1/kT$ is an undetermined multiplier, which must be eliminated between the equation for the magnetostriction and the similar equation for the parallel component of magnetization J_p, in order to obtain the former as a function of the latter. Thus for a single crystal

$$\lambda(l)=S_1(l)/S(l), \quad J_p(l)=S_0(l)/S(l), \tag{1}$$

where

$$S(l)=\sum_\sigma \exp\left[L_0HJ_{p\sigma}(l)\right],$$

$$S_0(l)=\sum_\sigma J_{p\sigma}(l)\exp\left[L_0HJ_{p\sigma}(l)\right], \tag{2}$$

$$S_1(l)=\sum_\sigma \lambda_\sigma(l)\exp\left[L_0HJ_{p\sigma}(l)\right].$$

For a polycrystalline specimen, Eqs. (12′) and (13′) of I show that Eqs. (1) are to be averaged over the unit sphere: thus

$$\lambda=\int\left[S_1(l)/S(l)\right]d\omega/4\pi,$$

$$J=\int\left[S_0(l)/S(l)\right]d\omega/4\pi \tag{3}$$

are the parametric equations of the magnetostriction-magnetization curve. The parameter is L_0H, and its range is from 0 to ∞; the Lagrangian multiplier L_0 ($=-L$ of I) is a positive quantity, but nothing in the theory as so far developed indicates that it is necessarily a constant, and therefore Eqs. (3) do not give the magnetization and magnetostriction as functions of the field strength H.

If the crystals are very small, so that each domain contains a large number of them, the domains may be treated as isotropic. There is then only one class of domain, so that instead of Eq. (3) we have

$$\lambda=S_1/S, \quad J=S_0/S; \tag{4}$$

but every direction is a direction of easy magnetization, so that the S's, instead of being sums over a finite number of such directions, are integrals over the unit sphere. Let $\lambda(\theta)$ and $J_p(\theta)$ be the magnetostriction and the parallel component of magnetization of a domain when it happens to be magnetized in a direction making an angle θ with the field direction: then

$$S=\int \exp\left[L_0HJ_p(\theta)\right]d\omega/4\pi,$$

$$S_0=\int J_p(\theta)\exp\left[L_0HJ_p(\theta)\right]d\omega/4\pi, \tag{5}$$

$$S_1=\int \lambda(\theta)\exp\left[L_0HJ_p(\theta)\right]d\omega/4\pi.$$

The case of isotropic domains is the simplest and will therefore be treated first.

Isotropic Domains

We have at once $J_p(\theta)=J_s\cos\theta$, where J_s is the saturation magnetization. To evaluate the longitudinal magnetostriction we shall first write down the thermodynamic potential F_{HX} whose partial derivatives with respect to the field- and stress-components (with sign reversed) give the magnetization- and strain-components. For a cubic crystal this function is given by Eq. (24) of I, with the substitutions mentioned after Eq. (23′). For an isotropic domain it simplifies to

$$F_{HX}=-J_s\sum H_i\alpha_i-\kappa_0\sum X_{ii} \\ -\kappa(\sum X_{ii}\alpha_i^2+2\sum X_{jk}\alpha_j\alpha_k)+W_e, \tag{6}$$

where W_e, the purely elastic part, is quadratic in the stress components X_{ij}. We are neglecting

[4] The symbol (l), standing of course for (l_1, l_2, l_3), corresponds to the superscript τ used to distinguish different classes of domains in the general theory.

terms of fourth degree in the direction cosines $(\alpha_1, \alpha_2, \alpha_3)$ of the domain magnetization. The form of (6) follows directly from symmetry considerations and the assumption that it is necessary to consider only the lowest order interaction terms (i.e., terms containing both mechanical and magnetic quantities). From (6) it follows that when the stresses are zero

$$e_{ii} = -\partial F_{HX}/\partial X_{ii} = \kappa_0 + \kappa\alpha_i^2 = \kappa(\alpha_i^2 - \tfrac{1}{3}), \quad (7)$$

$$e_{jk} = -\partial F_{HX}/\partial X_{jk} = 2\kappa\alpha_j\alpha_k. \quad (8)$$

The relation $\kappa_0 = -\frac{1}{3}\kappa$ used in (7) is necessary if the average strains are to be zero in the demagnetized state. From (7) and (8),[5]

$$\lambda(\theta) = \sum e_{ii}l_i^2 + \sum e_{jk}l_jl_k = \kappa[(\sum l_i\alpha_i)^2 - \tfrac{1}{3}] = \kappa(\cos^2\theta - \tfrac{1}{3}). \quad (9)$$

At saturation $\theta = 0$ for all domains, hence by (9) the saturation magnetostriction λ_∞ is equal to $2\kappa/3$, and to Eq. (27) of I we may add the corresponding equation for isotropic domains,

$$\kappa = 3\lambda_\infty/2. \quad (10)$$

When the domains are isotropic, there is only one stage of magnetization; it has been analyzed by Becker and Kersten[6] as a rotation process occurring under the joint action of the field and of internal stresses of a specified sort. Here we are regarding it as a limiting case of changes from one direction of easy magnetization to another, under the joint action of the field and of random influences of unspecified nature. The two theories, although different in their approach, will be seen to have many points in common.

Letting $\cos\theta = \gamma$ and $L_0HJ_s = \eta$, we now have from (5)

$$S = \tfrac{1}{2}\int_{-1}^{1} e^{\eta\gamma}d\gamma = (\sinh\eta)/\eta, \quad (11)$$

$$S_0 = J_s dS/d\eta, \quad S_1 = \kappa(d^2S/d\eta^2 - \tfrac{1}{3}S),$$

and hence from (4)

$$J/J_s = \coth\eta - 1/\eta, \quad (12)$$

$$\lambda/\lambda_\infty = 1 - 3(\coth\eta)/\eta + 3/\eta^2. \quad (13)$$

Eqs. (12) and (13) determine λ/λ_∞ as a function of J/J_s, say

$$\lambda/\lambda_\infty = \phi(J/J_s). \quad (14)$$

Calculations at low fields are more easily carried out by means of the series expansions

$$J/J_s = \tfrac{1}{3}\eta - (1/45)\eta^3 + (2/945)\eta^5 - (1/4725)\eta^7 + (2/93{,}555)\eta^9 - \cdots, \quad (15)$$

$$\lambda/\lambda_\infty = (1/15)\eta^2 - (2/315)\eta^4 + (1/1575)\eta^6 - (2/31{,}185)\eta^8 + \cdots. \quad (16)$$

The function ϕ is plotted in Fig. 1; numerical values of J/J_s and λ/λ_∞ as functions of η are given in Table I.

The right member of (12) will be recognized as the Langevin function. Differentiation with respect to H, on the assumption that L_0 is a constant of the material, leads to Gans's formula for reversible susceptibility.[7] We shall reserve for a later paper a full discussion of the question, but it should perhaps be mentioned now that an attempt to justify this procedure by interpreting L_0 as v_0/kT, where v_0 is the volume of a domain, would lead to a susceptibility 10^8 times too large.

[111] Domains

We next consider a polycrystalline specimen, say nickel at room temperature, whose domains are crystalline and have their magnetization vectors along the space-diagonals of the cubic lattice. By Eqs. (33), (35), and (27) of I we have, for a single crystal or a single class of domains,

$$J_p(l) = J_s(1/\sqrt{3})\sum l_i \tanh\eta l_i,$$
$$\lambda(l) = \lambda_{111}\sum l_jl_k \tanh\eta l_j \tanh\eta l_k, \quad (17)$$

where $$\eta = L_0HJ_s/\sqrt{3}. \quad (18)$$

Hence for a polycrystalline specimen, by (3),

$$\lambda/\lambda_{111} = \sum\int l_jl_k \tanh\eta l_j \tanh\eta l_k d\omega/4\pi, \quad (19)$$

$$J/J_s = \sum\int l_i \tanh\eta l_i d\omega/4\pi\sqrt{3}. \quad (20)$$

Eqs. (19) and (20) determine the function

$$\lambda/\lambda_{111} = \phi_{111}(J/J_s). \quad (21)$$

[5] Cf. M. Kersten, Zeits. f. Physik **76**, 505 (1932); F. Bitter, *Introduction to Ferromagnetism* (1937), p. 248.

[6] R. Becker, Zeits. f. Physik **62**, 253 (1930); R. Becker and M. Kersten, Zeits. f. Physik **64**, 660 (1930); M. Kersten, Zeits. f. Physik **71**, 553 (1931).

[7] R. Gans, Physik. Zeits. **12**, 1053 (1911); Ann. d. Physik **61**, 379 (1920).

Eq. (20) may be written in the equivalent form

$$J/J_s=\sqrt{3}\,(1/\eta^2)\int_0^\eta u\tanh u\,du. \qquad (22)$$

For low values of η, we may calculate the left members of (19) and (20) by means of the series expansions[8]

$$J/J_s=\tfrac{1}{3}\eta'-(1/45)\eta'^3 +(2/945)\eta'^5-(17/76{,}545)\eta'^7 +(62/2{,}525{,}985)\eta'^9-\cdots, \qquad (23)$$

$$\lambda/\lambda_{111}=(1/15)\eta'^2-(2/315)\eta'^4 +(1/1701)\eta'^6-(46/841{,}995)\eta'^8 +(34/6{,}567{,}561)\eta'^{10}-\cdots, \qquad (24)$$

where $$\eta'=\eta\sqrt{3}=L_0J_sH. \qquad (25)$$

For high values of η, we may use the rigorous formula

$$J/J_s=\sqrt{3}/2-(\sqrt{3}/2\eta^2)\{\pi^2/12-(2\eta+1)u +(4\eta+1)u^2/2^2-(6\eta+1)u^3/3^2+\cdots\}, \qquad (26)$$

where $$u=e^{-2\eta}, \qquad (27)$$

and the approximate formula (in which $e^{-2\eta}$ is neglected)

$$\lambda/\lambda_{111}=2/\pi-\pi/2\eta^2+13\pi^3/240\eta^4-\cdots. \qquad (28)$$

Numerical values of J/J_s and λ/λ_{111} as functions of η' are given in Table II. Values for $\eta'<1.25$ are identical with those given in Table I for J/J_s and λ/λ_∞ as functions of η. The values in Table II, if plotted in Fig. 1, fall only slightly below the curve for ϕ; the highest point is (0.866, 0.637).

TABLE I. *Isotropic domains.*

$\eta=L_0J_sH$	J/J_s	$\lambda/\lambda_\infty=\phi(J/J_s)$
0.1	0.033	0.001
0.2	0.067	0.003
0.3	0.099	0.006
0.4	0.132	0.011
0.5	0.164	0.016
0.6	0.195	0.023
0.7	0.226	0.031
0.8	0.256	0.040
0.9	0.285	0.050
1.0	0.313	0.061
1.25	0.379	0.090
1.5	0.438	0.124
1.75	0.491	0.158
2.0	0.537	0.194
2.5	0.614	0.264
3.0	0.672	0.328
4.0	0.751	0.437
5.0	0.800	0.520
7.5	0.867	0.654
10.0	0.900	0.730
20.0	0.950	0.858
100	0.990	0.970
∞	1.000	1.000

[8] The derivations are given in the Appendix; see also P. Debye, *Handbuch der Radiologie*, Vol. 6 (1925), p. 712.

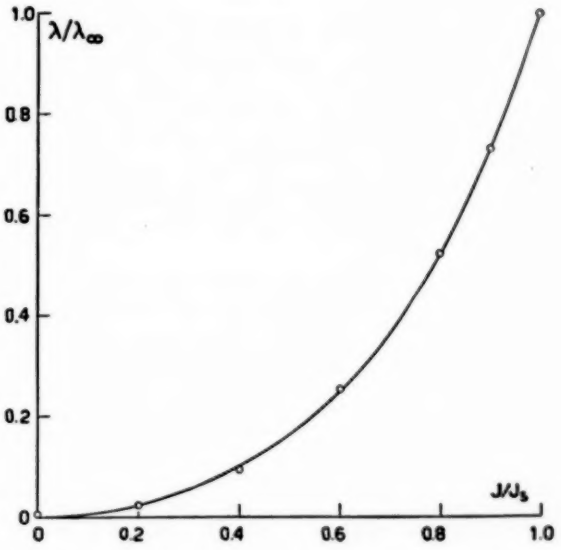

FIG. 1. Theoretical variation of magnetostriction with magnetization for polycrystalline material with isotropic domains: the function $\lambda/\lambda_\infty=\phi(J/J_s)$. The points show experimental values for nickel at 6°C, with a slight correction to the zero and to λ_∞ obtained from the straight-line plot of Fig. 4. Solid line, theoretical: $\lambda/\lambda_\infty=\phi(J/J_s)$; open circle, experimental: nickel, 6°C.

[100] DOMAINS

When the crystalline domains have the tetragonal axes as the directions of easy magnetization, a domain with magnetization along $\pm Ox_r$ contributes, by Eqs. (26′) of I,

$$J_{p(\pm r)}=\pm J_sl_r, \qquad (29)$$

$$\lambda_{\pm r}=\sum e_{ii}l_i^2=\kappa_1(l_r^2-\tfrac{1}{3}). \qquad (30)$$

Hence if $\eta=L_0J_sH$,

$$S(l)=\sum_r(e^{\eta l_r}+e^{-\eta l_r})=2\sum_i\cosh\eta l_i, \qquad (31)$$

$$S_0(l)=J_sdS/d\eta, \qquad (32)$$

$$S_1(l)=\kappa_1(d^2S/d\eta^2-\tfrac{1}{3}S), \qquad (33)$$

and (3) becomes

$$\frac{J}{J_s}=\frac{1}{4\pi}\int\left(\frac{\sum l_i\sinh\eta l_i}{\sum\cosh\eta l_i}\right)d\omega, \qquad (34)$$

$$\frac{\lambda}{\lambda_{100}}=\frac{3}{2}\frac{1}{4\pi}\int\left(\frac{\sum l_i^2\cosh\eta l_i}{\sum\cosh\eta l_i}\right)d\omega-\tfrac{1}{2}. \qquad (35)$$

For low values of η,

$$J/J_s=\tfrac{1}{3}\eta-(1/45)\eta^3+(2/945)\eta^5 -(2/8505)\eta^7+(8/280{,}665)\eta^9-\cdots, \quad (36)$$

$$\lambda/\lambda_{100}=(1/15)\eta^2-(2/315)\eta^4 +(9/17{,}010)\eta^6-(4/93{,}555)\eta^8+\cdots. \quad (37)$$

For high values of η ($e^{-\eta}$ being neglected),

$$J/J_s=0.8312-1.367/\eta^2 -0.8816/\eta^3-4.419/\eta^5+\cdots, \quad (38)$$

$$\lambda/\lambda_{100}=0.5513-2.721/\eta^2 -1.527/\eta^3+6.266/\eta^4+\cdots. \quad (39)$$

Numerical values of J/J_s and λ/λ_{100} as functions of η are given in Table II; values for $\eta<1.25$ are identical with those of J/J_s and λ/λ_∞ in Table I. The upper part of the ϕ_{100}-curve falls slightly below the ϕ_{111}-curve; the highest point is (0.831, 0.551).

The functions ϕ, ϕ_{111}, and ϕ_{100} are indistinguishable at low values of η, for the series formulas are identical to the fifth order of small quantities. On the other hand, at high values of η, where the differences become appreciable, the crystalline domain formulas are unreliable because rotation has been neglected. The slight differences between the functions therefore cannot be regarded as significant. Inferences may nevertheless be drawn in regard to the nature of the domains, from the range of magnetizations over which the theoretical relations hold, and from the magnitude of the constant by which the ϕ function must be multiplied in order to fit the data: for λ_∞, λ_{111}, and λ_{100} are quite different.

TABLE II. *Crystalline domains.*

η' or η $=L_0J_sH$	[111]		[100]	
	J/J_s	λ/λ_{111} $=\phi_{111}(J/J_s)$	J/J_s	λ/λ_{100} $=\phi_{100}(J/J_s)$
1.25	0.379	0.090	0.379	0.090
1.5	0.438	0.123	0.438	0.123
1.75	0.491	0.157	0.491	0.156
2.0	0.537	0.192	0.535	0.189
2.5	0.612	0.259	0.604	0.246
3.0	0.669	0.319	0.657	0.297
4.0	0.742	0.416	0.728	0.382
5.0	0.782	0.477	0.769	0.440
7.5	0.828	0.559	0.805	0.502
10.0	0.845	0.590	0.817	0.523
20.0	0.861	0.625	0.828	0.544
∞	0.866	0.637	0.831	0.551

Uniform Strain

If the strains rather than the stresses are assumed uniform, the average stresses must be expressed as functions of the strains and of the magnetization; then the longitudinal and transverse magnetostriction may be found by setting the average stresses equal to zero and solving for the strains. The average stresses are given to the first order in the assumed uniform strains by formulas of the type

$$X_{ij}'=X_{ij}'^0+\sum_{kl}(\partial X_{ij}'/\partial e_{kl})_3 e_{kl}, \quad (40)$$

where the primes indicate that the reference axes are the fixed ones, with Ox_3' now in the direction of the resultant vector magnetization. The derivatives $\partial X_{ij}'/\partial e_{kl}$ include a purely elastic part, and a magneto-mechanical part that could be evaluated by means of formula (20) of I. The quantities $X_{ij}'^0$ are the stresses developed when magnetostriction is prevented by applying external forces.

Written in full, Eqs. (40) in the case of a quasi-isotropic polycrystalline material take the form

$$\begin{aligned} X_{11}'&=X_{11}'^0+c_{11}'e_{11}'+c_{12}'e_{22}'+c_{13}'e_{33}',\\ X_{22}'&=X_{11}'^0+c_{12}'e_{11}'+c_{11}'e_{22}'+c_{13}'e_{33}', \quad (41)\\ X_{33}'&=X_{33}'^0+c_{13}'(e_{11}'+e_{22}')+c_{33}'e_{33}', \end{aligned}$$

$$X_{23}'=c_{44}'e_{23}', \quad X_{31}'=c_{44}'e_{31}', \quad X_{12}'=\tfrac{1}{2}(c_{11}'-c_{12}')e_{12}'. \quad (42)$$

The $X_{ii}'^0$'s and the c_{ij}''s are functions of the magnetization. The equality of certain of these coefficients and the vanishing of others is a consequence of symmetry requirements, and is not dependent on any theoretical assumptions except that the field and stress components for the polycrystalline material can be derived from a thermodynamic potential F_{Je}.[9] The basic formulas of the present theory, however, impose further restrictions on the coefficients in (41). For it follows from (26) and (26′) of I and from (7) above that there is no magnetization-dependent volume change when the stresses are uniform, and similarly no magnetization-dependent change of mean tension $(X_{11}'+X_{22}'+X_{33}')$ when the strains are uniform. If we add Eqs.

[9] Cf. A. E. H. Love, *Mathematical Theory of Elasticity* (1934), p. 160.

(41), therefore, the coefficients of the strains and the term not containing the strains must be independent of the magnetization and equal to their respective values in the demagnetized state. Thus we find

$$X_{11}'^0 = -\tfrac{1}{2}X_{33}'^0, \tag{43}$$

$$c_{11}'+c_{12}'+c_{13}' = 2c_{13}'+c_{33}' = 3k', \tag{44}$$

where k' is the bulk modulus and is independent of the magnetization. Eq. (44) reduces the number of independent elastic "constants" from five to four, say k', c_{11}', c_{33}', and c_{44}', of which all but k' vary with the magnetization.

Setting the left members of (41) equal to zero, solving for the strains, and using (43) and (44), we get for the magnetostriction

$$\lambda = e_{33}' = -2e_{11}' = -2e_{22}' = -2X_{33}'^0/3(c_{33}'-k'). \tag{45}$$

The formula for $X_{33}'^0$ with strain uniform is obtained from that for λ with stress uniform by substituting for the κ's the k's, given by Eq. (27′) of I:

$$k_2 = -c_{44}\kappa_2, \quad k_1 = -(c_{11}-c_{12})\kappa_1, \quad k = -2G_\infty\kappa. \tag{46}$$

The c's in the first two of these equations are the saturation values of the elastic constants of the crystals, referred to the crystal axes Ox_i; the third equation, in which G_∞ is the saturation value of the rigidity, is the form to which the others reduce when the domains are elastically isotropic. The ratio of the theoretical values of magnetostriction calculated by uniform strain and by uniform stress will therefore be $2c_{44}/3(c_{33}'-k')$ for [111] domains, $2(c_{11}-c_{12})/3(c_{33}'-k')$ for [100] domains, and $4G_\infty/3(c_{33}'-k')$ for isotropic domains. It is easily established moreover that

$$\frac{2}{3}\frac{1}{c_{33}'-k'} = \frac{3}{2}\left(s_{33}'-\frac{1}{9k'}\right) = \frac{3}{2}\left(\frac{1}{E}-\frac{1}{9k'}\right), \tag{47}$$

where E is Young's modulus in the field direction.

For consistency the variation of c_{33}' with magnetization should be computed theoretically at uniform strain, but for estimating the amount of divergence between the two results it suffices to consider the experimentally observed variation of E. This is about $\frac{1}{4}$ percent for iron at room temperature;[10] for nickel it is about 7 percent at room temperature, and rises to 19 percent at higher temperatures.[11] If we neglect this variation, we may replace c_{33}' by its value at saturation, when the substance is theoretically elastically isotropic. Then $3(c_{33}'-k')$ becomes $4G_\infty$. This is certainly justifiable for iron; for iron, therefore, uniform stress and uniform strain give the same theoretical magnetostriction curve except that the two values of the constant factor differ when the domains are crystalline. Nickel, on the other hand, is practically isotropic elastically,[12] so that if we neglect the variation of E with magnetization the formulas will be identical, but this variation may introduce some difference in the shapes of the two curves.

Comparison with Experiment

The comparison between theory and experiment is most easily made by plotting each experimental value of λ against the value of the appropriate ϕ-function corresponding to the experimental value of J/J_s. A straight line through the origin indicates agreement with the uniform stress formulas, and the slope gives the coefficient of the ϕ-function.

Iron

In Fig. 2 data obtained by the writer[13] on annealed Armco iron at 24°C are plotted in this way. The occurrence of positive magnetostriction at low magnetizations shows that the domains are crystalline and of course of the [100] type. The λ-ϕ_{100} plot is linear except at the top, where rotation begins to be appreciable, and at the bottom, where the wide divergence between the

[10] W. T. Cooke, Phys. Rev. **50**, 1158 (1936).

[11] S. Siegel and S. L. Quimby, Phys. Rev. **49**, 663 (1936).

[12] This is indicated by the measurements of J. Zacharias, Phys. Rev. **44**, 116 (1933), who found the Young's modulus of single and polycrystalline specimens to have nearly the same values. When a cubic crystal is nearly isotropic, the three principal elastic constants c_{11}, c_{12}, and c_{44} can be calculated from the observed Young's and rigidity moduli for the polycrystalline substance together with the value of Young's modulus for one direction in the crystal. The rigidity modulus of annealed polycrystalline nickel, as measured in this laboratory by Siegel, is 0.7608×10^{12} dynes/cm², while the Young's modulus of the same material is 2.069×10^{12}. If these results be combined with Zacharias' data on a single crystal, the resulting principal elastic constants at 23.6°C are $c_{11}=3.42$, $c_{12}=1.98$, $c_{44}=0.789$, all times 10^{12}.

[13] W. F. Brown, Phys. Rev. **50**, 1165 (1936).

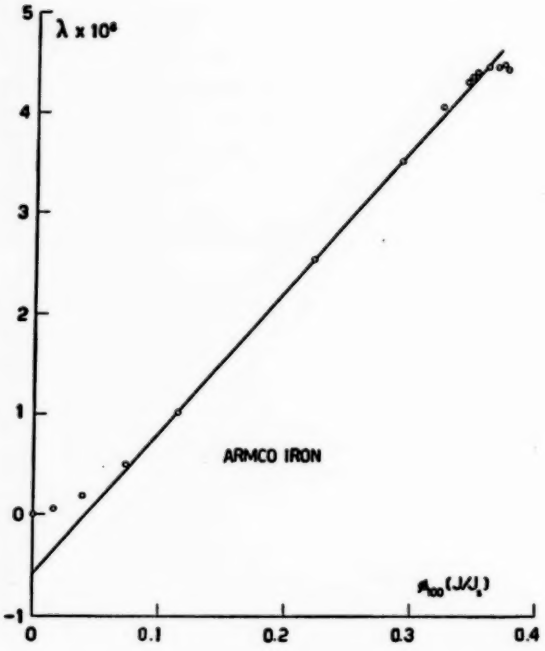

FIG. 2. Test of theoretical relation between magnetostriction and magnetization for Armco iron at room temperature. Experimental values of λ plotted against the theoretical function $\lambda/\lambda_{100}=\phi_{100}(J/J_s)$. J_s taken as 1710.

values on a normal magnetization curve and on a hysteresis loop indicates that the magnetostriction is not a function of the magnetization alone. These values have been plotted in Fig. 3, together with the theoretical curve $\lambda=\lambda_{100}\phi_{100}(J/J_s)$ calculated with $\lambda_{100}=14.13\times10^{-6}$, the slope of the straight line in Fig. 2. The zero of the experimental values in Fig. 3 has been shifted by 0.59×10^{-6}, the value of the y-intercept in Fig. 2, so that the ordinate at $J=0$ represents an excess over the theoretical value due to influences not taken into account in the theory.

This residual magnetostriction may perhaps be explained as follows. The specimen is an elongated ellipsoid (demagnetizing factor 0.0085), and its demagnetization is accomplished by continuous variation of a longitudinal field between positive and negative extremes of gradually decreasing magnitude. The final state is very likely one in which the domain magnetizations, although distributed equally in opposite directions, are oriented more often along [100] axes nearly parallel to the axis of the ellipsoid than along [100] axes nearly perpendicular to it. In such a state there would be a residual magnetostriction without residual magnetization.

From crystal measurements $\lambda_{100}=16.2\times10^{-6}$,[14] the coefficient of ϕ_{100} on the uniform strain theory is 9.2×10^{-6}. The value 14.13×10^{-6} required by the data is intermediate, but closer to the uniform stress value λ_{100}.

Nickel

Kirkham[15] has recently published values of the magnetostriction of annealed polycrystalline nickel as a function of magnetization at a number of temperatures from 6°C to the Curie point. If Kirkham's values of λ are plotted against ϕ, it is found that at the lowest five temperatures (153.2°C and below) all the points, including the saturation value, fall practically on a single straight line through the origin. At higher temperatures, however (192.8°C and above), only the lower part of the plot is linear; the values at high magnetizations fall below the straight line. Typical plots are shown in Fig. 4. The data at 6°C have also been plotted in Fig. 1; here the value of λ_∞ and the zero of ordinates used in plotting λ/λ_∞ are the values obtained from the straight line plot of Fig. 4.

We must conclude that at temperatures up to a little below 200°C, the domains in this specimen of nickel are isotropic, i.e., polycrystalline, but that above this point they are crystalline, so that at high fields magnetization occurs by rotation. Microphotographs of the surface of the ellipsoid show that the average linear dimensions of the crystals are about 0.2 mm. If the domains are polycrystalline at room temperature, they are considerably larger than the domains measured by Bozorth and Dillinger.[3] The maximum domain volume observed by them in nickel was 20×10^{-9} cm³, corresponding to linear dimensions of about 0.03 mm. These measurements were made on wires 60 cm long and 1 mm in diameter; Kirkham's magnetostriction measurements were made on a prolate spheroid 7 inches long[16] and 0.5 inch in diameter. There have been several

[14] Average value from measurements of K. Honda and Y. Mashiyama, Sci. Rep. Tohoku Imp. Univ. [1], **15**, 755 (1926).

[15] D. Kirkham, Phys. Rev. **52**, 1162 (1937).

[16] In reference 15, the length was erroneously stated to be 7.5 inches.

attempts[17] to account theoretically for the existence of domains; though a complete quantitative theory is still lacking, it seems clear that surface forces play an important part and that as a result the size and shape of the domains is dependent on the size and shape of the specimen. A computation based on the formula of Frenkel and Dorfman and the measurements of Bozorth and Dillinger shows that the domains in Kirkham's specimen, if crystalline, should have linear dimensions about half as great as those of the crystals. The formula involves constants whose values may be expected to be different for crystalline and for polycrystalline domains, and also for crystalline domains with different directions of easy magnetization. It is therefore not unreasonable to suppose that for this specimen larger, polycrystalline domains may correspond to a lower energy than smaller, crystalline domains when the direction of easy magnetization is [111], but to a higher when it is [100]. This would explain the transition near 200°C, since the direction of easy magnetization in nickel changes from [111] to [100] at about this temperature.[18]

In Siegel's[11] similarly heat treated but differently shaped specimen of the same material, a cylinder 7.2 cm long and 0.464 cm in diameter, the average linear dimensions of the crystals were 0.4 mm. The crystal size is larger, and the theoretical domain size smaller, for this specimen than for Kirkham's; and the ΔE-effect measurements were successfully analyzed[11, 2] on the assumption that the domains were crystalline at room temperature. The evidence is not entirely conclusive, however, for the initial susceptibility of the specimen is not known accurately. The assumption that the domains are isotropic would

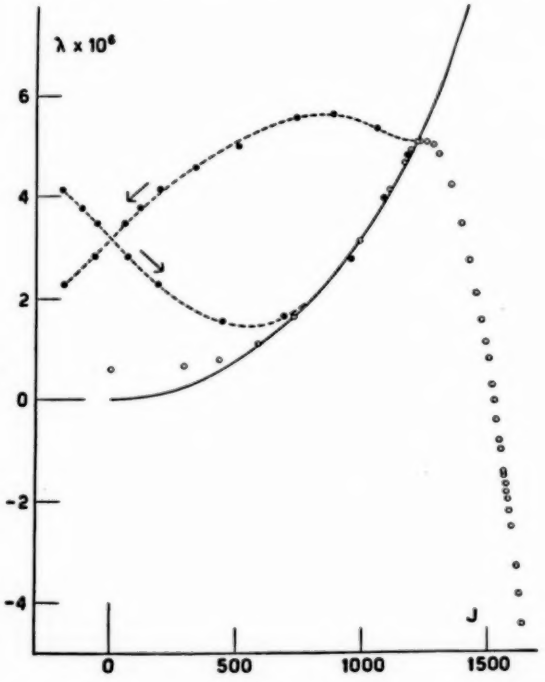

FIG. 3. Experimental and theoretical values of magnetostriction for Armco iron. The zero of the experimental values has been shifted to correct for the residual magnetostriction evident in Fig. 2. Solid line, theoretical. Experimental: open circle, normal magnetization; solid circle, hysteresis loop.

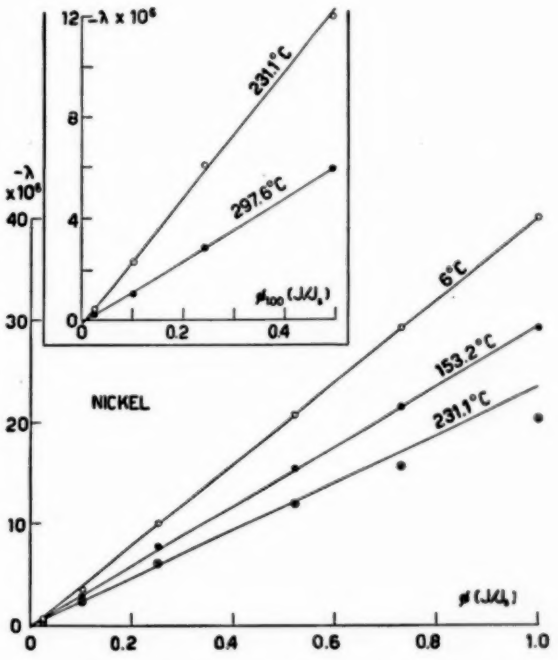

FIG. 4. Test of theoretical relations between magnetostriction and magnetization for nickel at various temperatures. Main plot, experimental values of λ plotted against the theoretical function $\lambda/\lambda_\infty = \phi(J/J_s)$ appropriate when the domains are isotropic. Insert, a similar plot against the theoretical function $\lambda/\lambda_{100} = \phi_{100}(J/J_s)$ appropriate when the domains are crystalline and have [100] as the direction of easy magnetization.

[17] J. Frenkel and J. Dorfman, Nature **126**, 274 (1930); F. Bloch, Zeits. f. Physik **74**, 295 (1932); R. Becker, Physik. Zeits. **33**, 905 (1932); L. Landau and E. Lifshitz, Physik. Zeits. Sowjetunion **8**, 153 (1935); E. Kondorsky, Physik. Zeits. Sowjetunion **11**, 597 (1937); F. Bitter, *Introduction to Ferromagnetism* (1937), pp. 185–192.

[18] K. Honda, H. Masumoto and Y. Shirakawa, Sci. Rep. Tohoku Imp. Univ. [1] **24**, 391 (1935); J. D. Kleis, Phys. Rev. **50**, 1178 (1936); reference 15, Fig. 6 and footnote 7.

change λ_{111} to λ_∞ in Eq. (56) of I and would require the initial susceptibility to be 7.7; the value required if the domains are crystalline is 16.2: the value obtained by Kirkham on a still thinner specimen of the same material, at 21.6°C, is 26.1.

It is now evident that at the higher temperatures, λ must be plotted against ϕ_{100}. If this is done, it is found that all points within the range of possible values of ϕ_{100} (0 to 0.551) fall on a straight line through the origin (see insert, Fig. 4).

This surprisingly good agreement shows that the assumption of uniform stress introduces no serious error in the general shape of the theoretical curves. In view of the approximate elastic isotropy of nickel there should also be a negligible error in the constant factor multiplying them. The slope of the straight line at any of the higher temperatures should therefore be equal to λ_{100}, the magnetostriction of a single crystal saturated in the [100] direction, at this temperature. The values of λ_{100} so obtained have been plotted in Fig. 5. Unfortunately no directly measured values are available for comparison, but it is possible to draw a reasonable curve through the values thus determined and the room temperature value.[19] The temperature 192.8°C is evidently in a transitional range.

The other curves in Fig. 5 give the observed saturation magnetostriction of the polycrystalline material, λ_∞, and the values of λ_{111} computed from the theoretical relation[20]

$$\lambda_\infty = (2\lambda_{100} + 3\lambda_{111})/5. \qquad (48)$$

The value of λ_{111} at room temperature deviates 20 percent from the directly measured value; if λ_∞ is calculated by (48) from Mashiyama's values of λ_{100} and λ_{111}, the deviation from the experimental value is 8.2 percent. Since this deviation may be partly due to actual differences in the materials, the values of λ_{111} above 190°C are not necessarily this much in error.

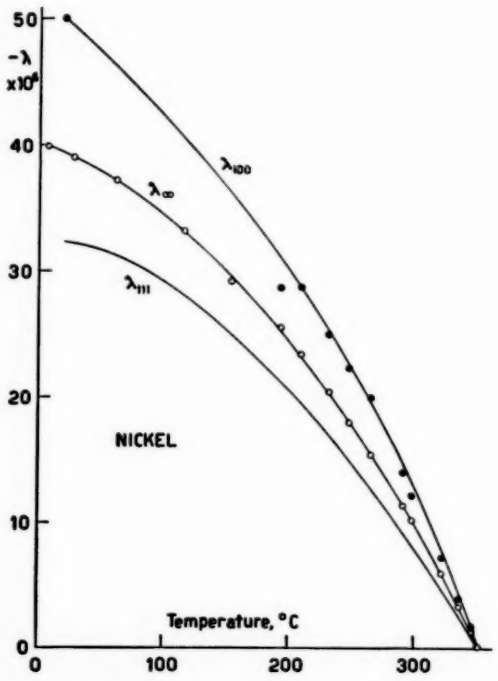

FIG. 5. Variation of saturation magnetostriction with temperature for polycrystalline nickel, and for nickel crystals magnetized in directions [111] and [100]. Polycrystalline values (λ_∞) are experimental (Kirkham). λ_{100} values above 200°C are deduced by theoretical analysis of Kirkham's λ-J curves for polycrystalline nickel; value at room temperature is Mashiyama's. λ_{111} curve is calculated from the smoothed out λ_∞ and λ_{100} curves by Akulov's formula.

There is almost no trace in nickel of the low field discrepancy found in iron; this may be related to the larger longitudinal demagnetizing factor of Kirkham's specimen. The disturbing effect of rotation in the transitional region is naturally less noticeable in nickel because λ_{100} and λ_{111} have the same sign.

The writer wishes to express his gratitude to Professor E. R. Jette and Mr. A. H. Marks of the department of metallurgy, Columbia University, for their assistance in the determination of the size of the crystals in the nickel ellipsoid: to Mr. Marks in particular for the excellent microphotographs which he obtained.

APPENDIX

Equations (23)–(24) and (36)–(37) may be obtained by expanding $J_p(l)$ and $\lambda(l)$ in powers of η and averaging the coefficients over the unit sphere, or (since only even functions of the l_i's occur) over the first octant. Sums $S_{2n} = \Sigma l_i^{2n}$ can be averaged at once by the formula $(l_i^{2n})_{Av} = 1/(2n+1)$. A power or product of such sums may be expressed as a sum of terms of the form

[19] Y. Mashiyama, Sci. Rep. Tohoku Imp. Univ. [1] **17**, 945 (1928).
[20] N. Akulov, Zeits. f. Physik **66**, 533 (1930).

$Y_{2\alpha,\,2\beta,\,2\gamma}=\Sigma l_i^{2\alpha}(l_j^{2\beta}l_k^{2\gamma}+l_k^{2\beta}l_j^{2\gamma})$, where the summation is as usual over the three sets of values $(i, j, k)=(1, 2, 3)$, $(2, 3, 1)$, $(3, 1, 2)$. The integral $\int l_i^{2\alpha}l_j^{2\beta}l_k^{2\gamma}d\omega$ is easily evaluated by Dirichlet's theorem, which gives the volume integral $\psi(r)=\int x^{2\alpha}y^{2\beta}z^{2\gamma}dV$ over the interior of the first octant of a sphere of radius r; the desired surface integral is $\psi'(1)$. Thus

$$(Y_{2\alpha,\,2\beta,\,2\gamma})_{A_0}=6[2(\alpha+\beta+\gamma)+3]\frac{P(\alpha)P(\beta)P(\gamma)}{P(\alpha+\beta+\gamma+2)}, \quad (49)$$

where $P(0)=1$, $P(n)=1\cdot3\cdot5\cdots(2n-1)$. $(n>0)$. (50)

In the evaluation of (19)–(20) for large η, integration over the first octant again suffices. The hyperbolic functions may be expanded in powers of $e^{-\eta l_i}$ and $e^{-\eta l_j}$; because of the behavior of the series near the boundaries $l_i=0$, $l_j=0$, no terms may be neglected, but the series may be integrated term by term since the resulting series are convergent. This integration offers no difficulties in the case of J. In λ, the integrals to be evaluated are of the forms

$$I_1=\int x^p y^q(1-x^2-y^2)^{r/2}e^{-\alpha x}dxdy,$$
$$I_2=\int x^p y^q(1-x^2-y^2)^{r/2}e^{-\alpha x-\beta y}dxdy, \quad (51)$$

the region of integration being the interior of the first quadrant of the unit circle in the xy-plane, and α and β being large if η is large. In I_2, because of the exponential factors, the only appreciable contribution to the integral is in the neighborhood of the origin; the algebraic factor may therefore be expanded in powers of x and y and integrated term by term over the entire region $0\leq(x, y)\leq\infty$. Only the first few terms are required, since higher-order terms give higher powers of $1/\eta$. In I_1, the integration with respect to y may be carried out without approximation; the resulting integrand may then be expanded in powers of x and integrated from 0 to ∞. The formulas thus obtained involve the quantities

$$\sigma_n''=1-\tfrac{1}{2}^n+\tfrac{1}{3}^n-\cdots, \quad (52)$$

whose values are known, and which are expressible in simpler form when n is even.[21]

To evaluate (34)–(35) for large η, we may use as the region of integration, Ω, the portion of the surface of the unit sphere bounded by the arcs $l_2=0$, $l_3=0$, $l_2=l_1$, and $l_3=l_1$.[22] For $\eta=\infty$ we have

$$(J/J_s)_\infty=\int l_1 d\omega/\Omega=(3\sqrt{2}/\pi)\sin^{-1}(1/\sqrt{3})=0.8312,$$
$$(\lambda/\lambda_{100})_\infty=(\tfrac{3}{2})\int l_1^2 d\omega/\Omega-\tfrac{1}{2}=\sqrt{3}/\pi=0.5513. \quad (53)$$

Let $\delta_J=J/J_s-(J/J_s)_\infty$: then by neglecting, in comparison with 1, exponential functions whose arguments are negative and of order of magnitude η at all points of Ω, we get

$$\delta_J=-2\int[ue^{-\eta u}/(1+e^{-\eta u}+e^{-\eta v})]d\omega/\Omega, \quad (54)$$

where $u=l_1-l_2$, $v=l_1-l_3$. Here two terms have been replaced by one, by making use of the symmetry of Ω with respect to l_2 and l_3.

Let δ_J' be the value obtained for δ_J by omitting $e^{-\eta v}$ in the denominator, and let $\delta_J''=\delta_J-\delta_J'$: then

$$\delta_J''=2\int[ue^{-\eta(u+v)}/(1+e^{-\eta u}+e^{-\eta v})(1+e^{-\eta u})]d\omega/\Omega. \quad (55)$$

After transformation to u and v as the variables of integration, δ_J' can be evaluated by a method similar to that used for I_1: thus

$$\delta_J'=-\frac{12}{\pi}\left\{\frac{1}{\sqrt{2}}\left(\sin^{-1}\frac{1}{\sqrt{3}}\right)\frac{\sigma_2''}{\eta^2}+\frac{1}{\sqrt{3}}\frac{\sigma_3''}{\eta^3}+\frac{10}{3\sqrt{3}}\frac{\sigma_5''}{\eta^5}+\cdots\right\}. \quad (56)$$

A treatment of δ_J'' similar to that used for I_2 gives

$$\delta_J''=\frac{4\sqrt{3}}{\pi}\left\{\frac{J_{10}}{\eta^3}+\frac{J_{30}-J_{21}+J_{12}}{3\eta^5}+\cdots\right\}, \quad (57)$$

where

$$J_{mn}=\int_0^\infty\int_0^\infty\frac{e^{-(x+y)}}{(1+e^{-x}+e^{-y})(1+e^{-x})}x^m y^n dydx. \quad (58)$$

A similar procedure gives

$$\delta_\lambda=-\frac{18}{\pi}\left\{\frac{1}{\sqrt{3}}\frac{\sigma_2''}{\eta^2}+\frac{2}{3}(\sigma_3''-J_{10})\frac{1}{\eta^3}-\frac{1}{\sqrt{3}}\left(2\sigma_4''+\frac{2J_{11}-J_{20}}{3}\right)\frac{1}{\eta^4}+\cdots\right\}. \quad (59)$$

The J_{mn}'s may be evaluated by numerical integration; but for $n=0$ and for $m=1$, it is easier to use the formulas

$$J_{m0}=m!\left\{\sigma_{m+1}''\log 2+\sum_{N=1}^{\infty}\frac{1}{N}\left(1-\frac{1}{2^N}\right)(\sigma_{m+1}''-\tau_{m+1,\,N})\right\}, \quad (60)$$

$$J_{1n}=n!\left\{\sigma_{n+2}''\log 2+\sum_{N=1}^{\infty}\frac{1}{N}\left(1-\frac{1}{2^N}\right)(\sigma_{n+2}''-\tau_{n+2,\,N})\right\}, \quad (61)$$

where $$\tau_{m,\,N}=\sum_{r=1}^{N}(-1)^{r+1}/r^m. \quad (62)$$

The first of these may be obtained by integrating with respect to y, expanding in powers of e^{-x}, and integrating term by term with respect to x; the second, by expanding in powers of e^{-y} and then integrating. These formulas give $J_{10}=0.5018$, $J_{20}=2J_{11}=1.1670$, $J_{30}=3J_{12}=3.7962$. By numerical integration, $J_{21}=1.3511$.

[21] G. Chrystal, *Algebra*, Part II (1906), pp. 366–367.
[22] Cf. R. Gans, Ann. d. Physik **15**, 28 (1932).

LETTERS TO THE EDITOR

Prompt publication of brief reports of important discoveries in physics may be secured by addressing them to this department. Closing dates for this department are, for the first issue of the month, the eighteenth of the preceding month, for the second issue, the third of the month. Because of the late closing dates for the section no proof can be shown to authors. The Board of Editors does not hold itself responsible for the opinions expressed by the correspondents.

Communications should not in general exceed 600 words in length.

Minimum Neutron Energy to Produce Neutron Loss Process and Its Application to the Measurement of Q Values

The cyclotron in Berkeley produces a beam of very high energy deuterons, which in bombardment of the light elements give rather high energy neutrons, especially in the forward direction.

Assumption of the conservation of energy and momentum gives the following formula

$$Q=\tfrac{1}{2}MV^2-\tfrac{1}{2}M_dV_d^2+(1/2Mn)\times(M^2V^2-2MM_dVV_d\cos\phi+M_d^2V_d^2), \quad (1)$$

where Q is the total energy evolved in the reaction which is usually expressed by the following type of formula

$$Z^A+{}_1H^2=(Z-1)^{A+1}+n+Q.$$

M, V, M_d and V_d are the mass and velocity of a neutron and of a deuteron respectively. Mn is the mass of residual nucleus, and ϕ the angle between the direction of the deuteron and that of the emitted neutron.

In the case of the Be target, for example, the energy of a neutron is expressed as follows

$$E_n=\frac{10}{11}Q+\frac{9}{11}E_d+\frac{MVM_dV_d}{11}\cos\phi,$$

where E_n and E_d are the energy of the neutron and of the deuteron. The maximum energy from the Be target varies by a fairly large amount, as a function of ϕ and E_d, especially when a value of E_d is as high as 8 Mev.

If the scattering from the materials around the target is negligible, it is possible to bombard a sample with a neutron beam of known maximum energy by placing it at various angles with the Be target or by changing the energy of the bombarding deuterons.

Since the end of 1936 it has been reported by several persons[1, 2] that neutron loss reactions can be observed on bombardment of certain elements by neutrons of sufficiently high energy. In other words, a high energy neutron can knock out one or more neutrons from a stable nucleus of certain elements, and the corresponding characteristic periods for neutron loss have been observed.

The detection of the presence of neutron-loss periods after bombardment with neutrons of known maximum energy makes it possible to determine the minimum energy of neutrons necessary to produce the neutron-loss process in measurable amount.

The results of some preliminary tests are as follows, some of which have been reported at the Stanford meeting.

Element	Limits of E_n (Mev)	T (min.)
N	$5.5>E_n>7$	10
P	$5>E_n>7$	2.8
Cu	$12>E_n>13$	10
Zn	$9.0>E_n>10$	35
Ga	$6>E_n>7$	66
Ge	$5.5>E_n>7$	30
Br	$9>E_n>13$	6
Mo	$12>E_n>13$	17
Ag	$5>E_n>7$	25
In	$12>E_n>13$	1
Sb	$5.5>E_n>7$	16

Although the minimum energies for the following elements are close to each other, it is still possible to detect which elements need higher energy than others, and this can be written in the following order:

$$\text{Ga}>\text{Ge}>\text{Sb}>\text{Ag}>\text{P}.$$

When these values are calibrated more accurately we shall be able to estimate roughly the maximum energy of neutrons from various targets subjected to deuteron bombardment by observing in what elements the neutrons are capable of producing neutron loss. Then using the formula (1) we can determine the Q value.

A test of this possibility was made on Al, Fe, Cu, and a rough estimate of the maximum energy of neutrons emitted gives the following figures:

	Al	Fe	Cu
Limits for E_n (Mev)	$6<E_n<9$	$5.5<E_n<7$	$5.5<E_n<7$
Q (Mev)	<3.5	<1.5	<1.5

It should be mentioned that the samples are not free from the bombardment of scattered neutrons and also those from the cyclotron walls or dees; but fortunately scattering turned out to be negligible and the maximum energy of the neutrons from copper is not very high so that the tests for neutron energies higher than that from Cu can be made fairly accurately.

The author wishes to express his gratitude to Professor Ernest O. Lawrence and the staff of the Radiation Laboratory for the privilege of the use of the cyclotron and for their valuable help and discussions. The financial support of the Research Corporation, the Chemical Foundation, and the Josiah Macy, Jr. Foundation, is greatly appreciated.

R. SAGANE

Radiation Laboratory, Department of Physics,
University of California,
Berkeley, California,
January 18, 1938.

[1] Heyn, Physica **4**, 161 (1937).
[2] Pool, Cork, Thornton, Phys. Rev. **52**, 239 (1937); Chang, Goldhaber, Sagane, Nature **139**, 962 (1937).
[3] Phys. Rev. **53**, 212 (1938).

On the Albedo of Slow Neutrons

Halpern, Lueneburg and Clark[1] have recently given a rigorous solution of the integrodifferential equation describing the diffusion of thermal neutrons in paraffin. Although the method used by these authors is very elegant and involves the overcoming of serious mathematical difficulties, the criticism given by them of our interpretation[2] of the experimental results does not seem to be correct.

The definition of albedo as "reflection coefficient for neutrons impinging on a plane surface limiting a large paraffin block" is not quite unique. We introduced, therefore, what we called "experimental albedo" by formula (10) of our paper in the *Physical Review*.[3] All measurements of the albedo are to be compared with this definition, and to the same definition the relationship

$$\beta = 1 - 2/(N)^{\frac{1}{2}}$$

refers, as proved in Fermi's paper.

Halpern, Lueneburg and Clark have instead calculated a different quantity viz., the reflection coefficient defined as the ratio of the number of reflected neutrons to the number of incident neutrons. Our definition rests on the measurement of the activity of a thin detector; now this activity is not simply a measure of the number of incident neutrons, but it also depends on their angular distribution, neutrons falling normally on the detector being less effective than neutrons falling at a large incidence angle (the probability of capture is proportional to $1/\cos\vartheta$). Since the angular distributions of the incident and reflected neutrons are different, the difference between Halpern's result and ours is easily explained.[4]

We must therefore maintain, that the average number of impacts of a thermal neutron in paraffin as given in our papers is correct, apart from the uncertainty of the experimental data.

E. Fermi
E. Amaldi

R. Università-Istituto Fisico,
Roma, Italy.

G. C. Wick

R. Università-Istituto Fisico,
Palermo, Italy,
January 14, 1938.

[1] O. Halpern, R. Lueneburg and O. Clark, Phys. Rev. **53**, 173 (1938).
[2] E. Amaldi, E. Fermi, Phys. Rev. **50**, 899 (1936); E. Fermi, Ricerca Scient. **7**, 13 (1936).
[3] See e.g. our paper, reference 2, page 910, column 2, line 11.
[4] It may be pointed out that in a paper by Wick, Lincei Rend. **23**, 775 (1936) the whole problem was based on the same integrodifferential equation as in Halpern's paper and a result in accordance with Fermi was obtained by a numerical method. The reflection coefficient, as defined by Halpern a.o., was also considered under the assumption of a cosine distribution of the incident neutrons, and a result in full accord with Halpern's result for this case was obtained.

Evidence of a Periodic Deviation from the Schottky Line for Tungsten

In the course of a study in this laboratory of the surface ionization of salts on tungsten it was found desirable to reinvestigate the thermionic emission of tungsten at high fields. Use was made of the thermionic cell designed by Clemens and Phipps.[1] Emission data were obtained over the range of temperature, 1560°K to 1940°K, and over the range of field at the surface of the filament, 1800 to 260,000 volts per cm. When the resulting values of log i were plotted against $E^{\frac{1}{2}}$ in order to test Schottky's relation, and the mean straight line was calculated by the method of least squares, it was found that the experimental points consistently fluctuate about the mean straight line, as shown in the sample curves given in Fig. 1, in which the deviation is given in the same units as log i. It is seen that the magnitude of the deviations from linearity is small, so that the deviations can be observed only with very precise measurements.

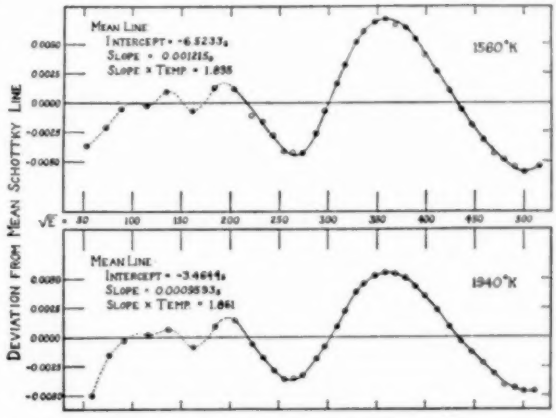

FIG. 1. Deviation from a mean straight line of the logarithm of the emission current from tungsten, at 1560°K and 1940°K, *vs.* the square root of E, the field at the filament surface in volts per cm.

In order to determine whether an inherent condition in the cell or in the circuit might have been responsible for the deviations, the experimental conditions were varied as follows: four different thermionic cells were employed in which filament diameters of 2 mil, 1 mil, and 0.5 mil were variously used: and in the course of the work two different experimental circuits were employed. In each case the resulting emission curves (six to nine isotherms for each 1 and 2 mil filament) showed the same deviation, the period and amplitude of the deviation curve increasing with increasing field. For a given cell and filament the maxima and minima in the deviation curves appeared at the same values of field strength for each isotherm. For different sized filaments the positions of the maxima and minima were shifted slightly.[2] The amplitude of the deviation curves decreases only slightly with increasing temperature.

A theoretical interpretation of these results is being undertaken by Professor H. M. Mott-Smith of the department of physics. To aid in this attempt it has been found desirable to obtain similar emission data for metals other than tungsten. At present we are attempting to do this and also to extend our measurements with tungsten to fields of the order of 10^6 volts per cm in an attempt to reach another maximum in the deviation curve and also possibly to reach the region of transition to field currents.

R. L. E. Seifert
T. E. Phipps

Department of Chemistry,
University of Illinois,
Urbana, Illinois,
February 22, 1938.

[1] Clemens and Phipps, Rev. Sci. Inst. **8**, 133 (1937).
[2] This may be attributed to uncertainties in the calculation of the conversion factor from applied voltage to field at the filament surface.

The Nature of the Penetrating Component of the Cosmic Radiation

The analysis by Bowen, Millikan and Neher[1] of their data on cosmic radiation intensity at various altitudes and latitudes shows among other things that the penetrating component[2] must be a secondary radiation produced (indirectly) by primary electrons whose behavior is much like that calculated for ordinary electrons according to current quantum mechanics.[3]

The observational material now available is commonly thought to be incapable of yielding further insight into the nature of the penetrating radiation or of eliminating certain of the hypotheses that have been put forward. The general supposition is that it is always possible to construct an energy distribution of particles to give any required absorption law. There are, however, in the present problem auxiliary, theoretical and observational restrictions sufficient to make this rather difficult. A serious attempt to satisfy all the conditions enhances one's regard for a satisfactory solution even before it has been shown to be unique.

An example of a thought widely held but actually untenable is the notion that the discrepancy between the cosmic ray ionization observed and that calculated for ordinary electrons can be attributed to particles which lose their energy only by collision and produce few secondaries which could lead to showers.

The data available at present can be used to calculate a lower limit for the number of such particles necessary to reproduce the observed absorption curve. The result is that more than 70 percent of the total ionization would have to be due to the non-shower producing secondaries and indeed they would predominate in number at all altitudes, and in all showers.

This is clearly incompatible with observation and theory. Further analysis, to be published in a more complete paper, strengthens the conclusion that the secondary cosmic radiation contains not merely penetrating particles of possibly diverse masses but also particles of intermediate properties which result in copious electron showers.

It is not necessary to invent quite new particles with *ad hoc* properties even if it were possible to do so with ease. A formulation in terms of present theory seems preferable. The appropriate interpretation is: *there are in the secondary cosmic radiation, electrons of the usual mass, electrons of much greater mass and electrons of intermediate mass.*

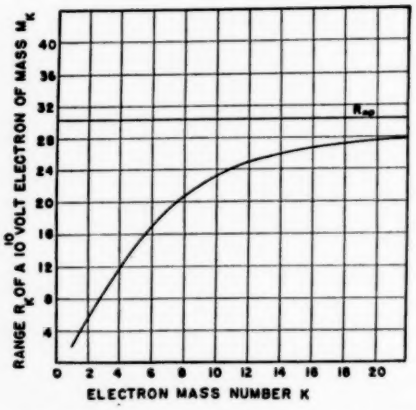

FIG. 1. Range in meters of water of 10^{10} volt electrons of mass $m_k = km_1$.

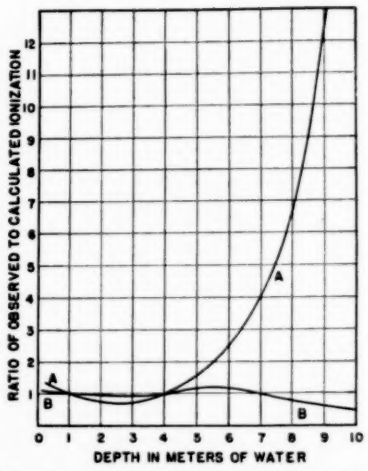

FIG. 2. (A) Ratio I_0/I_1 of observed cosmic radiation intensity in the 10^{10} volt band to that calculated from the theory of Carlson and Oppenheimer assuming all secondaries to be ordinary electrons. (B) Ratio $I_0/\Sigma I_k$ of the observed intensity to the intensity assuming that all integral mass heavy electrons occur.

Neddermeyer[4] has already presented such a hypothesis and discussed its advantages. The idea is to regard electronic mass as a quantized parameter

$$m_k = km_1, \tag{1}$$

where the quantum number k takes on a set of discrete values including unity. Merely tentatively and for definiteness this discussion will treat all integral values of k as possible. Some equally plausible alternatives give qualitatively similar results.

One of the very attractive features of the mass quantization hypothesis is that no special assumptions are necessary to describe the behavior of heavy electrons. The radiation theory of quantum mechanics can be invoked to predict all the properties required, no additional arbitrary constants are involved.

Figure 1 shows how rapidly the properties of heavy electrons change with their mass. The figure gives the range R_k for 10^{10} volt electrons of mass m_k. The range which is a measure of shower producing ability was computed from the formula

$$R_k = 45.5k^2 \ln (1+1/0.015k^2). \tag{2}$$

This expression, easy to derive, indicates the numerical values assigned to the radiation and collision energy loss constants which occur in the theory. In the sense of the present paper an electron of intermediate mass is evidently one with k considerably less than 10. A 10^{10} volt electron with $m_k > 10m_1$ is practically a nonradiating particle.

Figure 2 is intended to bring out the necessity of the assumption that penetrating particles exist and to show how remarkably well the mass quantization hypothesis satisfies the need for the 10^{10} volt band. The theory of

Carlson and Oppenheimer was used for $k=1$ and new calculations were made for $k>1$. The relative contributions of the different m_k are not arbitrary so that the fit of curve B is impressive. Of course both A and B were adjusted in absolute magnitude to give the total ionization observed. The agreement at the top of the atmosphere is probably fortuitous. The moderate discrepancy in the lower regions can be diminished by improving some of the approximations that were used.

The details of the present analysis will be published when the calculations for the other bands of the cosmic radiations have been completed.

R. M. LANGER

California Institute of Technology,
Pasadena, California,
February 3, 1938.

[1] I. S. Bowen, R. A. Millikan and H. V. Neher, Phys. Rev. **53**, 217 (1938); **52**, 80 (1937).
[2] C. D. Anderson and S. H. Neddermeyer, Phys. Rev. **50**, 263 (1936); S. H. Neddermeyer and C. D. Anderson, Phys. Rev. **51**, 884 (1937); J. C. Street and E. C. Stevenson, Phys. Rev. **52**, 1005 (1937).
[3] J. F. Carlson and J. R. Oppenheimer, Phys. Rev. **51**, 220 (1937); H. J. Bhabha and W. Heitler, Proc. Roy. Soc. **159**, 432 (1937).
[4] S. H. Neddermeyer, Phys. Rev. **53**, 102 (1938).

The Magnetic Moments of $_3Li^6$, $_3Li^7$ and $_9F^{19}$*

We have measured the nuclear moments of $_3Li^6$, $_3Li^7$ and $_9F^{19}$ with the new molecular beam method[1] in which the precession frequency ν of the nucleus in a uniform magnetic field H is measured directly. The moment μ is obtained from the relation $\nu=\mu H/ih$, where i is the spin in units of $h/2\pi$. The spins of these nuclei are known[2] from h.f.s. measurements, band spectra and from atomic beam experiments. With these values of i and our measurement of ν and H we obtain μ directly.

The nuclei were identified by observing resonance curves as in Fig. 1 of R.Z.M.K.[1] for LiCl, LiF and NaF. The common values of ν/H of LiCl and LiF are those of the Li isotopes, and the common ν/H of LiF and NaF is that of F. The values of ν/H obtained over a range of H which represents a threefold increase agree within a few parts in a thousand. The values of ν/H obtained from different molecules are equally concordant.

The values of μ in units of nuclear magnetons ($\mu_0/1838$) are given in Table I.

TABLE I.

Nucleus	Spin	Moment
$_3Li^6$	1	0.823 ± 0.005
$_3Li^7$	3/2	3.265 ± 0.016
$_9F^{19}$	1/2	2.635 ± 0.014

The ratio of the moments of the Li isotopes μ_7/μ_6 was found to be 3.89 by Manley and Millman.[2] The present experiments yield 3.97 for this value, an increase of 2 percent. For $_3Li^7$ Granath[2] found the moment to be 3.29 from the h.f.s. of Li II with the theory of Breit and Doerman;[3] Fox and Rabi found 3.20 from atomic beam experiment with the theory of Goudsmit, Fermi and Segrè[3] while Bartlett, Gibbons and Watson find 3.33 from the same data. Using the h.f.s. data of Campbell,[2] Brown and Bartlett[3] calculate values of the moment of $_9F^{19}$ ranging from 1.9 to 3.8. For a discussion of the accuracy and validity of these calculations see the conclusion of the papers by Bartlett[3] and his co-workers.

Our results for the ratio of the nuclear moments of $_3Li^7$ and $_3Li^6$ and the moment of $_3Li^7$ diverge even more widely from the calculations of Rose and Bethe[4] than did the previous results of Manley and Millman.

It is very noteworthy that the agreement between our value of the magnetic moment and the results of calculations from h.f.s. measurements is so very close in the case of $_3Li^7$.

I. I. RABI
S. MILLMAN
P. KUSCH
J. R. ZACHARIAS

Columbia University,
Hunter College (J.R.Z.),
New York, New York,
March 2, 1938.

* Publication assisted by the Ernest Kempton Adams Fund for Physical Research of Columbia University.

[1] Rabi, Zacharias, Millman and Kusch, Phys. Rev. **53**, 318 (1938).
[2] For $_3Li^6$ and $_3Li^7$, Schuler, Zeits. f. Physik **66**, 431 (1930); Harvey and Jenkins, Phys. Rev. **35**, 789 (1930); Guttinger and Pauli, Zeits. f. Physik **67**, 743 (1931); Goudsmit and Inglis, Phys. Rev. **37**, 328 (1931); Granath, Phys. Rev. **42**, 44 (1932); Fox and Rabi, Phys. Rev. **48**, 746 (1935); Manley and Millman, Phys. Rev. **51**, 19 (1936). For $_9F^{19}$, Gale and Monk, Astrophys. J. **69**, 77 (1929); J. S. Campbell, Zeits. f. Physik **84**, 393 (1933).
[3] Goudsmit, Phys. Rev. **43**, 636 (1933); Fermi and Segrè, Zeits. f. Physik **82**, 729 (1933); Breit and Doerman, Phys. Rev. **36**, 1732 (1930); Brown and Bartlett, Phys. Rev. **45**, 527 (1934); Bartlett, Gibbons and Watson, Phys. Rev. **50**, 315 (1936).
[4] Rose and Bethe, Phys. Rev. **51**, 205 (1937).

Evidence for a Band System of Antimony Nitride

In a discharge through a mixture of nitrogen and antimony vapor a new band system has been found extending from 2890A towards longer wave-lengths. The experimental arrangement differed little from the one used by Herzberg[1] and Spinks[2] for the production of the PN and AsN bands. The high melting temperature of Sb and low vapor pressures even at higher temperatures made the use of a quartz discharge tube necessary which was heated while the discharge was running. The spectrum has been photographed with a Hilger E3 and a Hilger E1 quartz spectrograph. The new system which consists of bands degraded towards the red has very likely the SbN molecule as carrier. It shows the same intensity distribution as the band spectra of PN and AsN. Some bands are overlapped by nitrogen bands, but the members of the diagonals are easily recognizable. Most of the bands could be fitted into a scheme. The vibrational quanta of the lower and upper state are about 925 cm^{-1} and 820 cm^{-1}, respectively. A detailed description will be published later together with results of experiments on BiN which are now in progress including a comparison of the nitrides of group $V(b)$ elements.

NETTIE H. COY
H. SPONER

Department of Physics,
Duke University,
Durham, North Carolina,
February 16, 1938.

[1] J. Curry, L. Herzberg and G. Herzberg, Zeits. f. Physik **86**, 348 (1933).
[2] J. W. T. Spinks, Zeits. f. Physik **88**, 511 (1934).

Further Evidence Against Heavy Beta-Particles

We have shown[1] that Champion's experiments on the collisions of beta-particles with electrons contradict the hypothesis of heavy beta-particles, in the form recently proposed by Jauncey.[2] Earlier, he suggested that heavy electrons in the cosmic rays might lose mass by ionization or by emitting gamma-radiation, and now he employs this suggestion[3] to explain the presence of "ordinary electrons" in his deflection experiments, and in those of Zahn and Spees. We are asked to believe that in the latter experiments practically all the radium E beta-particles start out in heavy form, but that they may revert to the ordinary form in the short time elapsing before they reach the detector. Presumably the same supposition could be employed to question our interpretation of Champion's results, so we wish to show that it does not agree with known facts. The idea that the excess energy is dissipated very quickly in the form of gamma-rays is incompatible with the very low amount of radiation emitted by radium E; this amounts to only 10^4 volts per disintegration.[4] On the other hand, the excess energy cannot be frittered away in ionization processes, for this would contradict the calorimetric experiments of Ellis and Wooster, who found the total energy liberated in the form of heat is $350{,}000 \pm 40{,}000$ volts per disintegration. Meitner and Orthmann's repetition gave $337{,}000 \pm 20{,}000$ volts.

Before Jauncey proposed the idea we have just considered, he discussed[5] the experiments of Meitner and Orthmann from another point of view, assuming that the lifetime of a heavy electron is long, or that any radiation it may emit escapes detection in experiments on the heat evolution of radium E. His hypothesis that all beta-particles from a given substance have the same total energy means that their *energy distribution* curve is shifted decidedly to lower energies, as compared with the classical one,[6] so that the average kinetic energy of the electrons is less than one-third of the maximum. He states that his hypothesis explains the Meitner-Orthmann result, provided that their experiment records only the kinetic energy of the particles.

We have done the computation over and used the data of Flammersfeld[7] on the shape of the radium E distribution curve. The average kinetic energy turns out to be 153 kev on Jauncey's hypothesis, while on the usual basis it is 331 kev, in excellent agreement with the calorimetric value, given above.

Additional evidence against the heavy particle hypothesis may be derived from data on elastic scattering of radium E beta-particles by electrons. Champion[8] obtained extensive cloud chamber evidence on the angular distribution of scattered electrons and the scattering cross section. His results agree closely with the theory of Möller, which takes into account both exchange effects and retardation. In these experiments the incident beta-particles had kinetic energies ranging from about 380 to about 880 kev. By the use of Jauncey's formulas these figures would become 165 and 570 kev, respectively. The predicted scattering would then be very different from the observed scattering, firstly because the average energy is much lower than the classical one, and secondly, because the incident particle and the one struck would not have the same rest mass.

No doubt many other types of experiment could be cited to show that there is no striking difference between the properties of beta-particles and electrons of the same velocity, calculated of course by the usual formulas. We are well aware that several observers have claimed that the energy loss formulas for electrons break down in the region below 10 Mev. The experiments of Turin and Crane[9] and the calculations of Jaeger[10] indicate that the trouble will be ironed out when more accurate numerical computations of cross sections become available. It is to be expected that present theories, properly applied, will be found to provide an adequate description of the behavior of electrons *outside* of nuclei and at energies for which the de Broglie wavelength is much larger than the classical electron radius.

ARTHUR RUARK
CREIGHTON C. JONES

University of North Carolina,
Chapel Hill, North Carolina,
February 16, 1938.

[1] Ruark and Jones, Phys. Rev. **53**, 264 (1938).
[2] Jauncey, Phys. Rev. **53**, 197 (1938).
[3] Jauncey, Phys. Rev. **53**, 265 (1938).
[4] Aston, Proc. Camb. Phil. Soc. **22**, 859 (1925).
[5] Jauncey, Phys. Rev. **53**, 106 (1938).
[6] Jauncey uses 2.06 mc^2 for the maximum *kinetic* energy. This is incorrect. In reference 1 we employed 2.44 mc^2 which corresponds to the Konopinski-Uhlenbeck extrapolation of O'Conor's data. The experimental end point is 2.28 ± 0.06 mc^2. Use of this value would not affect the conclusions in reference 1.
[7] Flammersfeld, Physik. Zeits. **38**, 973 (1937).
[8] Champion, Proc. Roy. Soc. **137**, 688 (1932).
[9] Turin and Crane, Phys. Rev. **52**, 63 and 610 (1937).
[10] Jaeger, Nature **140**, 108 (1937).

The Energy of the Neutrons from the Disintegration of Carbon by Deuterons

Recently Bethe and Livingston[1] have constructed new range energy curves for low energy protons which differ considerably from the old data. Because the old data of Blackett and Lees[2] were used in calculating the energy of the neutrons from carbon,[3] according to the reaction

$$C^{12}+H^2 \rightarrow N^{13}+n'+Q,$$

it was considered advisable to recalculate the data on the basis of the new range-energy curve.

The neutron energies are determined from that of the recoil protons recoiling in the forward direction (0–8°) to the 0.88 Mev deuterons. They were observed in a cloud chamber at an angle of $90° \pm 10°$ to the direction of the incident deuterons on the target. The stopping power of the methane in the cloud chamber was found to be 1.057 for polonium alpha-particles, and was corrected for the change in stopping power according to the procedure of Livingston and Bethe.[4] This gives a value of 1.16 for protons of 0.5 cm range.

The extrapolated range of the recoil protons is 0.58 ± 0.05 cm as determined from the integral range-number curve. This corresponds to a proton energy of 0.455 Mev according to the new data or to an energy of 0.33 Mev when Blackett's old data are used.

Corrections were then applied for range straggling, angular straggling, thick target corrections, etc., according to the procedure outlined by Livingston and Bethe.[4] This gives an energy of 0.46 ± 0.03 Mev for neutrons observed at 90° to the 0.88 Mev deuterons. The energy of disintegration is calculated from the relation $Q=14/13\,E_n-11/13\,E_H$. The numerical value is $Q=-0.25\pm0.05$ Mev. This value agrees well with that of -0.28 Mev as obtained by Cockcroft and Lewis[5] from the threshold value of the nuclear reaction. The difference between this and our old value of $Q=-0.37$ Mev is almost entirely due to the change in the range-energy curve for protons.

T. W. Bonner

Rice Institute,
Houston, Texas,
February 18, 1938.

[1] Private communication.
[2] Blackett and Lees, Proc. Roy. Soc. **A134**, 665 (1932).
[3] Bonner and Brubaker, Phys. Rev. **50**, 309 (1936).
[4] Livingston and Bethe, Rev. Mod. Phys. **9**, 275 (1937).
[5] Cockcroft and Lewis, Proc. Roy. Soc. **A154**, 261 (1936).